Fakultät für Physik der Universität Bielefeld

Light in the Inhomogeneous Universe:

Studies on light propagation in the averaged space-time

Samae Bagheri

November 11, 2014

Dissertation an der Fakultät für Physik

der Universität Bielefeld

To my parents, my brothers and sister
who have always supported me, each in their own way.

Abstract

In standard cosmology a background geometry is used to interpret observations of the large scale structure of the Universe. The *background* means a homogeneous, isotropic and flat Friedmann-Lemaître (FL) Universe, neglecting the details at small scales and local inhomogeneities of mass density.

Observational cosmology is based on light trajectories and the paths of light are null geodesics. One of the significant effects of inhomogeneity is on the light trajectories. Some aspects of this are very well understood and studied in great depth. For instance, CMB photons are related to density fluctuations by the Sachs-Wolfe effect, and gravitational lensing plays an important role for light propagation in the Universe.

Cosmic structures determine how light propagates through the Universe and consequently must be taken into account. In the standard cosmological model at the largest scales, such structures are either ignored or treated as small perturbations to an isotropic and homogeneous Universe. This isotropic and homogeneous model is commonly assumed to emerge from some averaging process at the largest scales.

However, averaging in general relativity is not a simple operation, due to the covariance of the theory and the non-linearity of Einstein equations. We review previous studies of the averaging and backreaction problem in cosmology. We also discuss some recent attempts, which addressed the averaging problem through propagation of light. Unfortunately, those works are restricted to either a toy model or a perturbative approach.

We then present our work on a more general result for the propagation of light in an averaged Universe. We assume that there exists an averaging procedure that preserves the causal structure of space-time. Based on that assumption, we study the effects of averaging the geometry of space-time and derive an averaged version of the null geodesic equation of motion. For the averaged geometry we then assume a flat FL model and find that light propagation in this averaged FL model is not given by null geodesics of that model, but rather by a modified light propagation equation that contains an effective Hubble expansion rate, which differs from the Hubble rate of the averaged space-time.

Contents

1. Introduction

The standard model of modern cosmology describes large-scale structures as perturbations of an isotropic and homogeneous Universe, the Friedmann-Lemaître (FL) model. In this way, confirmed by many observations, the Lambda Cold Dark Matter (ΛCDM) model of the Universe has been established to be the standard model. measurements of the Cosmic Microwave Background (CMB) from the Wilkinson Microwave Anisotropy Probe (WMAP) [1], and Planck [2], Supernova measurements [3, 4] and the Baryon Acoustic Oscillation (BAO) observations [5] confirm that the standard model is a good description of the Universe.

Despite of its success, the FL model is only a large scale approximation to highly non-linear structures at small scales. Consequently, one can ask how to justify this high degree of symmetry at the largest scales and how to connect the smallest scales to the largest ones. Eventually, we must not ignore the effects of local inhomogeneities from which an averaged space-time with certain symmetries seems to emerge. By *local* we refer to scales on which gravitationally bound structures exist, i.e. from $\sim$ 100 Mpc down to the Planck scale. Above the 100 Mpc, the Universe appears to be statistically homogeneous and isotropic, but on smaller scales, unlike the FL model, it is inhomogeneous. For testing large-scale homogeneity, several tests have been applied to the data from the Sloan Digital Sky Survey [6] and the WiggleZ Dark Energy Survey [7]. In both cases a transition to homogeneity at scales of about 100 Mpc is found.

In this thesis, we are specifically interested on the effects of the local inhomogeneities at and below the 100 Mpc scale on the propagation of light.

The thesis is organized as follows:

Before turning to the main topic of this work, the theoretical framework of cosmology based on an isotropic and homogeneous description of the Universe is reviewed in the following sections of chapter 1.

Chapter 2 highlights the necessary formalism of large scale structure, the perturbation theory and the results from the Planck mission up to now (October 2014).

Chapter 3 introduces the averaging problem in cosmology and presents a review of procedures to account the backreaction of inhomogeneity on the background have been addressed in them.

Chapter 4 contains the result of my research on trajectories of light-rays in the averaged Universe, some of it published in [8].

Finally, the conclusions are presented in chapter 5 and outlook for further research is given.

1.1. History of the Universe

The discovery of the expansion of the Universe by Edwin Hubble in 1929 was a big breakthrough in cosmology. This discovery is approved by observational cosmology and it is found that the Universe was hotter and denser in its past. At very early times the temperature was high enough to ionize the material that filled the Universe. The Universe therefore consisted of a plasma of nuclei, electrons and photons, and the number density of free electrons was so high that the mean free path for the Thomson scattering of photons was very short. As the Universe expanded, it has cooled, and transitioned from radiation dominated to matter-dominated state. Eventually, at a temperature of about 3000 K, the photon energies became too low to keep the Universe ionized. At this time, known as recombination, neutral atoms were ingredients of the Universe instead of the primordial plasma. Initial inhomogeneities present in the primordial plasma grew during the matter-dominated era into the structures we observe in the Universe today. This scenario after 13.7 billion years later has entered an epoch of accelerated expansion, with its energy density dominated by dark energy. Fig. 1.1 emphasizes the main events during the evolution history of the Universe. These events along the timeline of the Universe are summarized in Table 1.1.

The idea that the Universe was hot and dense in the past and has cooled by expansion is described by the Big Bang theory. The observational topics underlying the Big Bang theory are the Hubble diagram, Big Bang Nucleosynthesis (BBN) and the Cosmic Microwave Background (CMB).

However, several properties of the Universe such as anisotropies of the CMB, dark matter and dark energy cannot be explained within the standard model.

t	$\rho^{1/4}$	Event
10^{-42} s	10^{19} GeV	Inflation begins
10^{-32} s	10^{13} GeV	Inflation ends
100 s	0.1 MeV	Nucleosynthesis (BBN)
10^{4} yr	1 eV	Matter-radiation equality
10^{5} yr	0.1 eV	Photon decoupling and formation of the CMB
1 Gyr	10^{-3} eV	First structures form
14 Gyr	10^{-4} eV	Present time

Table 1.1. Corresponding time and energy density scales to the key events of the history of the Universe. Table re-provided from [9].

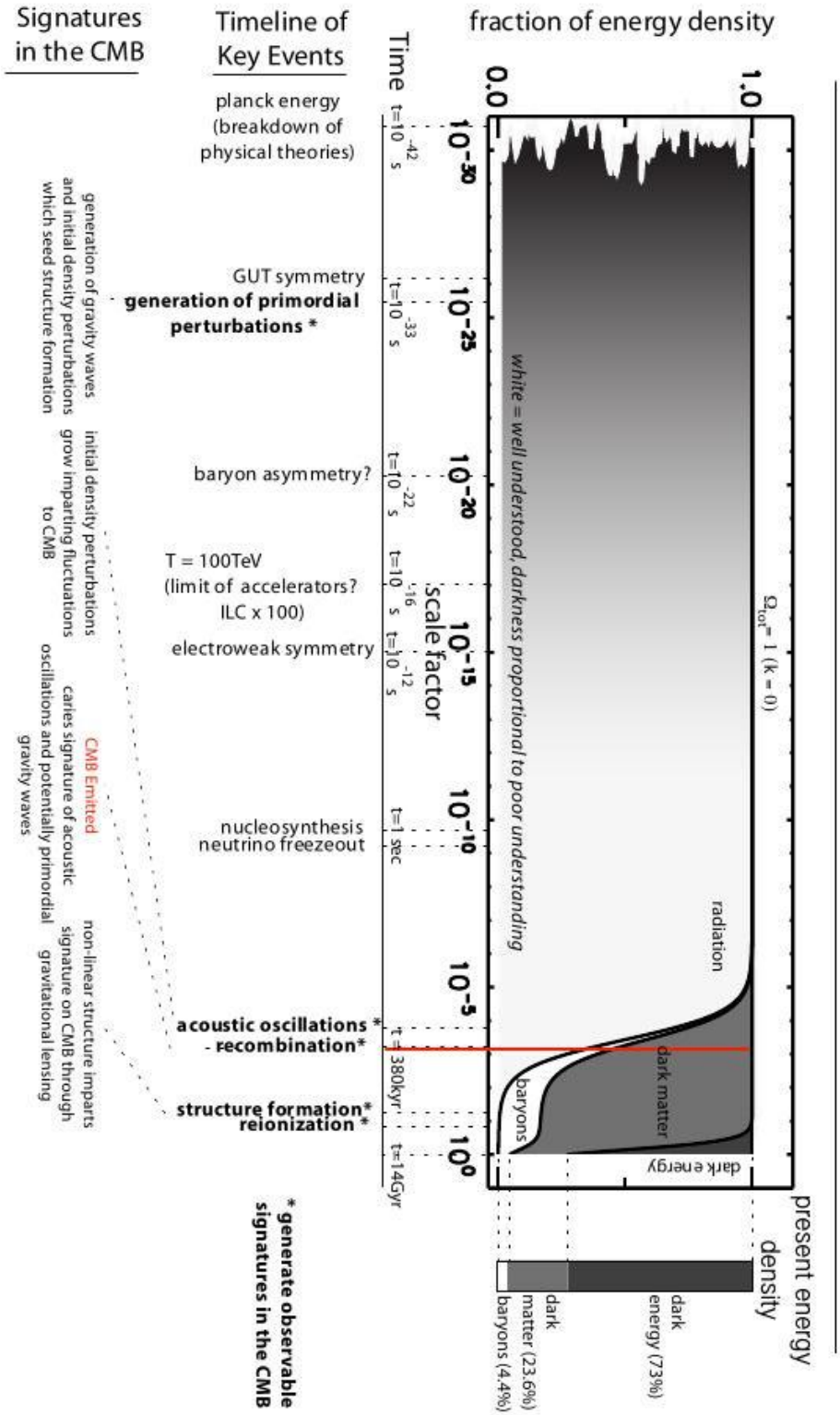

Figure 1.1. Key events of history of the Universe during the evolution.

On the largest scales, the Universe is assumed to be uniform (i.e. there is no preferred direction and no preferred observing position). This idea is called the cosmological principle implying the isotropy and homogeneity of the Universe.

The observational evidences have indicated that the Universe is expanding. This means that early in the history of the Universe, the distant galaxies were closer to us than they are today. It is convenient to describe the scaling of the coordinate grid in an expanding Universe by time dependent scale factor $a(t)$. In a smooth, expanding Universe, the scale factor connects the coordinate distance with the physical distance.

The observed Universe has the following properties:

- The Universe is homogeneous and isotropic when averaged over the largest scales.
- It is expanding with the Hubble rate.
- It was hotter in the past.
- It is locally inhomogeneous today (locally means on the scales smaller than 100Mpc).
- Its curvature is negligible.
- It contains a large percentage of unknown "dark energy", which causes acceleration.

We shall address these properties later in this chapter.

1.2. The metric

Most of the cosmology can be learnt with knowledge of general relativity (GR). We will need the concepts of metric and geodesic lines. Then we can apply Einstein equations to the Robertson-Walker metric, relating the metric parameters to the energy density of the Universe. In this section of the thesis, we will apply Einstein equations to the homogeneous Universe.

The metric is an essential tool to make quantitative predictions in an expanding Universe. In classical Newtonian mechanics, gravity is an external force, and particles move in a gravitational field. In GR, gravity is encoded in the metric, and the particles move in a curved space-time. Therefore a free falling particle follows a geodesic in space-time. The metric links the concepts of geodesic and space-time:

$$ds^2 = \sum_{\mu,\nu=0}^{3} g_{\mu\nu} dx^\mu dx^\nu, \tag{1.1}$$

where ds^2 is the proper interval, $g_{\mu\nu}$ is the metric tensor, and x^μ is a four-vector whereby $\mu, \nu \to 0, 1, 2, 3$. $x^0 = t$ represents the timelike coordinate, and x^i stands for the spacelike coordinates ($i = 1, 2, 3$).

If the Comoving distance today is x_0, the physical distance between two points at some earlier time t was $a(t)x_0$. In a flat Universe, the metric must be similar to the Minkowski metric (i.e. $\eta_{\mu\nu} = diag(-1, 1, 1, 1)$), except that the distance must be multiplied by the scale factor $a(t)$. Thus, the metric of a flat, expanding Universe is the Robertson-Walker metric:

$$g_{\mu\nu} = diag(-1, a^2(t), a^2(t), a^2(t)). \tag{1.2}$$

The evolution of the scale factor depends on the density of the Universe. When perturbations are introduced (see section 2.1), the metric will become more complicated, and the perturbed part of the metric will become determined by the inhomogeneities in the matter and the radiation.

1.3. The geodesic equation

1.3.1. Christoffel symbol

In Minkowski space, particles travel in straight lines unless they are acted upon by an external force. In more general space-times, the concept of a straight line gets replaced by the geodesic, which is the path followed by a particle in the absence of any external forces. The Newton's law with no forces, $\frac{d^2\vec{x}}{dt^2} = 0$, must be generalized to the expanding Universe. We will start with particle motion in an Euclidean 2D plane. In Cartesian coordinates $x^i = (x, y)$ the equations of motion for a free particle are

$$\frac{d^2x^i}{dt^2} = 0. \tag{1.3}$$

We start from the Cartesian equation and transform:

$$\frac{dx^i}{dt} = \left[\frac{\partial x^i}{\partial x'^j}\right]\frac{dx'^j}{dt}, \tag{1.4}$$

where the term in the brackets is a transformation matrix going from one basis to another. The basis vectors for polar coordinates are $r, \hat{\theta}$. This can be written as

$$\frac{d}{dt}\left[\frac{dx^i}{dt}\right] = \frac{d}{dt}\left[\frac{\partial x^i}{\partial x'^j}\frac{dx'^j}{dt}\right] = 0. \tag{1.5}$$

If the transformation was linear, the derivative acting on the transformation matrix would vanish, and the geodesic equation in the new basis would still be $d^2x'^i/dt^2$. In polar coordinates, the transformation is not linear, and using the chain rule, we have

$$\frac{d}{dt}\left[\frac{\partial x^i}{\partial x'^j}\right] = \frac{dx'^k}{dt}\frac{\partial^2 x^i}{\partial x'^k \partial x'^j}. \tag{1.6}$$

The geodesic equation therefore becomes,

$$\frac{d}{dt}\left[\frac{dx^i}{dx'^j}\frac{dx'^j}{dt}\right] = \frac{\partial x^i}{\partial x'^j}\frac{d^2x'^j}{dt^2} + \frac{\partial^2 x^i}{\partial x'^j \partial x'^k}\frac{dx'^k}{dt}\frac{dx'^j}{dt}. \tag{1.7}$$

Multiplying by the inverse of the transformation matrix, we obtain the geodesic equation in a non-Cartesian basis is:

$$\frac{d^2x'^l}{dt^2} + \left[\left((\frac{\partial x}{\partial x'})^{-1}\right)^l_i \frac{\partial^2 x^i}{\partial x'^j \partial x'^k}\right]\frac{dx'^k}{dt}\frac{dx'^j}{dt} = 0. \tag{1.8}$$

The term in the brackets is the Christoffel symbol,

$$\Gamma^l_{jk} = \left[\left((\frac{\partial x}{\partial x'})^{-1}\right)^l_i \frac{\partial^2 x^i}{\partial x'^j \partial x'^k}\right], \tag{1.9}$$

which is symmetric in j, k. In Cartesian coordinates, $\Gamma^l_{jk} = 0$ and the geodesic equation is simply $d^2x^i/dt^2 = 0$. In general $\Gamma^l_{jk} \neq 0$ describes geodesics in non-trivial coordinate systems. The geodesic equation is a useful concept, because in a non-trivial space-time e.g. the expanding Universe, it is not possible to find a fixed Cartesian coordinate system. So we need to know how particles travel in the more general case.

Considering an affine parameter λ , the geodesic equation becomes:

$$\frac{d^2x^\mu}{d\lambda^2} + \Gamma^\mu_{\alpha\beta}\frac{dx^\alpha}{d\lambda}\frac{dx^\beta}{d\lambda} = 0. \tag{1.10}$$

Rather than the previous definition of the Christoffel symbol obtained by transforming a Cartesian basis, it is more convenient to obtain it from the metric:

$$\Gamma^\mu_{\alpha\beta} = \frac{1}{2}g^{\mu\nu}\left[\frac{\partial g_{\alpha\nu}}{\partial x^\beta} + \frac{\partial g_{\beta\nu}}{\partial x^\alpha} - \frac{\partial g_{\alpha\beta}}{\partial x^\nu}\right]. \tag{1.11}$$

The components of the Christoffel symbol in the flat FL Universe are:

$$\Gamma^0_{00} = 0, \quad \Gamma^0_{0i} = 0, \quad \Gamma^i_{ij} = \delta_{ij}\dot{a}a, \quad \Gamma^i_{0j} = \frac{\dot{a}}{a}\delta^i_j, \quad \Gamma^i_{jk} = 0, \quad \Gamma^i_{00} = 0, \tag{1.12}$$

where overdots denote d/dt.

1.3.2. Particles traveling in an expanding Universe

In this section we apply the geodesic equation to a single particle. All observations in cosmology have to do with intercepting photons. Therefore we will consider a massless particle, which has four vector, $p^\alpha = (E, \vec{p})$, and use this to define the parameter λ:

$$p^\alpha = \frac{dx^\alpha}{d\lambda}, \tag{1.13}$$

by noting that $\frac{d}{d\lambda} = \frac{dx^0}{d\lambda}\frac{d}{dx^0} = E\frac{d}{dt}$, and the zero component of the geodesic equation,

$$E\frac{dE}{dt} = -\Gamma^0_{ij}p^i p^j = -\delta_{ij}\dot{a}ap^i p^j. \tag{1.14}$$

For a massless particle, the energy-momentum vector has zero magnitude:

$$g_{\mu\nu}p^\mu p^\nu = -E^2 + \delta_{ij}a^2 p^i p^j = 0. \tag{1.15}$$

Since $\vec{p}$ measures motion on the comoving grid, the physical momentum which measures changes in the physical distance is related to $\vec{p}$ by a factor of a. This leads to

$$\frac{dE}{dt} + \frac{\dot{a}}{a}E = 0. \tag{1.16}$$

We note that the energy of a massless particle decreases as the Universe expands:

$$E \propto \frac{1}{a}. \tag{1.17}$$

On the other hand, the energy of a photon with a frequency ω is given by

$$E = \hbar\omega, \tag{1.18}$$

where $\hbar$ is equal to the Planck constant h divided by 2π, i.e. $\hbar \equiv h/2\pi$.

The frequency of a photon emitted with ω_{em} will therefore be observed with a lower frequency ω_{obs} as the Universe expands:

$$\frac{\omega_{obs}}{\omega_{em}} = \frac{a_{em}}{a_{obs}}. \tag{1.19}$$

1.3.3. Redshift

Measuring the redshift of distant objects is one of the most basic observation. The above equation (1.19) can be explained in terms of the redshift z between two events, defined by the fractional change in wavelength:

$$z = \frac{\lambda_{obs} - \lambda_{em}}{\lambda_{em}} = \frac{\omega_{em} - \omega_{obs}}{\omega_{obs}}. \tag{1.20}$$

If the observation takes place today ($a_{obs} = a_0 = 1$), this implies

$$a_{em} = \frac{1}{1+z}. \tag{1.21}$$

So the redshift of an object gives us information about the scale factor when the photon was emitted.

1.4. The Einstein equations

Gravitation can be described by a metric. This is one important aspect of General Relativity which connects the metric to the matter and energy. It is described by the Einstein equations, which relates geometry to energy:

$$G_{\mu\nu} = R_{\mu\nu} - \frac{1}{2} g_{\mu\nu} R = 8\pi G T_{\mu\nu}, \tag{1.22}$$

where $G_{\mu\nu}$ is the Einstein tensor, $R_{\mu\nu}$ is the Ricci tensor

$$R_{\mu\nu} = \Gamma^{\alpha}_{\mu\nu,\alpha} - \Gamma^{\alpha}_{\mu\alpha,\nu} + \Gamma^{\alpha}_{\beta\alpha}\Gamma^{\beta}_{\mu\nu} - \Gamma^{\alpha}_{\beta\nu}\Gamma^{\beta}_{\mu\alpha}, \tag{1.23}$$

and $R = g^{\mu\nu} R_{\mu\nu}$ is the Ricci scalar. Finally, the energy-momentum tensor $T_{\mu\nu}$ is a symmetric tensor describing the constituents of the Universe.

Einstein general theory of relativity is somehow the starting point for a mathematical description of the Universe. However, solving the above Einstein equations (1.22) in general is highly complex. In practice, one should start with an ansatz for the metric $g_{\mu\nu}$ in order to simplify that. Some of the earliest models of the Universe to incorporate Einstein's general relativity were proposed independently by Alexander Friedmann in 1922 and Abbe Georges Lemaître in 1927. They derived solutions to Einstein's field equations which predicted that galaxies should be receding from each other due to cosmic expansion.

Howard Robertson and Arthur Geoffrey Walker explored the problem further during the 1930s. In 1935 Robertson and Walker proved that their obtained metric is the only one on a space-time that is spatially homogeneous and isotropic.

Hereby in this thesis, regarding this historical point of view, we call the standard model of cosmology as Friedman-Lemaître (FL) model and its corresponding metric, Robertson-Walker (RW) metric.

1.4.1. Energy momentum tensor

In Einstein equations, matter is incorporated through the energy momentum tensor $T^{\mu\nu}$. This is a symmetric tensor, such that $T^{\mu\nu} \equiv g^{\nu\alpha} T^{\mu}_{\alpha} = T^{\nu\mu}$.

On large scales of the Universe, matter can be approximated as a perfect fluid. The general form of the energy-momentum tensor for a perfect fluid is:

$$T^{\mu\nu} = (\rho + p) u^{\mu} u^{\nu} + p g^{\mu\nu}, \tag{1.24}$$

where ρ denotes the energy density, and p is the pressure of the fluid and $u^{\mu} = (1, 0, 0, 0)$ is the fluid four velocity. p and ρ depend on t and $u^{\mu} u_{\mu} = -1$. This equation reduces to $T^{\mu}_{\nu} = diag(\rho, p)$ in the rest frame, and is a tensor equation, therefore coordinate-independent and it must be valid in any frame. The choice of perfect fluid allows us to describe a wide variety of cosmological fluids, given their equation of state by

$$w = \frac{p}{\rho}. \tag{1.25}$$

Dust has $p = 0$, $w = 0$, radiation has $p = \frac{\rho}{3}$, $w = \frac{1}{3}$ and for vacuum energy $T^{\mu\nu} = -\rho_{vac} g^{\mu\nu}$, $P_{vac} = -\rho_{vac}$, $w = -1$. For the case where there is no gravity and velocities are negligible, the pressure and energy evolve as

$$\text{Continuity Equation :} \quad \frac{\partial \rho}{\partial \mathrm{t}} = 0, \tag{1.26}$$

$$\text{Euler Equation :} \quad \frac{\partial \mathrm{p}}{\partial \mathrm{x^i}} = 0. \tag{1.27}$$

Promoting this to a 4-component conservation equation for the energy-momentum tensor gives

$$\frac{\partial T^{\mu}_{\nu}}{\partial x^{\mu}} = 0. \tag{1.28}$$

However, in an expanding Universe, this must be modified, such that the conservation implies the vanishing of the covariant derivative

$$T^{\mu}_{\nu;\mu} \equiv \frac{\partial T^{\mu}_{\nu}}{\partial x^{\mu}} + \Gamma^{\mu}_{\alpha\mu} T^{\alpha}_{\nu} - \Gamma^{\alpha}_{\nu\mu} T^{\mu}_{\alpha}. \tag{1.29}$$

Thus the conservation law becomes

$$T^{\mu}_{\nu;\mu} = 0. \tag{1.30}$$

An important consequence for $\nu = 0$ yields the continuity equation:

$$\frac{\partial \rho}{\partial t} + 3\frac{\dot{a}}{a}(\rho + p) = 0. \tag{1.31}$$

1.5. Friedmann-Lemaître cosmology

1.5.1. The cosmological principle

At sufficiently large scales, the cosmological models are based on the idea of the Copernican principle which tells us that the Universe looks the same everywhere. This is encoded more rigorously in the following two statements:

- Isotropy : at each specified point on the manifold, space looks the same in every direction.
- Homogeneity : the metric is the same throughout the manifold.

If a space is smooth and isotropic everywhere, then it is also homogeneous. If a space is isotropic around one point and also homogeneous, it will be isotropic everywhere [10]. The CMB shows that the Universe is isotropic on the order of 10^{-5} [1], and since by the Copernican principle, we do not believe that we are the centre of the Universe.

1.5.2. Friedmann equations in a flat Universe

The scale factor is one of the fundamental concepts in general relativity and cosmology. Thus understanding the evolution of the scale factor in a homogeneous expanding Universe has a special significance. In this context, we consider the time-time component of the Einstein equation:

$$R_{00} - \frac{1}{2}g_{00}R = 8\pi G T_{00}, \tag{1.32}$$

leading to the first Friedmann equation for a spatially flat Universe:

$$\left(\frac{\dot{a}}{a}\right)^2 = \frac{8\pi G}{3}\rho. \tag{1.33}$$

The second Friedmann equation can be derived by considering the space-space component of Einstein equation:

$$R_{ij} - \frac{1}{2}g_{ij}R = 8\pi G T_{ij}. \tag{1.34}$$

Using the flat FL terms with $g_{ij} = \delta_{ij}a^2$, for the left hand side gives

$$\delta_{ij}[2\dot{a}^2 + \ddot{a}a] - \delta_{ij}\frac{a^2}{2}6\left[\frac{\ddot{a}}{a} + \left(\frac{\dot{a}}{a}\right)^2\right]. \tag{1.35}$$

The right hand side is obtained by noticing the perfect fluid energy-momentum tensor we see:

$$8\pi G T_{ij} = 8\pi G g_{ik}T^k_j = 8\pi G a^2 \delta_{ij} p. \tag{1.36}$$

Equating these terms gives

$$\frac{\ddot{a}}{a} + \frac{1}{2}\left(\frac{\dot{a}}{a}\right)^2 = -4\pi G p. \tag{1.37}$$

Combining with the first Friedmann equation (1.33), this leads us to the second Friedmann equation:

$$\frac{\ddot{a}}{a} = -\frac{4\pi G}{3}(\rho + 3p). \tag{1.38}$$

1.5.3. General RW metric and general Friedmann equations

Let us consider the line element

$$ds^2 = -dt^2 + a^2(t)d\sigma^2, \tag{1.39}$$

where t is a timelike coordinate, $a(t)$ is the scale factor, and $d\sigma^2$ is the metric on a maximally symmetric 3-manifold Σ:

$$d\sigma^2 = \gamma_{ij}dx^i dx^j, \tag{1.40}$$

where (x^1, x^2, x^3) are coordinates on Σ, and γ_{ij} is a maximally symmetric 3D metric.

The general RW metric on space-time describes one of these maximally symmetric hypersurfaces evolving in size:

$$ds^2 = -dt^2 + a^2(t)\Big[\frac{dr^2}{1-kr^2} + r^2 d\Omega^2\Big], \tag{1.41}$$

where k can take the values $[-1, 0, 1]$.

However, the Copernican principle only applies in space, not in time. Thus the maximally symmetric space-time (related to the perfect cosmological principle) does not describe our expanding Universe. With the assumption of the Universe being spatially homogeneous and isotropic, we thus replace the maximally symmetric with spherically symmetric space-time. So the metric can be written as

$$d\sigma^2 = \frac{d\tilde{r}^2}{1-k\tilde{r}^2} + \tilde{r}^2 d\Omega^2, \tag{1.42}$$

where $\tilde{r}$ denotes the radial coordinate, and $\Omega^2 = (d\theta^2 + \sinh^2\theta d\phi^2)$ is the metric on the 2-sphere. This become more convenient to redefine the radial coordinate as

$$d\chi = \frac{d\tilde{r}}{\sqrt{1-k\tilde{r}^2}}, \tag{1.43}$$

so that

$$d\sigma^2 = d\chi^2 + f_k^2(\chi) d\Omega^2, \tag{1.44}$$

where $f(\chi)$ is defined as

$$f(\chi) = \begin{cases} \sin\chi & k = +1 \\ \chi & k = 0 \\ \sinh\chi & k = -1 \end{cases} \tag{1.45}$$

Now the metric

$$ds^2 = -dt^2 + a^2(t)(d\chi^2 + f_k(\chi^2)(d\theta^2 + \sin^2\theta d\phi^2)), \tag{1.46}$$

represents a slicing of space-time with spatial slices Σ that are simply rescaled by the scale factor a as time goes on. If $k = 0$, we have a flat space, if $k = +1$, the space Σ describes a sphere, while if $k = -1$ we have an hyperbolic space.

We can also change coordinates in time to something called conformal time

$$\eta = \int_0^t \frac{dt}{a(t)}, \tag{1.47}$$

so that the RW metric becomes

$$ds^2 = a(\eta)^2[-d\eta^2 + d\chi^2 + f_k(\chi^2)(d\theta^2 + \sin^2\theta d\phi^2)]. \tag{1.48}$$

For general k, the first Friedmann equation (1.33) becomes:

$$\left(\frac{\dot{a}}{a}\right)^2 = \frac{8\pi G}{3}\rho - \frac{k}{a^2}, \tag{1.49}$$

and the second Friedmann equation does not change due to k:

$$\frac{\ddot{a}}{a} = -\frac{4\pi G}{3}(\rho + 3p). \tag{1.50}$$

Notice that, in an expanding Universe (i.e. $\dot{a} > 0$) filled with ordinary matter (i.e. matter satisfying the strong energy condition: $\rho + 3p \geq 0$), the second Friedmann equation (1.50) implies $\ddot{a} < 0$. Of course, this conclusion relies on the assumption that general relativity and the Friedmann equations are applicable to high energies. However, this assumption is certainly not true, and it is expected from the paradigm of inflation, that the Universe in its earliest stages undergoes a period of accelerated expansion i.e. $\ddot{a} > 0$ [11, 12, 13].

1.5.4. Dynamics of the FL Universe

The expansion rate of the FL Universe is characterized by the Hubble parameter,

$$H(t) = \frac{\dot{a}}{a}. \tag{1.51}$$

The expansion rate at the present epoch, $H(t_0)$, is called the Hubble constant. The usual convention of writing the Hubble constant at the present day is

$$H_0 = 100\ h\ \text{km s}^{-1}\ \text{Mpc}^{-1}, \tag{1.52}$$

where the dimensionless number h should not be confused with Planck's constant. The astronomical length scale of a megaparsec (Mpc) is equal to $3.0856 \times 10^{22} m$.

From the measurements of Planck + WMAP + BAO, the value of the Hubble constant is [14]

$$H_0 = 67.80 \pm 0.77\ \text{km s}^{-1}\ \text{Mpc}^{-1}. \tag{1.53}$$

The cosmological scales are set by the Hubble length,

$$d_H = H_0^{-1} c = 9.25 \times 10^{25} h^{-1} m = 4.22 \times 10^3 h^{-1} \text{Mpc}. \tag{1.54}$$

The Hubble time is,

$$t_H = H_0^{-1} = 4.35 \times 10^{17} h^{-1} s = 13.8 \times 10^9 h^{-1} yr. \tag{1.55}$$

Since we usually set $c = 1$, H_0^{-1} is referred to both the Hubble length and the Hubble time. The deceleration parameter,

$$q = -\frac{a\ddot{a}}{\dot{a}^2}, \tag{1.56}$$

measures the rate of change of the expansion.

The density parameter

$$\Omega = \frac{8\pi G}{3H^2}\rho = \frac{\rho}{\rho_{crit}}, \tag{1.57}$$

counts the energy density from all forms of constituents of the Universe.

The critical density

$$\rho_{crit} = \frac{3H^2}{8\pi G}, \tag{1.58}$$

changes with time, and is so called because the Friedmann equation can be written as

$$\Omega(a) - 1 = \frac{k}{H^2 a^2}. \tag{1.59}$$

Thus the sign of k is defined by the sign of $(\Omega - 1)$:

- $\rho < \rho_{crit} \leftrightarrow \Omega < 1 \leftrightarrow k < 0 \leftrightarrow Open$
- $\rho = \rho_{crit} \leftrightarrow \Omega = 1 \leftrightarrow k = 0 \leftrightarrow flat$
- $\rho = \rho_{crit} \leftrightarrow \Omega > 1 \leftrightarrow k > 0 \leftrightarrow closed$

The density parameter tells us which of the three FL geometries describes our Universe. Our observations are consistent with the flat case.

1.5.5. Evolution of the scale factor

Combining the two Friedmann equations, one can derive the continuity equation, which we previously obtained from the conservation of the energy-momentum tensor:

$$\frac{d\rho}{dt} + 3H(\rho + p) = 0. \tag{1.60}$$

This also follows from the first law of thermodynamics

$$\begin{aligned} dU &= -pdV \\ d(\rho a^3) &= -pd(a^3) \\ \Rightarrow \quad \frac{d\ln\rho}{d\ln a} &= -3(1+w), \end{aligned} \tag{1.61}$$

where w is the equation of state from (1.25). The continuity equation can be integrated to give

$$\rho \propto a^{-3(1+w)}. \tag{1.62}$$

Together with the Friedmann equation (1.49), this leads to the time evolution of the scale factor,

$$a \propto t^{\frac{2}{3}(1+w)}. \tag{1.63}$$

component	w_i	$\rho(a)$	$a(t)$
non-relativistic matter	0	a^{-3}	$t^{2/3}$
radiation/relativistic matter	$\frac{1}{3}$	a^{-4}	$t^{1/2}$
curvature	-$\frac{1}{3}$	a^{-2}	t
cosmological constant	-1	a^0	$e^{(Ht)}$

Table 1.2. Corresponding components of the Universe to the equation of state, energy and scale factor.

In particular, constituents of our Universe have the following scalings (see Table 1.2):

Thus the present ratio of the energy density relative to the critical density is defined as

$$\Omega_{i,0} \equiv \frac{\rho_0^i}{\rho_{crit,0}}, \tag{1.64}$$

and the corresponding equations of state

$$w_i \equiv \frac{p_i}{\rho_i}. \tag{1.65}$$

This allows one to rewrite the first Friedmann equation as

$$\left(\frac{H}{H_0}\right)^2 = \sum_i \Omega_{i,0} a^{-3(1+w_i)} + \Omega_{k,0} a^{-2}, \tag{1.66}$$

which implies

$$\sum_i \Omega_i + \Omega_k = 1. \tag{1.67}$$

The second Friedmann equation evaluated at $t = t_0$ becomes

$$\left(\frac{\ddot{a}}{a}\right)_{t=t_0} = -\frac{H_0^2}{2} \sum_i \Omega_i (1 + 3w_i). \tag{1.68}$$

Combined with results from prior experiments, Planck has revealed its first result that dark energy comprises 68.3% of the energy content of the Universe, down slightly from earlier estimates of 72.8%. Similarly, dark matter's contribution was boosted to 26.8 percent, while ordinary matter's share went from 4.5% to 4.9% [2].

1.6. Inflation

Inflationary cosmology has been introduced by Guth [11] in 1980. The theory was developed to overcome the problematic shortcomes of the hot big bang model of the Universe, like flatness, horizon and monopole problems. However, it also provides an

explanation for the origin of the structures. According to this theory, the Universe at very early stages of its evolution inflated rapidly. This led to an exponential growth of the scale factor $a(t)$. The theory of inflation has been accepted as the standard paradigm for the generation of the seed perturbations for the origin of structure in the Universe. Density perturbations were produced from quantum fluctuations, generated during inflation and seem to have a Gaussian distribution. After the era of inflation, the particles, which surround us, were produced and density perturbations grew into the observed large scale structure.

The theory is usually associated with a scalar fields that is slowly rolling down its potential. The slow roll inflation leads to an almost scale invariant power spectrum. In a better construction, inflation theory predicts an almost scale invariant, highly Gaussian spectrum of adiabatic perturbations, which can be probed experimentally by the measurements of temperature fluctuations in the CMB radiation as well as observations of large scale structure.

We assume that the flat homogeneous Friedmann Universe is filled by a spatially homogeneous scalar field (known as the inflation field). The energy density ρ and pressure p of a single field, $\phi(t)$, with potential $V(\phi)$ are

$$\rho = \frac{1}{2}\dot{\phi}^2 + V(\phi), \tag{1.69}$$

$$p = \frac{1}{2}\dot{\phi}^2 - V(\phi). \tag{1.70}$$

The Friedmann equations read $3H^2 = 8\pi G\rho$ and $\dot{H} = -4\pi G\dot{\phi}^2$. The Klein-Gordon equation is

$$\ddot{\phi} + 3H\dot{\phi} + \frac{\partial V(\phi)}{\partial \phi} = 0. \tag{1.71}$$

As long as the Universe is expanding, $\dot{a}$ is positive. The Friedmann equations can also be into

$$\frac{\ddot{a}}{a} = -4\pi G(\rho + 3p). \tag{1.72}$$

So the condition for accelerated expansion is $\rho + 3p < 0$. For

$$1/2\dot{\phi}^2 \ll V, \tag{1.73}$$

which is the first slow-roll condition, the condition $\rho + 3p < 0$ is satisfied.

If we want the first slow-roll condition to hold over an extended period, we must impose that the time derivative of this condition also holds $|\ddot{\phi}| \ll |\partial V/\partial\phi|$, which can be rewritten, by means of equation (1.71) as

$$|\ddot{\phi}| \ll 3H|\dot{\phi}|, \tag{1.74}$$

which is the second slow-roll condition.

When these two conditions hold, the Friedmann and Klein-Gordon equations become

$$3H^2 \simeq 8\pi G V(\phi), \tag{1.75}$$

$$H\dot{\phi} \simeq -\frac{1}{3}\frac{\partial V}{\partial \phi}. \tag{1.76}$$

The quantization of the scalar field ϕ, can be reduced to a harmonic oscillator. H is almost constant during inflation. This implies that the quantum fluctuations are Gaussian, as the only non-trivial information is encoded in the two-point function and they are scale invariant as H is constant [20].

1.7. Time and distance

Measuring distances in an expanding Universe has difficulties. These difficulties are simply because it is not easy to see which distance one should consider. Some obvious definitions of distances are:

- comoving distance which remains fixed as the Universe expands.
- physical distance which grows simply because of the expansion.

However, neither of these definitions is practically useful; e.g. a photon leaves a quasar at $z \sim 6$ when the scale factor was $\frac{1}{7}$ of its present value, and arrives on the earth today, when the Universe has expanded by a factor of 7. Thus the question is how one can relate the luminosity of the quasar to the observed flux.

1.7.1. Luminosity distance

A classical way of measuring distances in astronomy is to measure the flux from an object of known luminosity, a standard candle. The observed flux F at a distance d_L from a source of known luminosity L is

$$F = \frac{L}{4\pi d_L^2}. \tag{1.77}$$

However, this is in a case that the expansion has been neglected. In a flat FL Universe, the flux will be diluted.

The dilution comes from the fact that the individual photons redshift by a factor $(1+z)$ and from the time dilation effect between the emitter and the detector. Therefore we must have

$$\frac{F}{L} = \frac{1}{(1+z)^2 A}. \tag{1.78}$$

We now use equation (1.46) and consider that the physical distance between an observer at $\chi = 0$ and an object at comoving radial coordinate χ is $a(t)f(\chi_{em})$, where $f(\chi_{em})$ is a

function of the comoving distance χ_{em} from the object to the observer. Then the area A of a sphere centered at a comoving distance χ_{em} can be derived from the coefficient of $d\Omega^2$ in (1.46) and yields

$$A = 4\pi a_0^2(t) f^2(\chi_{em}), \tag{1.79}$$

we consider $a_0(t) = 1$ because the photons are being observed today. The obtained luminosity distance is

$$d_L = (1+z) f(\chi_{em}). \tag{1.80}$$

Using equations (1.39) and (1.44), on a radial null geodesic, we have

$$ds^2 = -dt^2 + a^2 d\chi^2, \tag{1.81}$$

where $ds^2 = 0$, so that

$$\chi = \int \frac{dt}{a} = \int \frac{da}{a^2 H(a)}. \tag{1.82}$$

Converting the scale factor to redshift by using $a = 1/(1+z)$ leads to

$$\chi(z) = \int_0^z \frac{dz'}{H(z')}, \tag{1.83}$$

where

$$H(z') = H_0 \sqrt{\Omega_m (1+z')^3 + \Omega_k (1+z')^2 + \Omega_\Lambda}. \tag{1.84}$$

Thus we can write the luminosity distance in terms of measurable cosmological parameters as

$$d_L = \frac{(1+z)}{H_0} \Big(\int_0^z \frac{dz'}{\sqrt{\Omega_m (1+z')^3 + \Omega_k (1+z')^2 + \Omega_\Lambda}} \Big). \tag{1.85}$$

Given the observables H_0 and Ω_i, we can calculate d_L to an object at any redshift z; conversely we can measure $d_L(z)$ for objects at a range of redshifts, and from that extract H_0 or $\Omega_{i,0}$.

1.7.2. Angular diameter distance

Another distance measurement in cosmology is to measure the angle $\delta\theta$ of an object of known physical size l, known as a standard ruler (see Fig. 1.2).

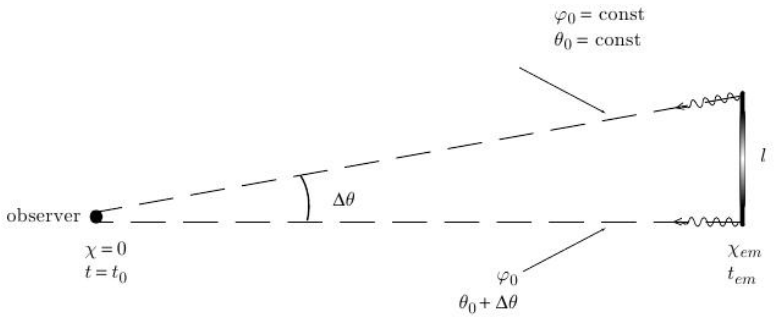

Figure 1.2. An object of a given size l at comoving distance $\chi_e m$ from an observer. The emitted photons from the observer at time t propagate along radial geodesics will arrive to the observer with an angular separation $\Delta\theta$. Figure credit: [15].

The angular diameter distance is defined as,

$$d_A = \frac{l}{\Delta\theta}, \tag{1.86}$$

where $\Delta\theta$ is small. Assume we are sitting at $\chi = 0$ of a comoving coordinate χ, and the object is at redshift z the time that the light is emitted. From the angular part of the metric, $l = a(t)f(\chi_{em})\Delta\theta$, and comparing with equation (1.86), we have the angular diameter distance as

$$d_A = af(\chi_{em}) = a\frac{d_L}{1+z}. \tag{1.87}$$

Furthermore, we can express d_A in terms of cosmological parameters, or simply in terms of luminosity distance as

$$d_A = (1+z)^{-2}d_L. \tag{1.88}$$

Let us compare two cases of a Universe with and without a cosmological constant, for a fixed H_0. Since the energy density and the expansion rate, are smaller in a Universe with a cosmological constant, both distances, d_A, d_L are larger in a such universe rather than in one without. Small H (i.e. slower expansion) on the early stages means that light had more time to travel from distant objects to us. Distant objects will therefore appear fainter in a Λ-dominated Universe than in a matter-dominated Universe today. Using this fact and using supernovae of Type Ia as standard candles lead to the Nobel prized discovery of dark energy at the end of the 1990's [3].

2. Large Scale Structure Formation

The real Universe is far from homogeneous and isotropic except on the largest scales. Fig. 2.1 shows slices through the 3D distribution of galaxy positions from the 2dF galaxy redshift survey [16] to a comoving distance of around 800 Mpc. The distribution of galaxies is not homogeneous; instead they are arranged into a cosmic web with galaxy clustering along filaments and leaving huge empty voids in between. However, if we smooth this picture on large scales to ~ 100 Mpc, it starts to look more homogeneous. Furthermore, during cosmological inflation, the initial perturbations were likely produced by quantum effects, and we know from the CMB that at the time of recombination, the Universe was smooth and fluctuations were at the level of only few parts in 10^5.

The aim of this part of the thesis is to study the growth of large-scale structure in an expanding Universe acting on small initial perturbations.

In section 2.1, we study the evolution of linear perturbations. In section 2.2, we aim to explain how the initial power spectrum of density fluctuations is processed by the evolution of the Universe, using linear perturbation theory. In section 2.3, we discuss the basic statistical properties of cosmological fields by assuming the physics of initial fluctuations. In section 2.5, we shortly review some main results of Planck. Surveys of the late time structure formation are introduced in section 2.6.

2.1. Perturbation from homogeneity

In the previous chapter, we have discussed the background solutions to the Einstein field equations assuming perfect homogeneity and isotropy. However, the real Universe is not perfectly homogeneous, and the structures have grown under the small matter perturbations since the early stages of the Universe.

In the early Universe, deviations from the homogeneous and isotropic FL background are small enough to be treated as first order perturbations. As the evolution goes on to the later time, other orders of perturbations become important and non-linear perturbation theory is needed to be taken account for transition from small scales to large scale structures. However, a full treatment of cosmological perturbation theory is beyond the scope of this chapter of the thesis.

The formalism to this subject can be found in a more details in [18, 19, 20].

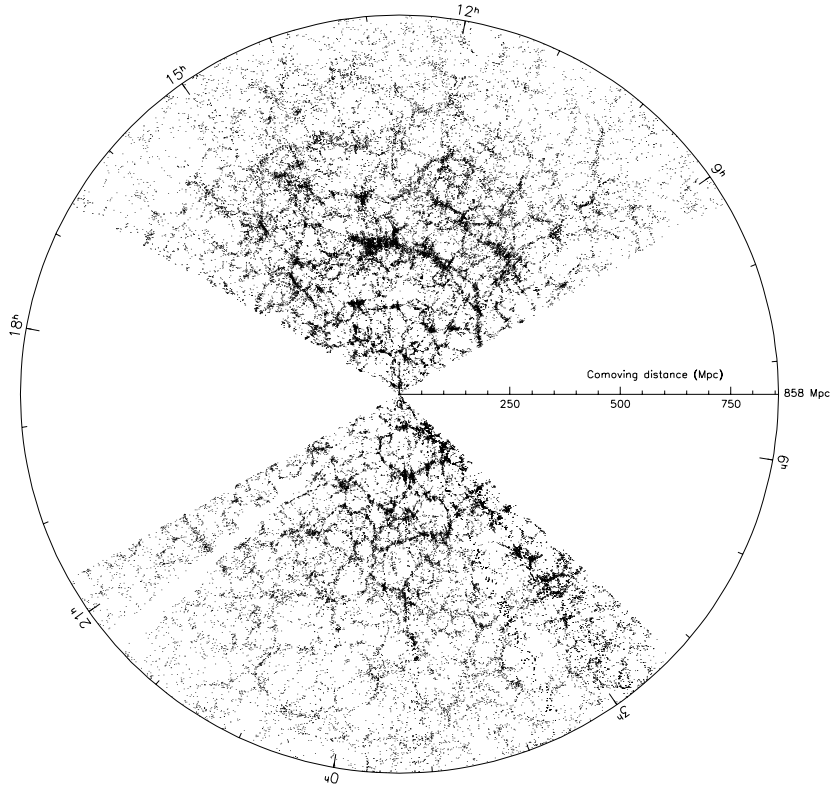

Figure 2.1. Slices through the 3D map of galaxy positions from the 2dF galaxy redshift survey. Figure credit: [17].

2.1.1. Evolution of perturbation

We account for deviations from the FL background by writing the perturbed metric as

$$g_{\mu\nu} = \bar{g}_{\mu\nu} + \delta g_{\mu\nu}, \tag{2.1}$$

where $\bar{g}_{\mu\nu}$ is the background metric and $\delta g_{\mu\nu}$ is a small perturbation. Then the Einstein equations can be written as

$$\delta R_{\mu\nu} - \frac{1}{2}\bar{g}_{\mu\nu}\delta R - \frac{1}{2}\delta g_{\mu\nu}\bar{R} = 8\pi G\delta T_{\mu\nu}, \tag{2.2}$$

where $\delta R_{\mu\nu}$, δR and $\delta T_{\mu\nu}$ denote the first order perturbations.

In this limit the Universe is homogeneous and isotropic, and its energy momentum tensor has the perfect fluid form, see equation (1.24). The energy momentum tensor continues to have the perfect fluid form and its perturbations are defined by the perturbations $\delta\rho$, δp and $\delta u^\mu = (0, v^i)$, where v^i is the three velocity of the fluid.

As it was first realized by Lifshitz in 1946, Einstein field equations yield a set of linear partial differential equations involving the metric perturbations, $\delta\rho$, δp and v^i. For the case of critical density, each perturbation can be expanded as a Fourier series. Note that the background geometry is isotropic and homogeneous, and to keep the Fourier analysis simple, we consider only the flat ($K = 0$) background case.

The following modes thus propagate independently:

- The perturbations $\delta\rho$ and δp, and the irrotational part of v^i.
- The rotational part of v^i (vorticity).
- Gravitation waves, characterized by the traceless transverse part of $\delta g_{\mu\nu}$.

Because of the spatial transformation properties of the metric components, these modes can be referred to as scalar, vector and tensor modes respectively; or more specifically, they are labeled as density, vorticity and gravitational wave modes, respectively.

Here, we are focused only on the density perturbation mode, which describes the perturbation in the density and motion of the matter and radiation in the Universe.

For a given perturbed geometry, the perturbations in the metric and the energy momentum tensor are defined when a definite coordinate choice has been made. A coordinate choice (or a set of coordinate choices) is called a gauge. For the density mode the choice of gauge has a strong influence on the appearance of the equations.

One of the widely used gauges is the synchronous gauge. This can be thought as a slicing of space-time into spatial hypersurfaces with constant time coordinate. The time coordinate is considered to be orthogonal to the hypersurfaces. Thus we have a choice of $\delta g_{oi} = 0$ and $\delta g_{00} = 1$ in equation (2.1). In the limit of early times, the solutions of the synchronous gauge equations are given with the corresponding geodesics [21].

Another important gauge is "comoving gauge". In this gauge, comoving worldline are used instead of geodesics, along with the hypersurfaces orthogonal to them, which are termed as "comoving hypersurfaces" [22].

Since we are interested only in scalar perturbations, we use the conformal Newtonian gauge (longitudinal gauge) in which the line element is

$$ds^2 = a^2(t)\Big[-(1+2\phi)dt^2 + (1-2\psi)dx^i dx^j\Big]. \tag{2.3}$$

This gauge is restricted as it does not include vector or tensor perturbations. An advantage is that ψ corresponds to the standard gravitational potential in the Newtonian limit. Also ψ and ϕ are related to the variables ϕ_A and ϕ_H of Bardeen [22]. Note that in the absence of anisotropic stresses, $\phi = \psi$ in equation (2.3).

2.2. Structure formation

In order to be able to use the framework for tracking the evolution of perturbations outlined in the previous section, we need to specify the perturbations at some initial time. The perturbations are believed to have originated as quantum fluctuation during an era of inflation. Such a mechanism yields an adiabatic Gaussian perturbation with an almost, but not precisely, scale invariant spectrum [23, 24].

The initial power spectrum of density fluctuations from inflation is called $P_i(k)$. This spectrum is processed by the evolution of the Universe, using linear perturbation theory.

The processing is quantified in terms of the transfer function

$$\delta_{\mathbf{k}}(t_0) = T(k)\delta_{\mathbf{k}}(t_i) \Rightarrow P(k) = T^2(k)P_i(k). \tag{2.4}$$

Related to this subject, in the following section we provide some basic formulas of key concepts of the power spectrum, the correlation function and the angular power spectrum, which will be needed to follow the discussion of the CMB anisotropies in section 2.4 and the Planck result in section 2.5.

2.3. Statistic of random fields

In cosmological theories, the fluctuations are treated as stochastic random variables, and theoretical predictions are made about the probability distribution functions of the perturbations. This probability distribution functions can be specified in terms of the spatial n-point correlation functions of the random fields. Thus the assumption of homogeneity and isotropy for the unperturbed Universe is replaced by the assumption of statistical homogeneity and isotropy of the perturbations.

2.3.1. Random fields in 3D Euclidean space

First of all let us consider a random field $f(\mathbf{x})$ where at each point $f(\mathbf{x})$ is some random number, and it has zero mean, $\langle f(\mathbf{x})\rangle = 0$[1]. The probability density of realizing field configuration is $P[f(\mathbf{x})]$, i.e. $\int \mathcal{D}f P[f] = 1$. Correlators of fields are expectation values of products of fields at different spatial points. Thus the two point correlator is

$$\xi(\mathbf{x},\mathbf{y}) \equiv \langle f(\mathbf{x})f(\mathbf{y})\rangle = \int \mathcal{D}f P[f] f(\mathbf{x})f(\mathbf{y}), \tag{2.5}$$

where the integral is a path integral over field configurations.

- *Statistical homogeneity* means that the statistical properties of the translated field,

$$\hat{T}_a f(\mathbf{x}) \equiv f(\mathbf{x}-\mathbf{a}), \tag{2.6}$$

[1]Note that the statistical average notation $\langle\ \rangle$ here, is different from the spatial average $\langle\ \rangle$ in chapters 3-5.

are the same as the original field, i.e. $P[f(\mathbf{x})] = P[\hat{T}_a f(\mathbf{x})]$, where $\hat{T}_a$ denotes the translation function. For the two-point correlation, this gives

$$\xi(\mathbf{x},\mathbf{y}) = \xi(\mathbf{x}-\mathbf{a},\mathbf{y}-\mathbf{a}) \Rightarrow \xi(\mathbf{x},\mathbf{y}) = \xi(\mathbf{x}-\mathbf{y}). \tag{2.7}$$

- *Statistical isotropy* means that the statistical properties of the rotated field,

$$\hat{R}f(\mathbf{x}) \equiv f(R^{-1}\mathbf{x}), \tag{2.8}$$

where R is a rotation matrix, are the same as the original field, $P[f(\mathbf{x})] = P[\hat{R}f(\mathbf{x})]$. For the two-point correlator, it gives

$$\xi(\mathbf{x},\mathbf{y}) = \xi(R^{-1}\mathbf{x}, R^{-1}\mathbf{y}). \tag{2.9}$$

Combining statistical homogeneity and isotropy gives us

$$\begin{aligned} &\xi(\mathbf{x},\mathbf{y}) = \xi(R^{-1}(\mathbf{x}-\mathbf{y})) \\ &\Rightarrow \xi(\mathbf{x},\mathbf{y}) = \xi(|\mathbf{x}-\mathbf{y}|), \end{aligned} \tag{2.10}$$

so the two-point correlator depends only on the distance modules between the two points.

To constrain the form of the correlators in Fourier space, we consider the symmetric Fourier convention, such that

$$\widetilde{f}(\mathbf{k}) = \int \frac{d^3\mathbf{x}}{(2\pi)^{3/2}} f(\mathbf{x}) e^{-i\mathbf{k}.\mathbf{x}} \quad \text{and} \quad \mathrm{f}(\mathbf{x}) = \int \frac{\mathrm{d}^3\mathbf{k}}{(2\pi)^{3/2}} \widetilde{\mathrm{f}}(\mathbf{k}) \mathrm{e}^{\mathrm{i}\mathbf{k}.\mathbf{x}}. \tag{2.11}$$

Note that $\widetilde{f}(\mathbf{k}) = \widetilde{f}^*(-\mathbf{k})$ for real fields. Under translations, the Fourier transform becomes

$$\begin{aligned} \hat{T}_a \widetilde{f}(\mathbf{k}) &= \int \frac{d^3\mathbf{x}}{(2\pi)^{3/2}} f(\mathbf{x}-\mathbf{a}) e^{-i\mathbf{k}.\mathbf{x}} \\ &= \int \frac{d^3\mathbf{x}'}{(2\pi)^{3/2}} f(\mathbf{x}') e^{-i\mathbf{k}.\mathbf{x}'} e^{-i\mathbf{k}.\mathbf{a}} \\ &= \widetilde{f}(\mathbf{k}) e^{-i\mathbf{k}.\mathbf{a}}. \end{aligned} \tag{2.12}$$

Invariance of the two-point correlator in Fourier space, this implies

$$\langle \widetilde{f}(\mathbf{k}) \widetilde{f}^*(\mathbf{k}') \rangle = \langle \widetilde{f}(\mathbf{k}) \widetilde{f}^*(\mathbf{k}') \rangle e^{-i(\mathbf{k}-\mathbf{k}').\mathbf{a}}, \tag{2.13}$$

thus we can write

$$\langle f(\mathbf{k}) f^*(\mathbf{k}') \rangle = F(\mathbf{k}) \delta(\mathbf{k}-\mathbf{k}'), \tag{2.14}$$

with $F(\mathbf{k})$ being a real function. Equation (2.13) tells us that different Fourier modes are uncorrelated, if the function f is statistically homogeneous.

Under rotations, the Fourier transform becomes

$$\begin{aligned}\hat{R}f(\mathbf{k}) &= \int \frac{d^3\mathbf{x}}{(2\pi)^{3/2}} f(R^{-1}\mathbf{x}) e^{-i\mathbf{k}.\mathbf{x}} \\ &= \int \frac{d^3\mathbf{x}}{(2\pi)^{3/2}} f(R^{-1}\mathbf{x}) e^{-i(R^{-1}\mathbf{k}).(R^{-1}\mathbf{x})} \\ &= f(R^{-1}\mathbf{k}).\end{aligned} \tag{2.15}$$

Additionally, applying invariance of the two-point correlator under rotations implies

$$\begin{aligned}\langle \hat{R}f(\mathbf{k})[\hat{R}f(\mathbf{k}')]^* \rangle &= \langle f(R^{-1}\mathbf{k}) f^*(R^{-1}\mathbf{k}') \rangle \\ &= F(R^{-1}\mathbf{k})\delta(\mathbf{k}-\mathbf{k}') \\ &= F(\mathbf{k})\delta(\mathbf{k}-\mathbf{k}'),\end{aligned} \tag{2.16}$$

where we have used $\delta(R^{-1}\mathbf{k}) = \det R\delta(\mathbf{k}) = \delta(\mathbf{k})$ here. Thus $F(\mathbf{k}) = F(k)$. Therefore the band power spectrum, $\mathcal{P}_f(k)$, of a homogeneous and isotropic field, $f(\mathbf{x})$, is defined as

$$\langle f(\mathbf{k}) f^*(\mathbf{k}') \rangle = \frac{2\pi^2}{k^3} \mathcal{P}_f(k) \delta(\mathbf{k}-\mathbf{k}'). \tag{2.17}$$

The normalization factor $2\pi^2/k^3$ in the definition of the power spectrum has been chosen for convention and will be clear from the following. The correlation function is the Fourier transform of the power spectrum:

$$\begin{aligned}\langle f(\mathbf{x}) f(\mathbf{y}) \rangle &= \int \frac{d^3\mathbf{k}}{(2\pi)^{3/2}} \frac{d^3\mathbf{k}'}{(2\pi)^{3/2}} \langle f(\mathbf{k}) f^*(\mathbf{k}') \rangle e^{i\mathbf{k}.\mathbf{x}} e^{-i\mathbf{k}'.\mathbf{y}} \\ &= \frac{1}{4\pi} \int \frac{dk}{k} \mathcal{P}_f(k) \int d\Omega_{\mathbf{k}} e^{i\mathbf{k}.(\mathbf{x}-\mathbf{y})}.\end{aligned} \tag{2.18}$$

We can evaluate the angular integral by taking $\mathbf{x}-\mathbf{y}$ along the $\mathbf{z}$-axis in Fourier space. Setting $\mathbf{k}.(\mathbf{x}-\mathbf{y}) = k|\mathbf{x}-\mathbf{y}|\mu$, the integral reduces to

$$2\pi \int_{-1}^{1} d\mu e^{ik|\mathbf{x}-\mathbf{y}|\mu} = 4\pi j_0(k|\mathbf{x}-\mathbf{y}|), \tag{2.19}$$

where $j_0(x) = \sin(x)/x$ is a spherical Bessel function of order zero. It follows that

$$\xi(\mathbf{x},\mathbf{y}) = \int_0^\infty \frac{dk}{k} \mathcal{P}_f(k) j_0(k|\mathbf{x}-\mathbf{y}|), \tag{2.20}$$

which only depends on $|\mathbf{x}-\mathbf{y}|$ as required by equation (2.10). The variance of the field is $\xi(0) = \int d\ln k \mathcal{P}_f(k)$. A scale free spectrum has $\mathcal{P}_f(k) = \mathcal{P}(k/k_0)^{n-1}$, with $n = 1$ denoting the scale-invariant case. k_0 is called the pivot scale.

2.3.2. Gaussian random fields

For a Gaussian random field, $P[f(\mathbf{x})]$ is a Gaussian functional of $f(\mathbf{x})$. The probability density function for f is specified by the correlation function:

$$\langle f_i f_j \rangle = \xi(|\mathbf{x}_i - \mathbf{x}_j|) \equiv \xi_{ij}, \tag{2.21}$$

where $f_i \equiv f(x_i)$ and

$$P(f) \propto \frac{e^{-f_i \xi_{ij}^{-1} f_j}}{\sqrt{det(\xi_{ij})}}. \tag{2.22}$$

Since $f(k)$ is linear in $f(x)$, the probability distribution for $f(k)$, i.e. $\mathcal{P}_f(k)$ is also a Gaussian field. Because different Fourier modes are uncorrelated as expressed by equation (2.13), $\widetilde{f}(k)$ and $f(\mathbf{x})$ are statistically independent for Gaussian fields. Thus for the Gaussian fields, $\mathcal{P}_f(k)$ contains all information.

Gaussian matter distributions are important in cosmology, because the initial fluctuations seem to have been Gaussian to a high degree of accuracy. Inflation predicts fluctuations that are very close to Gaussian. This property is preserved by linear evolution and observations of the CMB anisotropies which indicate that any non-Gaussianity, if present, is small.

2.3.3. Random fields on the sphere

Spherical harmonics form a basis for integrable functions on the sphere as:

$$f(\hat{n}) = \sum_{l=0}^{\infty} \sum_{m=-l}^{l} f_{lm} Y_{lm}(\hat{n}). \tag{2.23}$$

Here the Y_{lm} represents the position-space of the eigenstates of $\hat{L}^2 = -\nabla^2$ and $\hat{L}_z = -i\partial_\phi$ (from quantum mechanics)

$$\begin{aligned} \nabla^2 Y_{lm} &= -l(l+1) Y_{lm} \\ \partial_\phi Y_{lm} &= im Y_{lm}, \end{aligned} \tag{2.24}$$

with $l \geq 0$ and m and $|m| \leq l$. The spherical harmonics are orthonormal over the sphere,

$$\int d\hat{n} Y_{lm}(\hat{n}) Y^*_{lm}(\hat{n}) = \delta_{ll'} \delta_{mm'}, \tag{2.25}$$

such that the spherical multipole coefficients of $f(\hat{n})$ are

$$f_{lm} = \int d\hat{n} f(\hat{n}) Y^*_{lm}(\hat{n}). \tag{2.26}$$

For the two-point correlator, it turns out that in the case of an isotropic distribution of the real function $f(\hat{n})$, we have

$$\langle f_{lm} f^*_{l'm'} \rangle = C_l \delta_{ll'} \delta_{mm'}, \tag{2.27}$$

where C_l is the angular power spectrum of f, and

$$\begin{aligned} \langle f(\hat{n}) f(\hat{n}') \rangle &= \sum_{lm} \sum_{l'm'} \underbrace{\langle f_{lm} f^*_{l'm'} \rangle}_{C_l \delta_{ll'} \delta_{mm'}} Y_{lm}(\hat{n}) Y^*_{l'm'}(\hat{n}') \\ &= \sum_l C_l \underbrace{\sum_m Y_{lm}(\hat{n}) Y^*_{lm}(\hat{n}')}_{\frac{2l+1}{4\pi} P_l(\hat{n}.\hat{n}')} = C(\theta), \end{aligned} \tag{2.28}$$

where $\hat{n}.\hat{n}' = \cos\theta$. Here an addition theorem for spherical harmonics to express the sum of products of the Y_{lm} in terms of the Legendre polynomials $P_l(x)$ has been used. It follows that the two-point correlation function depends only on the angle between the two points, as required by statistical isotropy. The variance of the field is

$$C(0) = \sum_l \frac{2l+1}{4\pi} C_l \approx \int d(\ln l) \frac{l(l+1)C_l}{2\pi}. \tag{2.29}$$

It is conventional to plot $l(l+1)C_l/(2\pi)$ which we see is the contribution to the variance per log range in l and is called the angular band power. Finally we note that we can invert the correlation function to get the power spectrum by using orthogonality of the Legendre polynomials:

$$C_l = 2\pi \int_{-1}^{1} d(\cos\theta) C(\theta) \mathcal{P}_l(\cos\theta). \tag{2.30}$$

2.4. CMB anisotropies

Most of the background photons in the Universe are Cosmic Microwave Background photons. Their spectral distribution is in excellent agreement with the Planck spectrum of a black body at a temperature of 2.7255 ± 0.0006K [25]. This is in good correspondence with the prediction of Big Bang model of the Universe.

In the early universe, baryons and photons were strongly coupled by Thomson scattering of photons, where the temperature of the Universe became less than 3000K, the cosmic plasma recombined and the ionization rate x_e fell from 1 at $z > 1100$ down to $x_e < 10^{-3}$ at $z < 1100$. Consequently, the Universe became transparent to the background photons and these photons were propagating freely through the Universe. After that, only a small fraction of the electron density could be re-scattered. Therefore today we observe a thin shell of last scattering around us. From this last scattering surface, we know that the majority of photons have been interacting with baryons at a redshift of 1100, when the Universe was 380000 years old.

The temperature of the CMB is not exactly the same in all directions (i.e. it is anisotropic). An observed fractional deviation in temperature $\Delta T/T$ is only of order of $\sim 10^{-5}$. However, the temperature anisotropies $\Delta T(\hat{n}) \equiv T(\hat{n}) - T_0$ provide important information about the nature of primordial perturbations and the content of the Universe at late times [2].

The CMB temperature anisotropy is a function over a sphere. So the temperature anisotropy in direction of $\hat{n}$ in terms of spherical harmonics $Y_{lm}(\hat{n})$ is

$$\frac{\Delta T(\hat{n})}{T_0} = \sum_{lm} a_{lm} Y_{lm}(\hat{n}), \tag{2.31}$$

where the sum runs over $l = 1, 2, ...\infty$ and $m = -l, ..., l$, giving $2l + 1$ values of m for each l. The multipole coefficients a_{lm} are

$$a_{lm} = \int Y^*_{lm} \frac{\Delta T}{T_0} d\hat{n}. \tag{2.32}$$

Summing over the m corresponding to the same multipole number l in equation (2.25) we have

$$\sum_m |Y_{lm}|^2 = \frac{2l+1}{4\pi} P_l. \tag{2.33}$$

We also need the expansion of a plane wave in terms of spherical harmonics,

$$e^{i\mathbf{k}.\mathbf{x}} = 4\pi \sum_{lm} i^l j_l(kx) Y_{lm}(\hat{\mathbf{x}}) Y^*_{lm}(\hat{\mathbf{k}}), \tag{2.34}$$

where $\hat{\mathbf{x}}$ and $\hat{\mathbf{k}}$ are the unit vectors in the direction of $\mathbf{x}$ and $\mathbf{k}$, and j_l is the spherical Bessel function.

The CMB anisotropy is due to the primordial perturbation, hence it has a Gaussian nature. The a_{lm} are also Gaussian random variables. In theory we define the angular power spectrum, C_l as

$$C_l \equiv \langle |a_{lm}|^2 \rangle = \frac{1}{2l+1} \sum_m \langle |a^2_{lm}| \rangle. \tag{2.35}$$

Similar to equation (2.27), we have the relation $\langle a_{lm} a^*_{l'm'} \rangle = \delta_{ll'} \delta_{mm'} C_l$. The function C_l is analogous to $P(f)$ of Gaussian perturbations. C_l contains all the statistical information

[2] Also the velocity of the observer with respect to the Universe produces a dipole anisotropy with $\Delta T/T = v/c$ by the Doppler shift. The observed dipole indicates that the Solar System has speed $3.68 \times 10^5\ m/s^{-1}$ relative to the last scattering surface. The dipole is usually removed from the CMB map before analyzing it.

about the CMB temperature anisotropy. From equation (2.28) we can write

$$\begin{aligned}\Big\langle (\frac{\Delta T}{T})^2 \Big\rangle &= \Big\langle \sum_{lm} a_{lm} Y_{lm} \sum_{l'm'} a^*_{l'm'} Y^*_{l'm'} \Big\rangle \\ &= \sum_{ll'} \sum_{mm'} Y_{lm} Y_{l'm'} \langle a_{lm} a^*_{l'm'} \rangle \\ &= \sum_{l} C_l \sum_{m} |Y_{lm}|^2 \\ &= \sum_{l=1}^{\infty} C_l \Big(\frac{2l+1}{4\pi}\Big) \mathcal{P}_l.\end{aligned} \tag{2.36}$$

Although the expectation values, $\langle |a_{lm}|^2 \rangle$, from the random process is predicted in theory, we can observe only one realization of this random process. The observed angular power spectrum is the average of the observed values

$$C_l^{obs} = \frac{1}{2l+1} \sum_m |a_{lm}|^2. \tag{2.37}$$

Therefore, the variance of the observed temperature anisotropy is the average of $\Big(\Delta T/T\Big)^2$ over the celestial sphere,

$$\begin{aligned}\frac{1}{4\pi} \int \Big[\frac{\Delta T}{T}\Big]^2 d^2\hat{n} d^2\hat{n}' &= \frac{1}{4\pi} \int d^2\hat{n} d^2\hat{n}' \sum_{lm} a_{lm} Y_{lm} \sum_{l'm'} a^*_{l'm'} Y^*_{l'm'} \\ &= \frac{1}{4\pi} \sum_{lm} \sum_{l'm'} a_{lm} a^*_{l'm'} \int d^2\hat{n} d^2\hat{n}' Y_{lm} Y^*_{l'm'} \\ &= \sum_{l} C_l^{obs} \Big(\frac{2l+1}{4\pi}\Big) \mathcal{P}_l.\end{aligned} \tag{2.38}$$

The expectation value of the observed spectrum, C_l^{obs}, is equal to C_l, i.e. $\langle C_l^{obs} \rangle = C_l$. The expected squared difference between C_l^{obs} and C_l is called the cosmic variance.

For adiabatic initial perturbations, the initial conditions can be specified in terms of the potential ϕ in the conformal Newtonian gauge.

The gravitational redshift of photons and the change in the rate of expansion of the Universe (both due to ϕ) cause the well known Sachs-Wolfe effect (SW) [26]. This shifts the value of the redshift at which the Universe reaches the decoupling temperature $\sim 3000K$. The total effect is (see for example [27] for the detailed calculation)

$$\Big(\frac{\Delta T(\hat{n})}{T}\Big) = \frac{1}{3}\phi + 2\int \dot{\phi} dt. \tag{2.39}$$

The first part, $\frac{1}{3}\phi$ is called the Sachs-Wolfe effect, and the second part, $2\int \phi dt$, the integrated Sachs-Wolfe effect (ISW), since it evolves integrating along the line of sight.

As mentioned before, the CMB photons have travelled freely since last scattering, only redshifing due to the expansion of the Universe. Thus the anisotropies that we observed today arise from the following sources:

- Temperature fluctuations in the photon-baryon plasma at the time of last scattering at $z \sim 1100$.
- The Doppler effect of bulk velocities of the photon-baryon plasma at the last scattering.
- The gravitational redshift of photons due to fluctuations in the gravitational potential ϕ at last scattering i.e. SW effect.
- The gravitational redshift of photons due to time dependent fluctuations in ϕ along the line of sight between the last scattering surface and us, known as Integrated Sachs-Wolfe effect (ISW) (see [26] for more details).

2.5. CMB observations from Planck

In this part we discuss some aspects of the Planck project, as announced on March, 2013. This project is a very precise measurement of the temperature anisotropies of the Cosmic Microwave Background (CMB).

In the following sections, we describe some of the steps to obtain the results. Some of the relevant data from full sky maps at 9 different frequencies are also explained.

2.5.1. Pre-Planck CMB experiments

In the early Universe, quantum fluctuations generated the seeds for giving rise to the large scale structure (LSS) which we see today. The evolution of primordial fluctuations can be accurately followed. In order to account for the formation of large scale structure, their imprint as temperature fluctuations should have an rms of $\sim 10^{-4}$K in the presence of cold dark matter. Because of the smallness of these fluctuations it took long time to first detect them. The angular power spectrum C_l from spherical harmonics (see section 2.3), or the angular correlation function from temperature contrast δ_T is needed to be compute, in order to analyze the statistical properties.

The first detection of the CMB anisotropies was made by the DMR instrument in a satellite called Cosmic Background Explorer (COBE) in 1992 [28, 29]. COBE was orbiting the earth, with a ten degree beam and a signal to noise per resolution element around unity. This detection was done for the large scale, low frequency, Sachs-Wolf effect at low multipole. The first acoustic peak of the spectrum was drafted by 1999. Later on, many other aspects of inflationary cosmology were probed by several ground and balloon experiments.

The later detection result of nine years of operation was done by a space experiment, Wilkinson Microwave and Anisotropy Probe (WMAP) and its findings were released in 2012 [30, 31]. (For more detailed explanations about CMB experiments before Planck, see [32]).

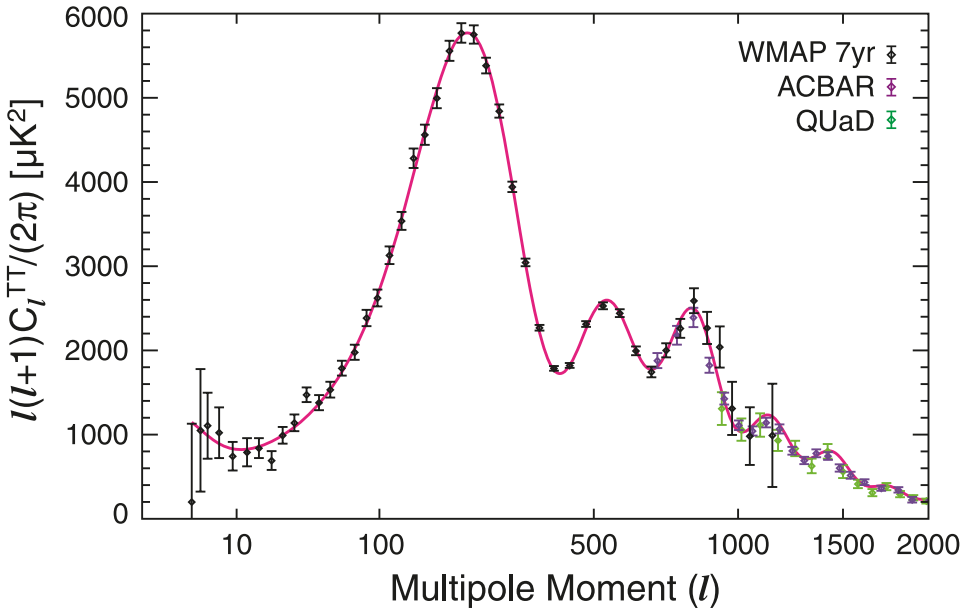

Figure 2.2. Angular power spectrum of the primordial fluctuations of the CMB temperature field. The angular power is given in terms of the magnitude of the coefficients C_l in the expansion of the two-point correlation function into spherical harmonics. Figure Credit: WMAP7 [1].

Until the release of the data from the Planck Satellite, the best measurement of the cosmic microwave background at large scales was from the WMAP. The angular power spectrum of the temperature field is shown in Fig. 2.2. Arcminute Cosmology Bolometer Array Receiver (ACBAR) and QUEST at DASI (QUaD), in this figure, are two South Pole based CMB experiments.

The fit of the theoretical curve in Fig. 2.2 to the measured data was already very precised and the measurement of the temperature correlations had a high accuracy.

2.5.2. The Planck mission

The Planck project was selected by the European Space Agency (ESA) in March 1996, contemporary with WMAP which was selected by NASA. The Planck satellite was launched on May 2009, and the first results were released on March 2013.

The goals of the Planck experiment include a coverage of the full sky and a good angular resolution in order to access all scales on which that CMB anisotropies contain cosmological information. This also includes a coverage of a large frequency range to be able to remove the astrophysical foreground contributions. These tasks require to map the full sky at 9 frequencies from 30 GHz to 1 THz, to determine the CMB properties (see Fig. 2.3).

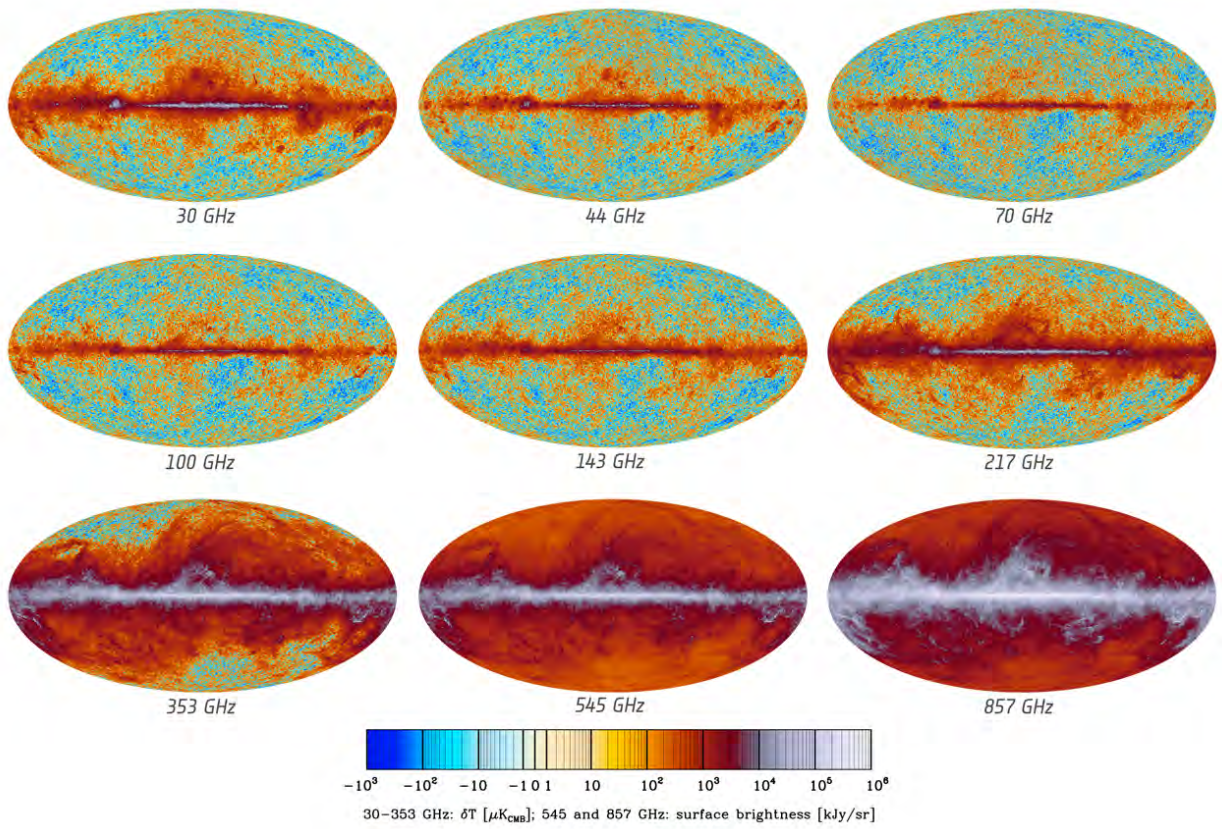

Figure 2.3. Nine sky maps of combination of coverage, sensitivity, resolution and accuracy from Planck data. Figure Credit: [2].

In order to achieve the high resolution and sensitivity in each frequency band, the Planck team proposed the High Frequency Instrument (HFI) [33, 34]. 52 detectors were used in the HFI instrument, surrounded by the 11 larger detectors from the Low Frequency Instrument (LFI) [35, 36]. The LFI detectors cover three bands at 30, 40 and 70 GHz.

One of the contribution in the detector data is from the Solar dipole which is referred to cosmological dipole and is induced by the motion of the Solar system through the CMB. Another contribution comes from the orbital dipole induced by the motion of the satellite within the Solar system. This is not constant on the sky and must be removed before creating the sky map. The Solar dipole is used as a calibration source at lower HFI and all LFI frequencies. The dipoles are computed in the non-relativistic approximation.

Furthermore, the multiplicative effect on the angular power spectrum is encoded in the effective beam window function [37] which includes the appropriate weights of each multipole for analyzing maps across detector sets or frequencies. Fig. 2.4 displays an example of positional variation of the effective beam at 100 GHz.

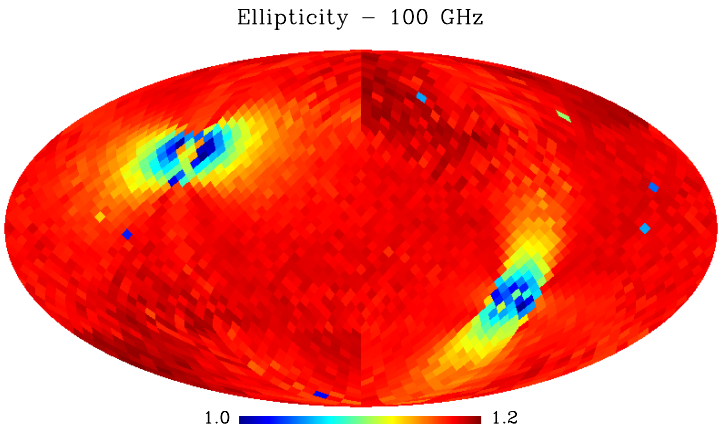

Figure 2.4. The best Gaussian fit of the 100 GHz effective beam across the sky in Galactic coordinates. Figure Credit: [2].

2.5.3. CMB maps

In order to clean the background CMB map from foreground emissions, Planck has used four different approaches which combine the various frequency maps differently.

The first approach is a parameterized model approach in pixel space. This was used to obtain Galactic foregrounds maps.

For CMB non-Gaussianity studies, a harmonic space approach, called SMICA has been used to generate the CMB map.

The third approach called NILC allows checking the benefits of spatial localization.

And finally a spatial template based approach, SEVEM, allows producing different CMB maps.

Each different approach produces a CMB map, a so-called mask i.e. confidence map and and a noise estimate map.

The analyses are based on model fitting firstly by a Bayesian parameter fitting approach which works in the pixel domain. This can be done by fitting a parameterized model of the CMB and the foreground contribution to the data. This model fitting has been used for frequencies from 30 to 353 GHz.

The second model fitting approach is SMICA, which performs spectral matching in the harmonic domain. In this sense the CMB model and noise contributions can be fit to the auto-spectra and cross-spectra of the maps from 30 to 857 GHz.

NILC stands for internal linear combination (ILC) working in wavelet (needlet) domain. This makes an internal linear combination at each wavelet independently. This has been used for frequencies from 44 to 857 GHz.

SEVEM is based on minimizing the variance of the CMB component by template fitting. The templates are used to clean the 143 and 217 GHz maps.

Based on the simulation performance, the SMICA map has been selected for the high resolution CMB map, which has minimized the sum of noise and foreground residuals at

each scale (Fig. 2.5).

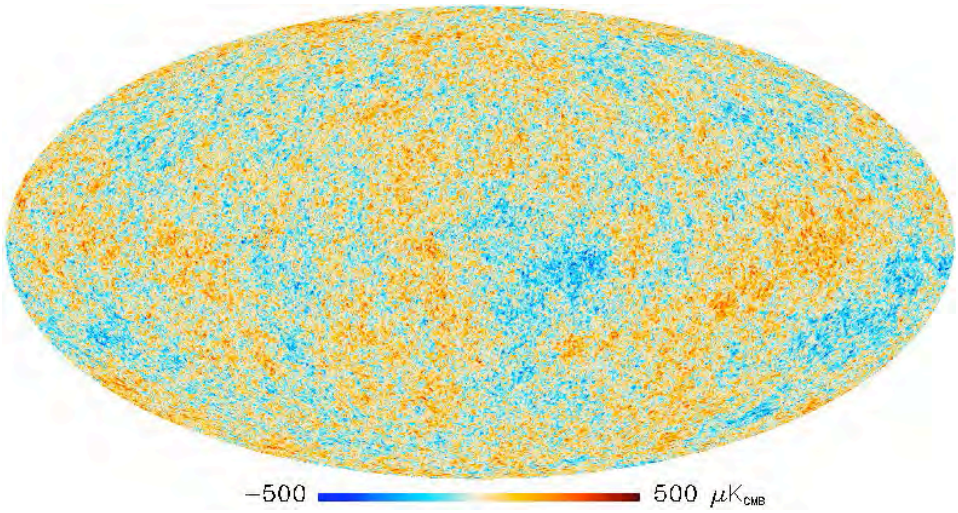

Figure 2.5. Planck CMB map by SMICA. Figure Credit: [2].

2.5.4. CMB spectra and likelihood

Planck uses a pixel-based maximum likelihood approach to map the CMB sky. This is a straightforward approach to check whether a given theoretical angular power spectrum C_l is a good match to the Planck determination of the CMB spatial distribution. Details of the approach are explained in [38].

The full Planck CMB likelihood is given by the product of the low frequency pixel-based likelihood and of the high frequency pixel-based, with a transition at $l = 50$. The resulting foreground-subtracted temperature power spectrum is displayed in Fig. 2.6. The power spectrum at low multipoles i.e. $l = 2 - 49$ is plotted on a logarithmic multipole scale in Fig. 2.6. Multipoles at $50 \leq l \leq 2500$ plotted on a linear multipole scale which shows the best fit CMB spectrum. The blue points show averages in bands of width $\Delta l \approx 31$ with 1σ errors. The red line shows the temperature spectrum for the best fit based on ΛCDM model. The green lines in the lower panel shows the $\pm 1\sigma$ errors on the power spectrum estimates at high multipoles.

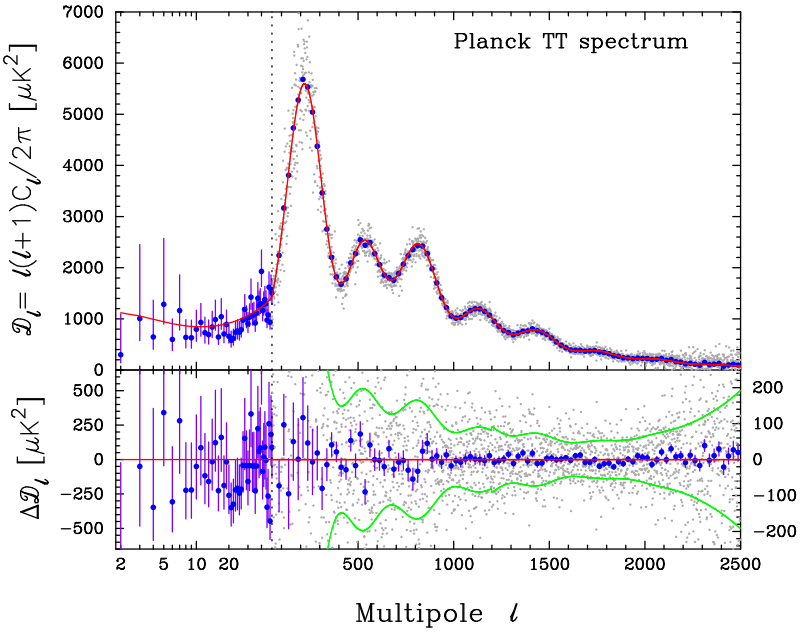

Figure 2.6. Planck foreground subtracted temperature power spectrum with foreground parameters fixed to their best fit values for the standard ΛCDM model. Figure Credit : [14].

2.5.5. CMB lensing spectrum

The large scale structures of the Universe between us and CMB last scattering surface induce small but coherent deflections of the observed CMB temperature and polarization anisotropies [39]. These so-called gravitational lensing effects blur the acoustic peaks [40] and generate non-Gaussianity [41]. It also convert a portion of the E-mode polarization to B-mode [42].

Some methods to calculate the effects of lensing on the CMB power spectrum have been investigated in [43]. Also some optimal estimators for the distinct statistical signatures of lensing exist [44].

The resulting spectrum of individual 143 and 217 GHz reconstructions and their minimum variance combination is shown in Fig. 2.7. They are in good agreement with the best fit ΛCDM model, and with the determination from ACT (Atacama Cosmology Telescope [45] and SPT (South Pole Telescope) [46].

The use of the lensing map and cross correlations with the ISW effect and other probes has been further explained in [47].

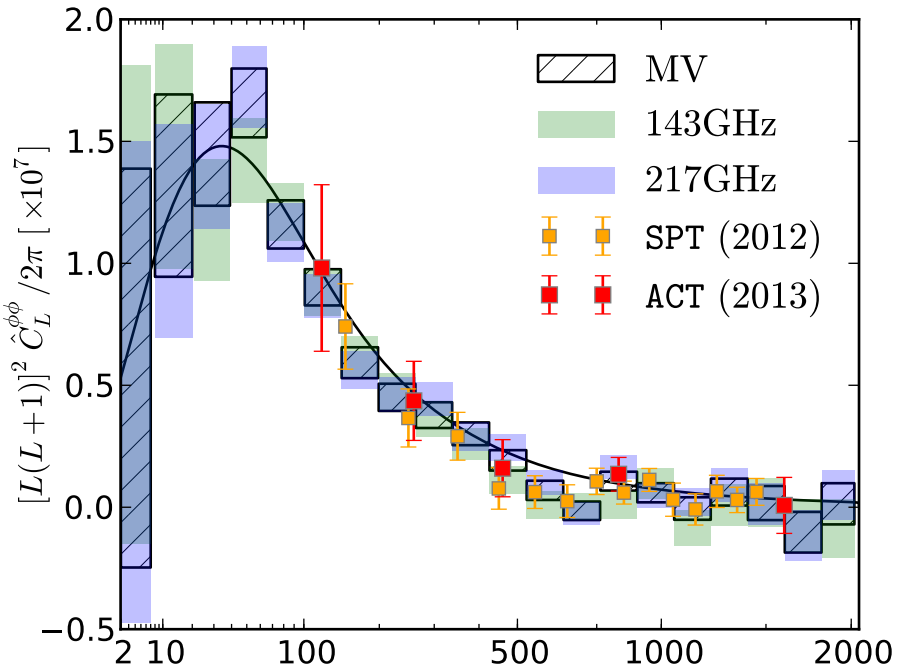

Figure 2.7. Planck measurement of the lensing power spectrum compared to the prediction for the best fitting Planck+WMAP+ΛCDM model parameters, and to the SPT and ACT bandpowers. All three experiments are consistent between them and with the ΛCDM predictions. Figure Credit: [47].

2.5.6. The cosmological consequences

By using the Planck likelihood on temperature and lensing, we find a good match with the standard ΛCDM model with a minimal set of cosmological parameters i.e. $\omega_b, \omega_c, \theta, \tau, n_s, A_s$. The Planck cosmological parameters are explained in Table 2.2. The detailed description can be found in [14].

Fig. 2.8 shows the constraints on pair of these parameters. This also allows comparing their posterior marginals, in case of using Planck alone (CMB+lensing, in color coded samples), or adding WMAP polarization information (red contours) where both of which are more precise than the WMAP-9 alone constraints (grey contours).

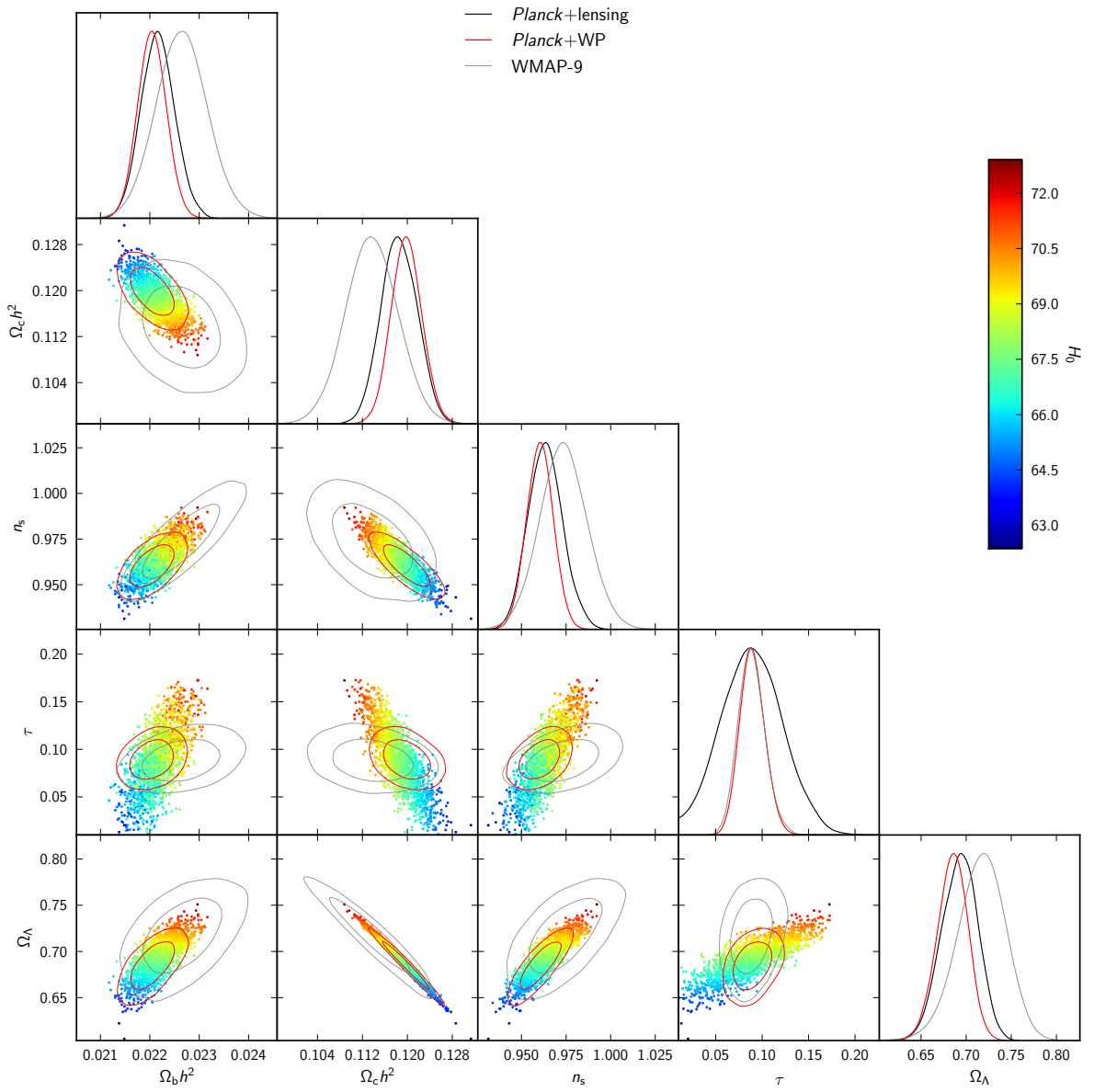

Figure 2.8. Comparison of the standard ΛCDM model parameters for Planck+lensing only (color code samples), and the 68% and 98% constraint contours adding WMAP low-l polarization (red contours), compared to WMAP-9 (grey contours). Figure Credit: [14].

The Planck (CMP+lensing) constraints on the standard ΛCDM model are displayed in Table. 2.1. It is worth noting that the 68% limit on the power law index of the scalar spectrum n_s, by Planck alone is 0.9635 ± 0.0094 (i.e. 0.9% accuracy), this means that the exact scale invariance is excluded at the 3.9σ level. One should also note that Planck leads to a low value of $H_0 = 67.9 \pm 1.5 \mathrm{km\,s^{-1}\,Mpc^{-1}}$, a matter density $\Omega_m = 0.307 \pm 0.019$

and an Universe with an age of $13.796 \pm 0.058\,Gyr$ which is also fully consistent with BBN constraints, but in tension with local determinations of H_0, which forms values of $H_0 = 72.7 \pm 2.0$ km s^{-1} Mpc [3, 141].

In other words, within the standard ΛCDM context, the Planck CMB fit is completely compatible with BAO data, and shows some tension with some of the measurements of H_0 and Ω_m from low redshift measurements. Note that BAO stands for Baryon Acoustic Oscillation, which are the analogue to the wiggles in the CMB power. They form when the over-density in the baryons from the initial sound waves are distributed in the whole matter distribution [5].

	Planck (CMB+lensing)		*Planck*+WP+highL+BAO	
Parameter	Best fit	68 % limits	Best fit	68 % limits
$\Omega_b h^2$	0.022242	0.02217 ± 0.00033	0.022161	0.02214 ± 0.00024
$\Omega_c h^2$	0.11805	0.1186 ± 0.0031	0.11889	0.1187 ± 0.0017
$100\theta_{MC}$	1.04150	1.04141 ± 0.00067	1.04148	1.04147 ± 0.00056
τ	0.0949	0.089 ± 0.032	0.0952	0.092 ± 0.013
n_s	0.9675	0.9635 ± 0.0094	0.9611	0.9608 ± 0.0054
$\ln(10^{10} A_s)$	3.098	3.085 ± 0.057	3.0973	3.091 ± 0.025
Ω_Λ	0.6964	0.693 ± 0.019	0.6914	0.692 ± 0.010
σ_8	0.8285	0.823 ± 0.018	0.8288	0.826 ± 0.012
z_{re}	11.45	$10.8^{+3.1}_{-2.5}$	11.52	11.3 ± 1.1
H_0	68.14	67.9 ± 1.5	67.77	67.80 ± 0.77
Age/Gyr	13.784	13.796 ± 0.058	13.7965	13.798 ± 0.037
$100\theta_*$	1.04164	1.04156 ± 0.00066	1.04163	1.04162 ± 0.00056
r_{drag}	147.74	147.70 ± 0.63	147.611	147.68 ± 0.45

Table 2.1. Cosmological parameter values for the Planck-only best-fit 6-parameter ΛCDM model (Planck temperature data plus lensing) and for the Planck best-fit cosmology including external data sets (Planck temperature data, lensing, WMAP polarization [WMAP] at low multipoles, high frequency experiments, and BAO, labelled [Planck+WMAP+high-l+BAO]). The six fitted parameters are above the line; those below are derived. Table from [14].

Table. 2.3 illustrates the Planck status of some extensions to the standard ΛCDM model. This has been done regarding single parameter extensions. The current table also exhibits the constraints from Planck+WMAP alone when either BAO or high frequency CMB information, or both are added. When not specified, the numbers in the text below are 95% confidence level from the joint constraints from Planck+WMAP+High-l+BAO.

Parameter	Definition
$\omega_b \equiv \Omega_b h^2$	Baryon density parameter today
$\omega_c \equiv \Omega_c h^2$	Cold dark matter density parameter today
Ω_K	Curvature parameter today with $\Omega_{\rm tot} = 1 - \Omega_K$
Ω_Λ	Dark energy density parameter today
Ω_m	Matter density today divided by the critical density
z_*	Redshift for which the optical depth equals unity
$r_* = r_s(z_*)$	Comoving size of the sound horizon at $z = z_*$
$100\theta_{\rm MC}$	100× approximation to r_*/D_A
$100\theta_*$	100× angular size of sound horizon at $z = z_*(r_*/D_A)$
τ	Thomson scattering optical depth due to reionization
n_s	Scalar spectrum power-law index (spectral index)
A_s	Amplitude of primordial scalar perturbations
$\ln(10^{10}A_s)$	Log power of the primordial curvature perturbations
σ_8	RMS matter fluctuations today in linear theory
$z_{\rm re}$	Redshift at which Universe is half reionized
H_0	Current expansion rate in km s^{-1}Mpc^{-1}
$z_{\rm drag}$	Redshift at which baryon-drag optical depth equals unity
$r_{\rm drag} = r_s(z_{\rm drag})$	Comoving size of the sound horizon at $z = z_{\rm drag}$
w	Dark energy equation of state parameter
$\sum m_\nu$	The sum of neutrino masses in eV
$N_{\rm eff}$	Effective number of neutrino-like degrees of freedom
$Y_{\rm P}$	Fraction of baryonic mass in helium
$dn_s/d\ln k$	Scale dependence of the spectral index
$r_{0.002}$	Ratio of tensor primordial power to curvature power

Table 2.2. Explanation of cosmological parameters from Planck analysis, used in Fig. 2.8 and tables 2.1 and 2.3. Table re-provided from [14].

Fig. 2.9 allows comparing the constraints in the $n_s - r$ plane with predictions from a number of common inflation models. The figure shows that concave potentials are preferred, with both $\dot{\phi}^2$ and $\dot{\phi}^2/\rho$ increasing during slow-roll inflation. Main analyses and results of this context is presented in [48].

Parameter	*Planck*+WP		*Planck*+WP+BAO		*Planck*+WP+highL		*Planck*+WP+highL+BAO	
	Best fit	95% limits	Best fit	95% limits	Best fit	95% limits	Best fit	95% limits
Ω_k	− 0.0105	$-0.037^{+0.043}_{-0.049}$	0.0000	$0.0000^{+0.0066}_{-0.0067}$	− 0.0111	$-0.042^{+0.043}_{-0.048}$	0.0009	$-0.0005^{+0.0065}_{-0.0066}$
w	−1.20	$-1.49^{+0.65}_{-0.57}$	−1.076	$-1.13^{+0.24}_{-0.25}$	−1.20	$-1.51^{+0.62}_{-0.53}$	−1.109	$-1.13^{+0.23}_{-0.25}$
Σm_ν [eV]	0.022	< 0.933	0.002	< 0.247	0.023	< 0.663	0.000	< 0.230
$N_{\rm eff}$	3.08	$3.51^{+0.80}_{-0.74}$	3.08	$3.40^{+0.59}_{-0.57}$	3.23	$3.36^{+0.68}_{-0.64}$	3.22	$3.30^{+0.54}_{-0.51}$
$Y_{\rm P}$	0.2583	$0.283^{+0.045}_{-0.048}$	0.2736	$0.283^{+0.043}_{-0.045}$	0.2612	$0.266^{+0.040}_{-0.042}$	0.2615	$0.267^{+0.038}_{-0.040}$
$dn_s/d\ln k$	−0.0090	$-0.013^{+0.018}_{-0.018}$	−0.0102	$-0.013^{+0.018}_{-0.018}$	−0.010(	$-0.015^{+0.017}_{-0.017}$	−0.0103	$-0.014^{+0.016}_{-0.017}$
$r_{0.002}$	0.000	< 0.120	0.000	< 0.122	0.000	< 0.108	0.000	< 0.111

Table 2.3. Constraints on one-parameter extensions to the base ΛCDM model. Table from [14].

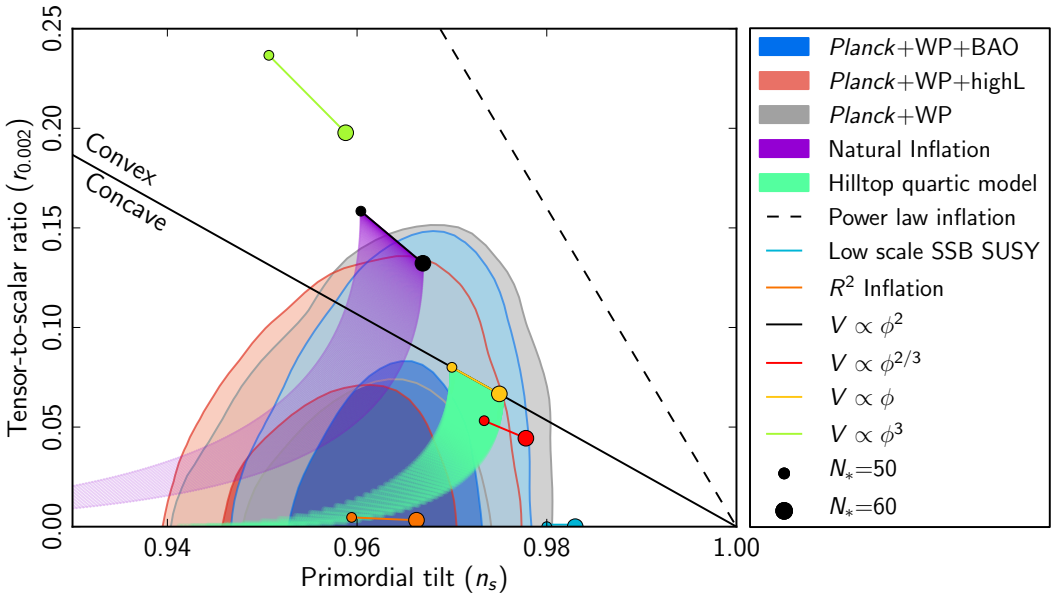

Figure 2.9. Marginalized 68% and 95% confidence levels for n_s (the scalar spectral index of primordial fluctuations) and $r_{0.002}$ (the tensor to scalar power ratio at the pivot scale $k = 0.002$ Mpc^{-1}) from Planck+WMAP, alone and combined with high frequency and BAO data, compared to the theoretical predictions of selected inflationary models. Figure Credit: [48].

Planck in [48] provided the constraints when $r_{0.002}$ and other extensions ($N_{eff}, Y_{\rm P}, w, m_\nu$) were allowed to vary for various data combination. Introducing N_f and $Y_{\rm P}$ shift the preferred value of n_s to higher values and weak the exclusion of the $n_s = 1$ to only two sigma. Because of uncertainties from the end of inflation to the end of entropy generation,

Planck explored a number of scenarios to see how $n_s - r$ constraints can be modified. First they searched for features by performing a reconstruction of the primordial scalar spectrum or of the best fitting inflation potential.

Concerning these results, we find that the standard ΛCDM model with 6 cosmological parameters is in a good match with Planck temperature spectra with parameters $(n_s, \Omega_b, \Omega_c, \theta)$ with the remaining (A_s, τ) reduced by adding the large scale polarization constraint from WMAP.

The standard ΛCDM model is fully consistent with CMB lensing and polarization power spectra observations from Planck.

Considering CMB from Planck+WMAP polarization+ACT and SPT+BAO constraints, exact scale invariance is excluded at $\sim 7\sigma$.

The single field slow-roll inflation model survived the tests of Gaussianity performed to data.

2.6. Experiments on large scale homogeneity

Large scale structure surveys determine the distribution of galaxies and question the homogeneity at different scales. In contrast to the measurement of the initial conditions of structure formation, by looking at the CMB, these experiments are applied to the late times of the Universe. The known large scale structure surveys are the 2dF survey [16], the Sloan Digital Sky Survey (SDSS) [49], the WiggleZ survey [50] and the Baryon Oscillation Spectroscopic Survey (BOSS) [51].

The analysis of an estimation of the two-point correlation function from the seventh data release of the SDSS project has been done in [52] The comparison with the ΛCDM model correlation function shows good agreement on small and intermediate scales. Besides the estimation of the correlation function, one can also determine the power spectrum of the fluctuations from the data [53]. The result is shown in Fig. 2.10.

Baryon acoustic oscillations act as standard ruler for the determination of the angular diameter distance. They can also be probed in all epochs of the Universe by measuring the matter correlation function at the respective time. Existence of the BAO has first been detected in [5]. Later on, the corresponding data from SDSS as it is shown in Fig. 2.10 made a strong confirmation for their existence. They have also been found in the WiggleZ [50] and in the BOSS [51] data. In [54] it has been explained how their existence make strong constraints on deviations of the distance redshift relation from the ΛCDM prediction.

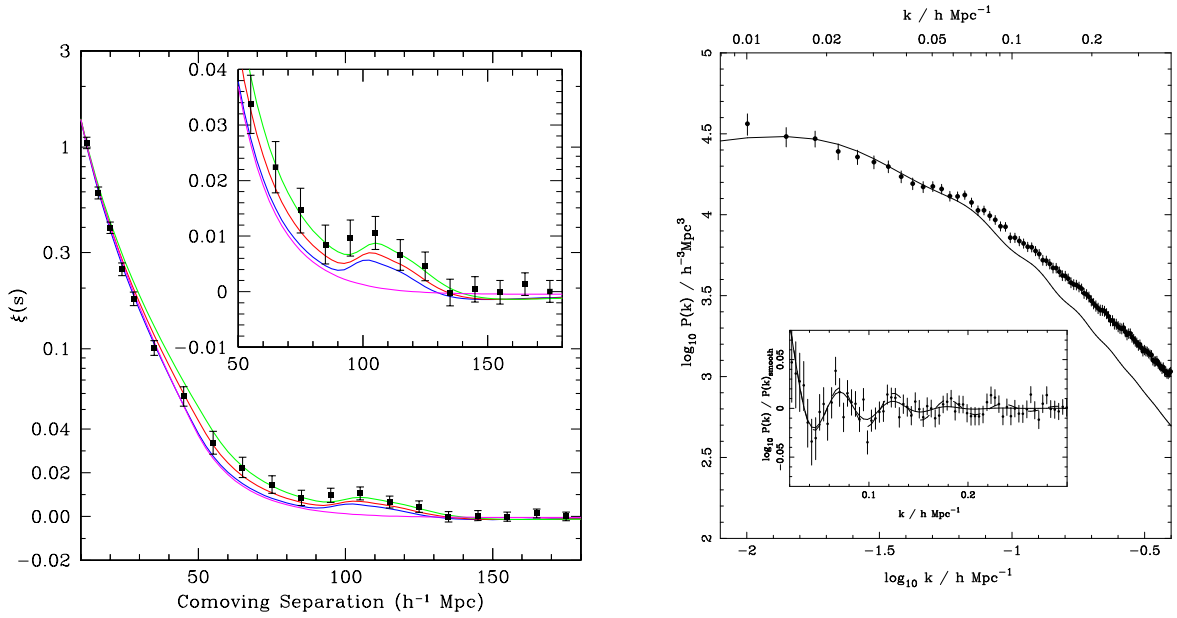

Figure 2.10. Measurements of the BAO in the SDSS DR5 galaxy data. The first detection of the BAO peak by using the correlation function is shown in the left plot, and by using the estimation of the power spectrum is shown in the right one. Figure Credit: The left plot from [5] and the right one from [53].

3. Averaging Problem in Cosmology

The reader might have skipped reviewing the basic knowledge which has been explained in the first two chapters of this thesis. In order to proceed the problem of averaging in cosmology, here we shortly point out some of the topics of interest from the previous chapters, in section 3.1. Then we open up the discussion of averaging problem in section 3.2. The history of studying this subject is presented in section 3.3. To make progress in solving this problem, it is first essential to have a reliable averaging scheme at hand. We therefore highlight two of the most important directions of dealing with the mentioned problem. First, the spatial scalar averaging approach of Buchert in sections 3.4 and 3.5 and the recent attempt of Skarke in 3.6. Finally the second direction, which is a fully tensorial averaging approach, introduced by Zalaletdinov, is explained in section 3.7.

3.1. Introduction

Einstein's theory of general relativity is the most accepted fundamental theory of gravity, and its application to cosmology has been studied by many, including Einstein himself, deSitter, Lemaître, Friedmann, etc.

A simple model of the Universe is described by the homogeneous and isotropic geometry, characteristic for the Friedmann-Lemaître (FL) model with the so-called Robertson-Walker (RW) metric. Describing the FL space-time by the ΛCDM model of the Universe (or as it is called the *concordance model*) is the highly successful attempt to fit a large amount of cosmological observations. The hot Big Bang theory tells us that the Universe was very hot and dense at early times and cooled as it expanded, with tiny fluctuations in the era of recombination that have grown to form structures such as galaxies today.

A central assumption in the standard model of cosmology is that the Universe on large scales is homogeneous and isotropic [19]. But the real Universe on the small scales is neither homogeneous nor isotropic; we see a rich variety of structure around us from galaxies to clusters of galaxies and even larger structures in different directions [55].

In the previous chapter, we discussed the so-called *cosmic structure*. In the following items we only briefly review some aspects of that to address the importance of inhomogeneity and anisotropy.

- The CMB anisotropies is one of the most central topic of cosmology. These anisotropies have primordial origin, and they are generated in the early Universe i.e. at the epoch of recombination. The COBE [28], WMAP [1] and recently Planck [2]

collaborations have provided a precise picture of the observed Universe. In fact, study of the anisotropies of the CMB is a useful and suitable way to understand the gravitational fluctuations imprinted on the last scattering surface in the early times of the Universe.

- Different from CMB anisotropies, the distribution of matter at the present time of the Universe have been probed by redshift and galaxy surveys. Filaments of galaxies known as *great walls* have been observed for instance by the CfA Redshift Survey [56][1]. Up to now, the largest structure is the Sloan Great Wall, based on the SDSS result [17] [2].

- Devoid of rich clusters of galaxies, we also have some mostly empty places in our Universe, known as *voids*. Study of these voids in theoretical and observational parts of research have made us quite sure that there exists some huge large voids. Among them, the Northern Local Void is the closest super-void, and the Boötes Super-void with an approximately spherically shaped region is known as *great void* [57].

As we see from the first item above, the CMB observations hold the assumption of homogeneity unchanged, nevertheless the Universe is no longer locally homogeneous, when density perturbation become non-linear at late times. The formation of these non-linear structures from primordial perturbations has been most studied in GR using linear perturbation theory, or accompanied with analytical work in Newtonian gravity by means of Newtonian N-body and fluid simulations. Perhaps one of the biggest successes in this area of research is the explanation of how statistical properties of the large scale structure (e.g. statistical homogeneity and isotropy, statistical Gaussianity) arise [58]. The relevant calculations are largely based on linear perturbation theory (i.e. linearizing Einstein equations around the smooth FL solution) which is valid at all length scales of interest at early times and on large scales at late times [15, 20]. Dynamics on small scales at late times involves non-linear theory. One should have in mind that the effects of perturbations at the linear order vanishes on average by construction, but they have a significant effect on the expansion rate once they enter the non-linear regime [59]. In chapter 4, we will investigate their effect on the propagation of light-rays.

Based on the second and third items above, we can say the Universe is a collection of regions with high matter density (walls) and regions with low matter density (voids). In particular, the homogeneous and isotropic, spatially flat model ΛCDM model fits observations of the distance scale and the expansion rate well by introducing vacuum energy. However, the Universe is known to be far from exact homogeneity and isotropy at late times due to the formation of non-linear structures. We can refine these inhomogeneities

[1] This has been done in 1989. In fact the (CfA) Redshift Survey was the first attempt to map the large-scale structure of the Universe.

[2] These filaments are as large as a few hundred Mpc.

through a process of averaging also known as smoothing. These inhomogeneities can affect the curvature of the space and cause an extrinsic curvature, additional to the Ricci curvature tensor. However, this curvature has been assumed to averaged out to zero, while passing to the Friedmannian picture. We express this extrinsic curvature in terms of an expansion tensor, later in section 3.4.

3.2. The averaging problem

We go from the local scale to the large scale by averaging. In order to do so, the first trivial question that comes to mind is: how can we obtain the averaged values of the cosmological parameters? Theoretically, this could be done by obtaining the average of their values in different regions with voids and walls in the Universe. However, averaged and time-evolving are not commutative operations i.e. $[\partial_t, \langle\,\rangle_{\mathcal{D}}] \neq 0$. Non-commutativity of average and time evolution for an arbitrary operation, O, gives us, $\langle\dot{O}\rangle \neq \dot{\langle O\rangle}$, as time evolution is non-linear (e.g. $\dot{O} = O^2 \Rightarrow \dot{\langle O\rangle} \neq \langle O\rangle^2$).

Moreover, since most of the cosmological parameters are tensorial objects, another problem is how to average a tensor.

Regarding these problems, we have two options. First, in the classical approach to standard cosmology, we first obtain the average of matter distributions and geometries in different regions at the early Universe, and then plug these smooth quantities into the Einstein equations to derive the homogeneous geometry from the evolution in the time of average. However, the more proper approach would be to let the parameters evolve with time in different regions and then obtain an average of the evolved values in the late time Universe; so that we first plug the inhomogeneous quantities into Einstein equations and solve these equations for different regions' geometries, then let the results evolve in time, and then average over the final results.

Because the Einstein equations are non-linear, these two approaches are not equivalent:

$$\langle G_{\mu\nu}(g_{\alpha\beta})\rangle \neq G_{\mu\nu}(\langle g_{\alpha\beta}\rangle), \tag{3.1}$$

where $\langle\,\rangle$ stands for averaging. The content of equation (3.1) is that the average behavior of an inhomogeneous space-time is not the same as the behavior of the corresponding smooth space-time.

Fig. 3.1 shows a scheme that the result of the two approaches would not coincide at the end of the day[3].

[3] Recently, Skarke [60, 61] realized that one could avoid the non-commutativity of averaging and time evolution of scalars by utilizing a mass weighted averaging scheme. We shall explain this model in section 3.6.

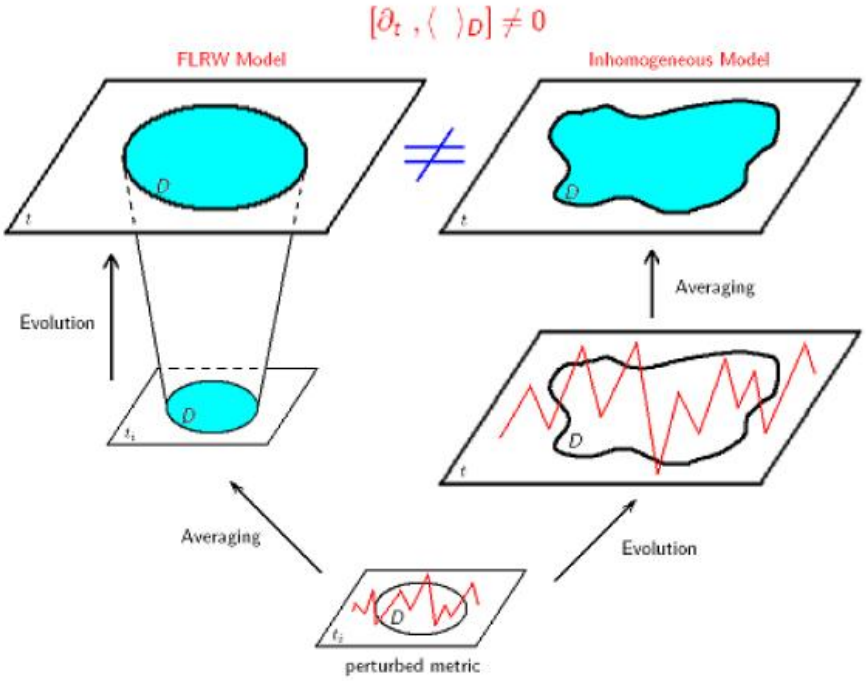

Figure 3.1. Sketch of the difference of the averaged inhomogeneous model to the homogeneous FL model, due to the non-commutativity of time derivations and spatial averaging. Figure credit: Julien Larena, a given talk in the second Kosmologietag, Bielefeld University [63].

The influence of inhomogeneity and anisotropy on the average behavior is also known as *backreaction* term. In order to correct the problem of tensorial equations that appears when we first average the matter density in different regions and then solve Einstein equations, we have to introduce a term of correction, which is known as backreaction term.

As we mentioned, averaging involves the integration of tensors. Therefore, changing the coordinates will change the result in an arbitrary way. One can try to handle this problem by defining a covariant averaging procedure, (e.g. via bi-tensors) which has complexities in its algebra, or one can use part of field equations which only involves scalars.

Another worth to mention problem is the conceptual meaning of the *scale factor*. As we have been convinced, the reason behind using a homogeneous and isotropic model is that the Universe appears to be homogeneous and isotropic when averaged over sufficiently large scales. While the FL scale factor has been very successful in fitting observations, it is difficult to understand the matter content implied by the FL equations which relate to the scale factor. Noticing the fact that the averaged properties of the Universe are well described by an overall scale factor does not imply that the scale factor entirely evolves

according to the Friedmann equations, since the Universe is not completely homogeneous and isotropic.

These difficulties do not allow us to take a straight forward averaging procedure in the context of general relativity and cosmology. In the next section, we shortly introduce the historical attempts to solve the averaging problem in cosmology.

3.3. History of the averaging problem

The problem of averaging in general relativity has a history going back 1960's. It was for the first time introduced by Shirkov and Fisher in 1963 [64]. They proposed a space-time averaging procedure, but it was not covariant such that a tensor did not remain to be a tensor after applying averaging.

A few years later, the problem of second order effects of gravitational waves on the large scale background metric was studied by Isaacson in 1968 [65]. Isaacson used an averaging operation which he called the "BH assumption" after Brill and Hartle [66], which was suited to studying the effects of perturbative gravitational waves in a region surrounded by different wavelengths. An attempt to generalize Isaacson's results was made by Noonan [67], which could be applied to perturbative inhomogeneities. However, the issue of averaging problem was not very well known until 1984 when Ellis gave a comprehensive description of the concept of *backreaction* from small to large structures [68]. He called that task of finding the smooth metric which best fits the average of the real clumpy Universe the *fitting problem*.

The question was further considered for instance by Zotov and Stoeger [69], whose procedure was equivalent to the one by Shirkov and Fisher, hence not covariant and by Futamase [70, 71] who studied the gravitational correlation by employing the metric perturbations. Futamase introduced a spatial averaging procedure after performing a $3+1$ splitting of space-time, and computed backreaction terms arising from averaging second order perturbations. Another example is the work of Boersma [72], who attempted to construct a gauge-invariant (i.e. coordinate independent) averaging procedure in perturbation theory, and also estimated that backreaction effects remain negligibly small at the present day. The reader might be interested in other early works done on this subject [73, 74, 75, 76].

Two breakthroughs in the study of the averaging problem and backreaction were achieved by Zalaletdinov [77, 78] in a covariant and exact way and by Buchert [79, 80], who restricted the problem to scalar quantities only.

Nowadays we know despite of its success, the FL model is only a large-scale approximation to highly non-linear structures at small scales. Releasing more data has revealed more certainty that at small scales, the standard model does not agree with observations. Therefore, the study of backreaction became more and more important in [81, 82, 83, 84, 85].

In the next two sections, we introduce the concept of averaging of scalar quantities,

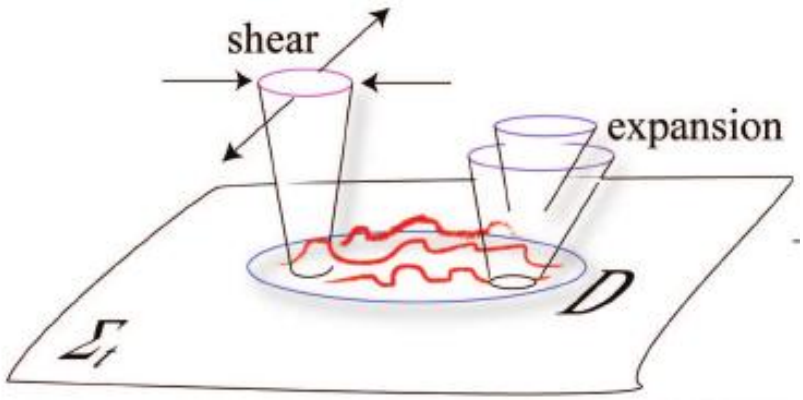

Figure 3.2. A pictorial representation of expansion and shear, while considering in the real inhomogeneous Universe. The fluctuations in the local expansion and shear generate a kinematical backreaction Figure credit: Buchert and Carfora [86].

based on Buchert's approach. The kinematics of the procedure is restricted to the irrotational dust Universe, explained in section 3.4.

We then proceed the dynamics of the current procedure in section 3.5. Another attempt on scalar averaging, different from Buchert's approach is discussed in 3.6. Finally, the exact and covariant tensor averaging approach of Zalaletdinov is explained in 3.7.

3.4. Kinematics of scalar averaging

In order to understand the kinematics of the Universe, one should consider not only the expansion, but also the shear and rotation. These geometrical variables have been detailed in this section. In the next section 3.5 we will neglect the rotation (see Fig. 3.2).

We consider a set of observers comoving with the cosmic medium with the 4-velocity $u^\mu \equiv dx^\mu/d\tau$, where τ is the proper time.

For the comoving observers we can set $u^\mu u^\nu_{;\mu} = 0$, and we define $h^\mu_\nu \equiv \delta^\mu_\nu + u^\mu u_\nu$, where h^μ_ν projects orthogonally to u^μ. Now we can describe the kinematics of the Universe as

$$u^\mu_{;\nu} \equiv \theta^\mu_\nu = h^\mu_\alpha h^\beta_\nu u^\alpha_{;\beta} = w^\mu_\nu + \sigma^\mu_\nu + \frac{1}{3}h^\mu_\nu\theta, \tag{3.2}$$

where w^μ_ν, σ^μ_ν and θ are the rotation tensor, shear tensor and expansion scalar respectively, and are defined as (see e.g. [87])

$$w^\mu_\nu \equiv \frac{1}{2}h^\mu_\alpha h^\beta_\nu (u^\alpha_{;\beta} - u_\beta{}^{;\alpha}), \tag{3.3}$$

$$\sigma^\mu_\nu \equiv h^\mu_\alpha h^\beta_\nu (\frac{1}{2}u^\alpha_{;\beta} + u_\beta{}^{;\alpha}) - \frac{1}{3}h^\alpha_\beta u^\lambda_{;\lambda}, \tag{3.4}$$

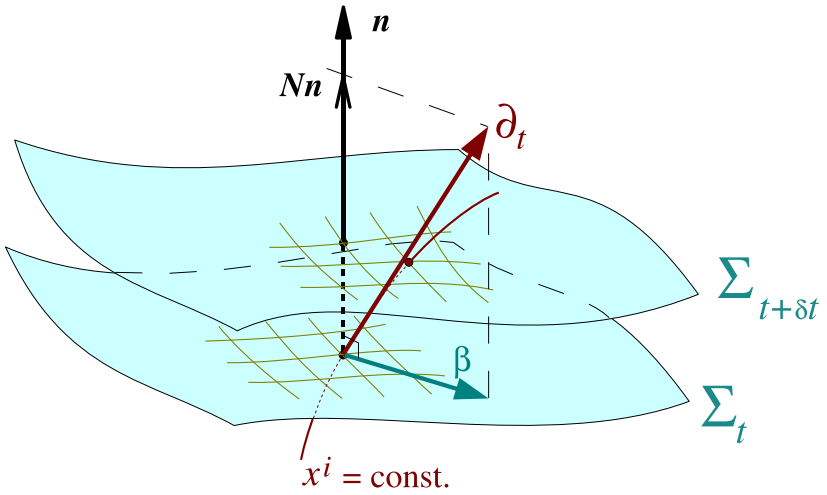

Figure 3.3. Foliation of the space-time by a set of spacelike hypersurfaces. Each line $x^i = const$ of the Coordinates, x^i, on the hypersurfaces, Σ_t, cuts across the foliation. Figure credit: Gourgoulhon, [89].

$$\theta \equiv u^{\lambda}{}_{;\lambda}. \tag{3.5}$$

Here we restrict our attention to the irrotational Universe, i.e. $w^{\mu}_{\nu} = 0$ (see [88] for the case of non-zero rotation), and use the synchronous coordinate system (see the review discussion in [89]). As we mentioned earlier, the choice of synchronous gauge allows us to foliate the space-time to constant time hyperspheres with $\tau = t$ and set the time axis orthogonal to them (see Fig. 3.3).

The metric of the inhomogeneous Universe thus can be expressed in terms of synchronous coordinates:

$$ds^2 = -dt^2 + {}^{(3)}g_{\mu\nu}dx^{\mu}dx^{\nu}, \tag{3.6}$$

where now $d\tau = dt$, and ${}^{(3)}g_{\mu\nu}$ is the metric on hypersurfaces of constant t. The coordinate system in the three hypersurfaces is attached to the cosmic fluid and therefore called comoving. The 4-velocity u^{μ} of comoving observers becomes

$$u^{\mu} = (1, 0), \quad u_{\mu} = (-1, 0). \tag{3.7}$$

From equation (3.2) we have

$$\theta^{\mu}_{\nu} = \sigma^{\mu}_{\nu} + \frac{1}{3}\theta\delta^{\mu}_{\nu}. \tag{3.8}$$

Notice that from equation (3.8) we get $\sigma^{\mu}_{\mu} = 0$, and the shear scalar can be defined as

$$\sigma^2 \equiv \frac{1}{2}\sigma^{\mu}_{\nu}\sigma^{\nu}_{\mu} = \frac{1}{2}(\theta^{\mu}_{\nu}\theta^{\nu}_{\mu} - \frac{1}{3}\theta^2). \tag{3.9}$$

One should keep in mind that two types of curvature, i.e. an extrinsic curvature and an intrinsic curvature, arise from the formalism. The extrinsic curvature tensor, K^{μ}_{ν}, is equivalent to the expansion tensor, i.e. $K^{\mu}_{\nu} \equiv \theta^{\mu}_{\ \nu} = h^{\mu}_{\ \alpha} h^{\beta}_{\ \nu} u^{\alpha}_{\ ;\beta}$. The intrinsic curvature tensor, R^{μ}_{ν}, comes from Einstein equation, $G_{\mu\nu} + \Lambda g_{\mu\nu} = 8\pi G T_{\mu\nu}$, and is expressed as

$$\begin{aligned} g^{\mu\nu} R_{\mu\nu} &= g^{\mu\nu}\Big(\Gamma^{\rho}_{\ \nu\mu,\rho} - \Gamma^{\rho}_{\ \mu\rho,\nu} + \Gamma^{\rho}_{\ \mu\nu}\Gamma^{\epsilon}_{\ \rho\epsilon} - \Gamma^{\epsilon}_{\ \mu\rho}\Gamma^{\rho}_{\ \nu\epsilon}\Big) \\ &\quad + g^{\mu\nu}\Big(\Gamma^{0}_{\ \mu\nu,0} + \Gamma^{0}_{\ \mu\nu}\Gamma^{\rho}_{\ 0\rho} - \Gamma^{\rho}_{\ 0\mu}\Gamma^{0}_{\ \nu\rho} - \Gamma^{0}_{\ \mu\rho}\Gamma^{\rho}_{\ 0\nu}\Big) \\ &\equiv \mathcal{R} + g^{\mu\nu}\Big(\Gamma^{0}_{\ \mu\nu,0} + \Gamma^{0}_{\ \mu\nu}\Gamma^{\rho}_{\ 0\rho} - \Gamma^{\rho}_{\ 0\mu}\Gamma^{0}_{\ \nu\rho} - \Gamma^{0}_{\ \mu\rho}\Gamma^{\rho}_{\ 0\nu}\Big), \end{aligned} \tag{3.10}$$

where $\mathcal{R}$ is the Ricci curvature of the spatial hypersurfaces, and the spatial 3-dimensional curvature tensor is

$$\mathcal{R}^{\mu}_{\nu} \equiv g^{\mu\kappa}\Big(\Gamma^{\epsilon}_{\ \rho\nu,\epsilon} - \Gamma^{\epsilon}_{\ \rho\epsilon,\nu} + \Gamma^{\epsilon}_{\ \rho\nu}\Gamma^{\kappa}_{\ \epsilon\kappa} - \Gamma^{\kappa}_{\ \rho\epsilon}\Gamma^{\epsilon}_{\ \nu\kappa}\Big). \tag{3.11}$$

To proceed to the dynamics of scalar averaging procedure, we need the following decomposition of the Einstein equations, only in the scalar parts (for irrotational dust: $w_{\mu\nu} = 0$, $p = 0$) [90][4]:

$$\dot{\theta} + \frac{1}{3}\theta^2 = -4\pi G\rho - 2\sigma^2 + \Lambda, \tag{3.12}$$

$$\frac{1}{3}\theta^2 = 8\pi G\rho - \frac{1}{2}\mathcal{R} + \sigma^2 + \Lambda, \tag{3.13}$$

$$\dot{\rho} + \theta\rho = 0, \tag{3.14}$$

where the overdots stand for a derivative with respect to the time t. Note that we have neglected the term w in equations (3.12) and (3.13).

The Raychaudhuri equation (3.12) shows the local acceleration, equation (3.13) is equivalent to the flat Friedmann equation for the case that $p = 0$. The continuity equation (3.14) shows that the energy density is proportional to the inverse of the volume.

Similar to equation (3.9), we decompose the 3-dimensional Ricci tensor into its trace part (i.e. the Ricci scalar R) and its traceless part r^{μ}_{ν} [61],

$$\mathcal{R}^{\mu}_{\nu} = \frac{\mathcal{R}}{3}\delta^{\mu}_{\nu} + r^{\mu}_{\nu}. \tag{3.15}$$

The time evolution of the 3-dimensional Ricci tensor gives us

$$\dot{\mathcal{R}}_{\mu\nu} = \theta^{\epsilon}_{\mu;\nu\epsilon} + \theta^{\epsilon}_{\nu;\mu\epsilon} - \theta_{\mu\nu;\epsilon\lambda} g^{\epsilon\lambda} - \theta_{;\mu\nu}, \tag{3.16}$$

where the semicolon denotes covariant spatial derivative. Splitting equation (3.16) into its trace and traceless parts and using equation (3.9-3.16) we arrive at the evolution equations for $\mathcal{R}$ and r^{μ}_{ν} as

$$\dot{\mathcal{R}} + \frac{2}{3}\theta\mathcal{R} = -2\sigma^{\mu}_{\nu} r^{\nu}_{\mu}, \tag{3.17}$$

[4]The Arnowitt-Deser-Misner (ADM) formalism is used in Buchert's approach to decompose the Einstein equations into the time- and spatial components, in the scalar parts.

$$\dot{r}^{\mu}_{\nu} + \frac{2}{3}\theta r^{\mu}_{\nu} = -\frac{5}{4}\sigma^{\mu}_{\epsilon}r^{\epsilon}_{\nu} + \frac{3}{4}\sigma^{\epsilon}_{\nu}r^{\mu}_{\epsilon} + \frac{1}{6}\delta^{\mu}_{\nu}\sigma^{\epsilon}_{\lambda}r^{\lambda}_{\epsilon} + Y^{\epsilon\mu}{}_{\nu;\epsilon}, \tag{3.18}$$

where last term in equation (3.18) is given by

$$Y^{\epsilon}{}_{\mu\nu} = \frac{3}{4}(\sigma^{\epsilon}_{\mu;\nu} + \sigma^{\epsilon}_{\nu;\mu}) - \frac{1}{2}g_{\mu\nu}\sigma^{\epsilon}_{\lambda;}{}^{\lambda} - \sigma_{\mu\nu;}{}^{\epsilon}. \tag{3.19}$$

3.5. Dynamics of scalar averaging

A technically simple approach has been proposed by Buchert. He decomposed Einstein equations into a set of dynamical equations for scalar quantities. We now turn to the dynamics of Buchert's scalar averaging approach. We first review the averaging definition based on this approach in subsection 3.5.1. We then yield the modified Friedmann equations[5] in subsection 3.5.2. We assume that the matter is a pressureless ideal irrotational fluid, or *dust* (for discussion of non-dust matter see [80, 88, 91, 92, 93, 94]) and the four-velocity of observers, u_{μ} is comoving with the dust. We express the integrability condition for the backreaction term in subsection 3.5.3 and consequences on the cosmological parameters in the last subsection 3.5.4.

3.5.1. Averaging procedure

The spatial average of a scalar physical quantity $f(t,\mathbf{x})$ on hypersurfaces of a comoving domain $\mathcal{D}$ is defined as [79]

$$\langle f\rangle_{\mathcal{D}}(t,\mathbf{x}) = \frac{1}{V_{\mathcal{D}}}\int_{\mathcal{D}} d^3\mathbf{x}\sqrt{g(t,\mathbf{x})}f(t,\mathbf{x}), \tag{3.20}$$

where $V_{\mathcal{D}}(t) \equiv \int_{\mathcal{D}} d^3\mathbf{x}\sqrt{g(t,\mathbf{x})}$ is the volume of the domain. The averaged scale factor is defined via the comoving volume on spatial hypersurfaces

$$a_{\mathcal{D}}(t) = \Big(\frac{\int_{\mathcal{D}} d^3x\sqrt{g(t,\mathbf{x})}}{\int_{\mathcal{D}} d^3x\sqrt{g(t_0,\mathbf{x})}}\Big)^{1/3} \simeq \Big(\frac{V_{\mathcal{D}}(t)}{V_{\mathcal{D}}(t_0)}\Big)^{1/3}. \tag{3.21}$$

Using equation (3.21) we find

$$\langle\theta\rangle_{\mathcal{D}} = \frac{1}{V_{\mathcal{D}}}\int_{\mathcal{D}}\theta\sqrt{g(t,\mathbf{x})}d\mathbf{x} = \frac{\dot{V_{\mathcal{D}}}}{V_{\mathcal{D}}} = 3\frac{\dot{a_{\mathcal{D}}}}{a_{\mathcal{D}}}. \tag{3.22}$$

The effective Hubble expansion rate is thus defined as

$$H_{\mathcal{D}} \equiv \frac{\dot{a_{\mathcal{D}}}}{a_{\mathcal{D}}} = \frac{1}{3}\langle\theta\rangle_{\mathcal{D}}. \tag{3.23}$$

[5]These equations are known in the literature as the Buchert equations.

A key point corresponding to equation (3.20) here is that the time evolution and spatial averaging do not commute

$$\partial_t\langle f\rangle - \langle\partial_t f\rangle = \langle f\theta\rangle - \langle f\rangle\langle\theta\rangle, \tag{3.24}$$

which causes the existence of the backreaction terms in following subsection.

3.5.2. Buchert equations

The formalism introduced above leads to the modified Friedmann equations or the so-called Buchert equations [79], see also [80, 81, 95] for a more detailed discussion. For an irrotational dust Universe[6] with a cosmological constant, the equations are:

$$3\frac{\dot{a}_{\mathcal{D}}^2}{a_{\mathcal{D}}^2} = 8\pi G\langle\rho\rangle_{\mathcal{D}} - \frac{1}{2}\langle\mathcal{R}\rangle_{\mathcal{D}} - \frac{1}{2}\mathcal{Q}_{\mathcal{D}} + \Lambda, \tag{3.25}$$

$$3\frac{\ddot{a}_{\mathcal{D}}}{a_{\mathcal{D}}} = -4\pi G\langle\rho\rangle_{\mathcal{D}} + \mathcal{Q}_{\mathcal{D}} + \Lambda, \tag{3.26}$$

where $\mathcal{R}_{\mathcal{D}}$ denotes the 3-Ricci scalar, and $\mathcal{Q}_{\mathcal{D}}$ is the kinematic backreaction term, defined as

$$\mathcal{Q}_{\mathcal{D}} \equiv \frac{2}{3}(\langle\theta^2\rangle_{\mathcal{D}} - \langle\theta\rangle_{\mathcal{D}}^2) - 2\langle\sigma^2\rangle_{\mathcal{D}}. \tag{3.27}$$

The quantities $\mathcal{Q}_{\mathcal{D}}$ and $\langle\mathcal{R}\rangle_{\mathcal{D}}$ have to obey to the integrability condition (introduced in the next subsection). Note that equations (3.25) and (3.26) can be obtained by averaging the equations (3.12) and (3.13).

From the above equations we see that the evolution of the inhomogeneous Universe strongly depends on three quantities of $\langle\rho\rangle_{\mathcal{D}}$, $\mathcal{Q}_{\mathcal{D}}$ and $\langle\mathcal{R}\rangle_{\mathcal{D}}$.

To compare the original Friedmann equations for a spatially flat Universe with the equations (3.25) and (3.26), we may introduce the effective energy density ρ_{eff} and pressure p_{eff} as

$$\rho_{\text{eff}} \equiv \langle\rho\rangle_{\mathcal{D}} - \frac{\mathcal{Q}_{\mathcal{D}} + \langle\mathcal{R}\rangle_{\mathcal{D}}}{16\pi G}, \tag{3.28}$$

$$p_{\text{eff}} \equiv -\frac{1}{16\pi G}\left(\mathcal{Q}_{\mathcal{D}} + \frac{1}{3}\langle\mathcal{R}\rangle_{\mathcal{D}}\right). \tag{3.29}$$

[6] Another example model of a space-time filled with an irrotational dust perfect fluid is the Swiss-cheese model [96, 97, 98]. The model describes a Universe dominated by many voids, and the cheese regions are the over-dense matter content. One of the solutions in the context of Swiss-Cheese models is by using the Lemaître metric, known as Lemaître-Tolman-Bondi (LTB) solution. The LTB solution describes a spherically symmetric space-time for the case of irrotational dust Universe. This model is a useful toy for studying backreaction effects because of the advantage of the symmetry property which allows quantitative studies without any use of approximations. However, it remains merely far away from a realistic description of the real Universe.

Thus equations (3.25) and (3.26) become

$$H_{\mathcal{D}} = \frac{8\pi G}{3}\rho_{\text{eff}} + \frac{\Lambda}{3}, \tag{3.30}$$

$$\frac{\ddot{a}_{\mathcal{D}}}{a_{\mathcal{D}}} = -\frac{4\pi G}{3}\Big(\rho_{\text{eff}} + 3p_{\text{eff}}\Big) + \frac{\Lambda}{3}. \tag{3.31}$$

One should keep in mind that the above set of averaged equations has a different physical meaning than the Friedmann equations due to the different meaning of the scale factor. The scale factor $a(t)$ in the standard Friedmann equations is part of the metric and the evolution of any volume in the space is given by the same scale factor, while the scale factor $a_{\mathcal{D}}(t)$ in Buchert's equations is not part of the metric, and it only corresponds to the volume of a the region which the average is taken[7].

Moreover, we can define the modified equation of state as

$$\omega_{\text{eff}} \equiv \frac{p_{\text{eff}}}{\rho_{\text{eff}}} = \frac{\langle\mathcal{R}\rangle_{\mathcal{D}} - 3\mathcal{Q}_{\mathcal{D}}}{2\langle\theta\rangle_{\mathcal{D}}^2}. \tag{3.32}$$

3.5.3. Integrability condition

The averaged quantities $\mathcal{Q}_{\mathcal{D}}$ and $\langle\mathcal{R}\rangle_{\mathcal{D}}$, which determine the evolution of the inhomogeneous Universe, can be related by an integrability condition.

The continuity equation (3.14) for an irrotational dust Universe can be written as

$$\dot{\rho} = -\theta\rho, \tag{3.33}$$

which after spatial averaging gives us

$$\langle\dot{\rho}\rangle_{\mathcal{D}} + \langle\theta\rho\rangle_{\mathcal{D}} = \dot{\langle\rho\rangle}_{\mathcal{D}} + \langle\theta\rangle_{\mathcal{D}}\langle\rho\rangle_{\mathcal{D}} = 0. \tag{3.34}$$

From the Buchert's equations (3.30) and (3.31) and equation (3.34), we obtain the integrability condition for $\mathcal{Q}_{\mathcal{D}}$ and $\langle\mathcal{R}\rangle_{\mathcal{D}}$ as [79]

$$a_{\mathcal{D}}^{-2}\Big(a_{\mathcal{D}}^2\langle\mathcal{R}\rangle_{\mathcal{D}}\Big)^{\cdot} + a_{\mathcal{D}}^{-6}\Big(a_{\mathcal{D}}^6\mathcal{Q}_{\mathcal{D}}\Big)^{\cdot} = 0. \tag{3.35}$$

The integrability condition is an exact result and $\mathcal{Q}_{\mathcal{D}}$ and $\langle\mathcal{R}\rangle_{\mathcal{D}}$ have to obey it. This condition is essential in Buchert's formalism so that it can be applied to any order in perturbation theory.

[7] Differences between $a(t)$ from Friedmann equations and $a_{\mathcal{D}}$ from averaged equations will be discussed in more details in section 3.6.

3.5.4. Cosmological parameters

The quantities $\mathcal{Q}_{\mathcal{D}}$ and $\langle\mathcal{R}\rangle_{\mathcal{D}}$ in the right hand side of Buchert's equations can be considered as terms in the modified energy momentum tensor. For our discussion we introduce four averaged energy densities for the large scale

$$\Omega_m^{\mathcal{D}} \equiv \frac{8\pi G\langle\rho\rangle_{\mathcal{D}}}{3H_{\mathcal{D}}^2}, \quad \Omega_\Lambda^{\mathcal{D}} \equiv \frac{\Lambda}{3H_{\mathcal{D}}^2}, \quad \Omega_{\mathcal{R}}^{\mathcal{D}} \equiv -\frac{\langle\mathcal{R}\rangle_{\mathcal{D}}}{6H_{\mathcal{D}}^2}, \quad \Omega_{\mathcal{Q}}^{\mathcal{D}} \equiv -\frac{\mathcal{Q}_{\mathcal{D}}}{6H_{\mathcal{D}}^2}. \tag{3.36}$$

We shall call them cosmological parameters, but they are scale dependent variables. The normalization condition thus reads

$$\Omega_m^{\mathcal{D}} + \Omega_\Lambda^{\mathcal{D}} + \Omega_{\mathcal{R}}^{\mathcal{D}} + \Omega_{\mathcal{Q}}^{\mathcal{D}} = 1. \tag{3.37}$$

To compare $\Omega_{\mathcal{R}}^{\mathcal{D}}$ and $\Omega_{\mathcal{Q}}^{\mathcal{D}}$ with the contribution of curvature parameter in the standard model, we shall introduce the pair [99]

$$\Omega_k^{\mathcal{D}} \equiv -\frac{k_{\mathcal{D}_i}}{a_{\mathcal{D}}^2 H_{\mathcal{D}}^2}, \quad \Omega_{\mathcal{Q}_N}^{\mathcal{D}} \equiv \frac{1}{3a_{\mathcal{D}}^2 H_{\mathcal{D}}^2}\int_{t_i}^{t} dt' \mathcal{Q}_{\mathcal{D}} \frac{d}{dt'} a_{\mathcal{D}}^2(t'), \tag{3.38}$$

which are related to the previous pair of parameters by $\Omega_k^{\mathcal{D}} + \Omega_{\mathcal{Q}_N}^{\mathcal{D}} = \Omega_{\mathcal{R}}^{\mathcal{D}} + \Omega_{\mathcal{Q}}^{\mathcal{D}}$. Therefore, the normalization condition from equation (3.37) becomes

$$\Omega_m^{\mathcal{D}} + \Omega_\Lambda^{\mathcal{D}} + \Omega_k^{\mathcal{D}} + \Omega_{\mathcal{Q}_N}^{\mathcal{D}} = 1. \tag{3.39}$$

The most important result of Buchert's approach is that it is possible to cast a spatially volume averaged irrotational dust model in the form of a FL model with an effective mass density and pressure. The disadvantage of this approach is that firstly an assumption like an effective equation of state has to be introduced. Secondly, the set of scalar equations is not closed. This means there are four unknown variables, $a_{\mathcal{D}}$, $\langle\rho\rangle_{\mathcal{D}}$, $\langle\mathcal{Q}\rangle_{\mathcal{D}}$ and $\langle\mathcal{R}\rangle_{\mathcal{D}}$, and only three independent constraints (two of them are the Buchert equations and one is the integrability condition). In order to close them, introducing another relation based on some physical statement is necessary. This has been done by means of cosmological perturbation theory in [100].

3.5.5. Arguments on perturbations

Attempts to address the averaging problem for an irrotational dust Universe are in general in non-perturbative frameworks [99, 101, 102, 103, 104, 105, 106]. However, this leads to a complexity which requires simplifying assumptions. The problem has been furthermore analyzed mainly within perturbation theory [100, 85, 107, 108, 109, 110], where one can assume that the Universe is describable by the split into a *background* that is the standard homogeneous case and small perturbations to this background. The main result at the first perturbative level is that the corrections are perturbatively small and their contribution to the energy is of the order of 10^{-5} at the Hubble scale.

Although the average of first order perturbation vanishes [84, 112], the effect on the average expansion rate is not negligible at higher order [111, 107].

Simply put, metric perturbations around FL space-time are small at all times. This might imply the smallness of metric perturbations causes the average evolution to remain close to the FL case. However, this does not necessarily mean that backreaction would be small at the perturbative level, because the perturbation of the expansion rate depends on first and second derivative of metric perturbations. Thereby the second derivation of metric perturbations i.e. perturbations of the curvature might not be small; e.g. there is a deviation of order unity in the local expansion rate and in the spatial curvature [113].

However, as we mentioned earlier in this chapter and also according to [111], there have been doubts concerning the validity of perturbation theory in the late Universe, whereby all orders of perturbations become important. In [100, 114], the backreaction effect as a function of averaging scale in a perturbative approach up to higher order has been studied. The result show that the effects on the second order are as efficient as the first order, such that the averaged kinematical backreaction term, $\langle \mathcal{Q} \rangle_{\mathcal{D}}$, found to be a second order term, and the averaged spatial curvature, $\langle \mathcal{R} \rangle_{\mathcal{D}}$, has both the first and second order terms. However, the dominant contribution comes from $\langle \mathcal{R} \rangle_{\mathcal{D}}$, up to scales of ~ 200Mpc. Also, the kinematical backreaction, $\langle \mathcal{Q} \rangle_{\mathcal{D}}$, due to second order perturbations becomes important, within ~ 30Mpc. This indicates that the perturbative approach cannot be applied to both too small or too large scales, where non-perturbative effects dominate, but only in a range of $\sim 30 - 200$Mpc.

Calculation of the averaged physical quantities up to third order of perturbation can be found in [115].

3.5.6. Mimicking dark energy by backreaction

Connecting dark energy to backreaction was first proposed by [83] and proceeded by [85, 116, 117, 107], who attempted to explain dark energy by means of a backreaction of small scale structures on the large scale evolution of the Universe. However, such claims have been controversial. A number of authors have argued that the backreaction cannot lead to acceleration of the scale factor [118, 119, 120, 121, 122, 123, 124, 112]. The question is still open. So far nobody could present a proof that would exclude this idea and nobody could prove that the backreaction effects are large enough to explain dark energy. However, it seems to be generally accepted that backreaction effects cannot be neglected if one is interested in precision cosmology. The idea has been later on discussed in [125, 126, 127, 100, 108, 128] and many others.

To make the topic of this section more clear, let us highlight some of the related discussions:

In order to mimic dark energy by backreaction terms, one should consider the case of a vanishing cosmological constant, Λ, and ask whether the backreaction terms can mimic Λ or at least have influence on the evolution of background space-time.

Consider the effective fluid ρ_{eff} in equation (3.28) with dust and dark energy. Let us

consider the number density of dust particles as n and their corresponded mass as m, then we have $\langle n\rangle_{\mathcal{D}} = \langle n\rangle_{\mathcal{D}_0}(a_{\mathcal{D}_0}/a_{\mathcal{D}})^3$ for any comoving domain. We know that the energy density of the dust Universe is $\rho(t,\mathbf{x}) = mn(t,\mathbf{x})$, thus we denote $\rho_m \equiv \langle\rho\rangle_{\mathcal{D}} = m\langle n\rangle_{\mathcal{D}}$. The energy density of dark energy contribution according to equation (3.28) would thus be

$$\rho_{\text{de}} = -\frac{\langle\mathcal{Q}\rangle_{\mathcal{D}} + \langle\mathcal{R}\rangle_{\mathcal{D}}}{16\pi G}, \tag{3.40}$$

and from equation (3.32) we get

$$\omega_{\text{de}} \equiv \frac{p_{\text{de}}}{\rho_{\text{de}}} = \frac{p_{\text{eff}}}{\rho_{\text{eff}}} = -\frac{1}{3} + \frac{4\langle\mathcal{Q}\rangle_{\mathcal{D}}}{3(\langle\mathcal{Q}\rangle_{\mathcal{D}} + \langle\mathcal{R}\rangle_{\mathcal{D}})}. \tag{3.41}$$

The latter equation leads to the claim that if

$$\langle\mathcal{Q}\rangle_{\mathcal{D}} = -\frac{1}{3}\langle\mathcal{R}\rangle_{\mathcal{D}}, \tag{3.42}$$

we will have $\omega_{\text{de}} = -1$, corresponding to $\Lambda = \langle\mathcal{Q}\rangle_{\mathcal{D}}$ [101]. This states that the effects of the inhomogeneities appear to be large enough to let the terms $\mathcal{Q}_{\mathcal{D}}$ and $\Omega_{\mathcal{Q}}^{\mathcal{D}}$ replace Λ and $\Omega_{\Lambda}^{\mathcal{D}}$ [107].

One of the criticism to this claim is that the probable magnitude of the backreaction is not large enough to explain the apparent expansion of the Universe and as a consequence, the backreaction is not a possible substitute for dark energy [129].

Similar calculation as [129] in [130, 131] shows that the effects of backreaction are real, but insufficient to explain the accelerated expansion of the Universe. Therefore dark energy cannot be an effect of the backreaction.

In 2007, Li and Schwarz presented some estimates regarding these effects [108], which show that the effects of the backreaction on the Hubble constant are scale dependent, i.e. the variation of the Hubble constant depends on the inverse square distance ($Q_D \sim 1/r^2$). Moreover, the above result from equation (3.42) could only happen at third order of the perturbation [115].

One should have in mind that the above result is only valid for the perturbative approach. In fact in the non-perturbative regime, $\langle\mathcal{Q}\rangle_{\mathcal{D}}$ and $\langle\mathcal{R}\rangle_{\mathcal{D}}$ are strongly coupled in a *morphon field* description [101].

3.6. Scalar averaging based on mass weighted average method

Another method for analyzing the dynamics of an inhomogeneous irrotational dust Universe was presented recently by Skarke [60, 61].

The model is in line with [107, 127] and [132], and tries to relate the accelerated expansion to inhomogeneity effects. However, its construction differs completely from

Buchert's approach. While one uses the ordinary volume average of scalar quantities in Buchert's approach, this method uses the mass weighted average instead, and its advantage is that averaging commutes with taking time derivatives.

The basic idea is, if we consider a large domain $\mathcal{D}$ in an irrotational dust Universe, by means of synchronous gauge, we could divide the domain $\mathcal{D}$ into a number of infinitesimal regions $\mathcal{D}_n$. In fact, these regions are small in cosmic terms, but large enough for the usage of irrotational dust approximation. One can thus obtain the volume of $\mathcal{D}$, $V_{\mathcal{D}}$, by adding the contribution of the volume of each of regions $\mathcal{D}_n$.

3.6.1. The local scale factor

The scale factor which has been used in the analysis of the current model plays a different role than $a_{\mathcal{D}}$ in Buchert's approach (and the one in the homogeneous and isotropic FL model). We shall specify them in the following:

- The scale factor used in the homogeneous Universe, $a_{FL}(t)$, is related to the metric $g_{\mu\nu}$ such that, $g_{\mu\nu} = diag(-1, a^2_{FL}(t), a^2_{FL}(t), a^2_{FL}(t))$. Yet, on the level of linear perturbation, where the metric is modified by tiny Gaussian perturbations, we use the same scale factor $a_{FL}(t)$ to treat the perturbations.

- The scale factor used in Buchert's scalar averaging approach, $a_{\mathcal{D}}(t)$, for a given domain $\mathcal{D}$ characterizes the evolution of the volume $V_{\mathcal{D}}$ and their relation is described as
$$a_{\mathcal{D}}(t) = \left(\frac{V_{\mathcal{D}}(t)}{V_{\mathcal{D}}(t_0)}\right)^{1/3}. \tag{3.43}$$

- The *local* scale factor used in Skarke's approach, $a_l(t, x)$, is expressed in terms of a fixed quantity of energy density, $\hat{\rho}$, and is defined as
$$a_l(t, x) = \left(\frac{\hat{\rho}}{\rho(t, x)}\right)^{1/3}, \tag{3.44}$$
where $\rho(t, x)$ is the energy density. The connection between a_l and $a_{\mathcal{D}}$ can be seen in equation (3.49) below.

From the expansion scalar $\theta^{\mu}_{\nu} \equiv \theta = (\sqrt{-g}\,)^{\cdot}/\sqrt{-g}$ and the continuity equation $\dot{\rho} + \theta\rho = 0$ (see the kinematics of dust Universe introduced in section 3.4), we find
$$\frac{d}{dt}\left(\rho(t, x)\sqrt{-g(t, x)}\right) = 0, \tag{3.45}$$
and therefore we obtain the mass content $m_{\mathcal{D}}$ as
$$m_{\mathcal{D}} = \int_{\mathcal{D}} \rho(t, x)\sqrt{g(t, x)}d^3x, \tag{3.46}$$

which is a time-independent quantity i.e. $\dot{m}_{\mathcal{D}} = 0$.

Now we can introduce the mass weighted average definition [60] of a scalar quantity $F(t,x)$ as

$$\langle F\rangle^m_{\mathcal{D}}(t) = \frac{1}{m_{\mathcal{D}}}\int_{\mathcal{D}} F(t,x)\rho(t,x)\sqrt{g(t,x)}d^3x, \tag{3.47}$$

which as mentioned earlier has the property that averaging and time derivation do commute, $\langle F\rangle^{\cdot}_{\mathcal{D}} = \langle \dot{F}\rangle_{\mathcal{D}}$.

Therefore, the volume $V_{\mathcal{D}}$ can be computed as

$$V_{\mathcal{D}} = \int_{\mathcal{D}} \sqrt{g(x,t)}d^3x = m_{\mathcal{D}}\langle\rho^{-1}\rangle^m_{\mathcal{D}} = \frac{m_{\mathcal{D}}}{\hat{\rho}}\langle a_l^3\rangle^m, \tag{3.48}$$

and since $a_{\mathcal{D}}$ can be written as $a_{\mathcal{D}} = \left(V_{\mathcal{D}}/V_{\mathcal{D}_0}\right)^{1/3}$, the relation between the latter two scale factor is

$$a^3_{\mathcal{D}} = \frac{1}{V_{\mathcal{D}_0}}\Big(\frac{m_{\mathcal{D}}}{\hat{\rho}}\Big)\langle a_l^3\rangle. \tag{3.49}$$

Equation (3.49) shows that in general $a_{\mathcal{D}} \neq a_l$ and the relation $a_{\mathcal{D}} = \langle a_l^3\rangle^{1/3}$ holds only if $V_{\mathcal{D}_0} \equiv m_{\mathcal{D}}/\hat{\rho}$.

3.6.2. Evolution of the local scale factor

With considering the kinematics of the irrotational dust Universe and equations (3.8-3.14), the definition of the local scale factor in equation (3.44) together with the continuity equation (3.14) gives the following expression for the expansion rate θ

$$\theta(t,x) = -\frac{\dot{\rho}(t,x)}{\rho(t,x)} = 3\frac{\dot{a}_l(t,x)}{a_l(t,x)}. \tag{3.50}$$

The scale factor a_l as a solution of this equation for some initial time t_{in} [60] is:

$$a_l(t,x) = a_{in}(x)\exp\left(\frac{1}{3}\int_{t_{in}}^{t}\theta(\tilde{t},x)d\tilde{t}\right). \tag{3.51}$$

We now introduce the rescaled quantities (with hatted sign)

$$\hat{\rho} = a_l^3\rho, \quad \hat{\sigma}^\mu_\nu = a_l^3\sigma^\mu_\nu, \quad \hat{R} = a_l^2 R, \quad \hat{r}^\mu_\nu = a_l^2 r^\mu_\nu, \tag{3.52}$$

with the evolution equations

$$\begin{gathered}\dot{\hat{\rho}} = 0, \quad \dot{\hat{\sigma}}^\mu_\nu = -a_l\hat{r}^\mu_\nu, \quad \dot{\hat{R}} = -2a_l^{-3}\hat{\sigma}^\mu_\nu\hat{r}^\nu_\mu, \\ \dot{\hat{r}}^\mu_\nu = a^{-3}\Big(-\frac{5}{4}\hat{\sigma}^\mu_\epsilon\hat{r}^\epsilon_\nu + \frac{3}{4}\hat{\sigma}^\epsilon_\nu\hat{r}^\mu_\epsilon + \frac{1}{6}\delta^\mu_\nu\hat{\sigma}^\epsilon_\lambda\hat{r}^\lambda_\epsilon\Big) + a_l^2 Y^{\epsilon\mu}{}_{\nu;\epsilon},\end{gathered} \tag{3.53}$$

which are needed to compute the evolution of the local scale factor a_l [61].

Therefore, equation (3.13) can be written in terms of the new rescaled quantities as

$$\theta^2 = 8\pi G\hat{\rho}a_l^{-3} + \hat{\sigma}^2 a_l^{-6} - \frac{1}{2}\hat{R}a_l^{-2} + \Lambda. \tag{3.54}$$

Moreover, we can compute the evolution of $\hat{R}$ from equation (3.53) for some initial time

$$\begin{aligned}\hat{R}(t) &= \hat{R}(t_{in}) - 2\int_{t_{in}}^{t} a_l^{-3}(\tilde{t})\ \hat{\sigma}^{\mu}_{\nu}(\tilde{t})\ \hat{r}^{\nu}_{\mu}(\tilde{t})\ d\tilde{t} \\ &= \hat{R}(t_{in}) + 2\int_{t_{in}}^{t} a_l^{-4}(\tilde{t})\ \hat{\sigma}^{\mu}_{\nu}(\tilde{t})\ \dot{\hat{\sigma}}^{\nu}_{\mu}(\tilde{t})\ d\tilde{t} \\ &= \hat{R}(t_{in}) + 2\ a_l^{-4}(t)\ \hat{\sigma}^2(t) - 2a_l^{-4}(t_{in})\hat{\sigma}^2(t_{in}) \\ &\quad + \frac{8}{3}\int_{t_{in}}^{t} \theta(\tilde{t})a_l^{-4}(\tilde{t})\ \hat{\sigma}^2(\tilde{t})d\tilde{t}.\end{aligned} \tag{3.55}$$

Using the latter expression together with equation (3.54) we finally obtain the evolution of the local scale factor

$$3(\frac{\dot{a}_l^2}{a_l^2}) = a_l^{-6}\Big(\hat{\sigma}_{in}^2 - \frac{4}{3}\int_{t_{in}}^{t} \theta(\tilde{t})\hat{\sigma}^2(\tilde{t})d\tilde{t}\Big) + a_l^{-3}(8\pi G\hat{\rho}) - a_l^{-2}(\frac{1}{2}\hat{R}_{in}) + \Lambda. \tag{3.56}$$

The assumptions on initial values are compatible with linear perturbation theory. Simply put, one can refer to the linear perturbation regime to compute the initial values a_{in}, $\hat{\sigma}_{in}$ and $\hat{R}_{in}$ in equation (3.56). The initial scalar perturbations can be parameterized in terms of scalar Gaussian random fields, where the resulting contributions can be expressed in only one time-dependent function [100]. So that for the case of a flat FL background, the first order expressions for the perturbed metric, the Ricci and expansion tensors depend only on this single function. Using the results from linear perturbation theory, one is able to find the initial values of the mentioned quantities and to compute the volume of the domain $V_{\mathcal{D}}$, which is in general a function of time t, the cosmological constant Λ and the background curvature (see [61] for the detailed calculations). In order to completely fix the evolution of the volume of the Universe and compare the results with the observations, the case of zero cosmological constant and flat background has been considered; so that the scale of the time parameter only needs to be determined. Fig. 3.4 displays different lines corresponding to a plot of $a_{\mathcal{D}}$ over t.

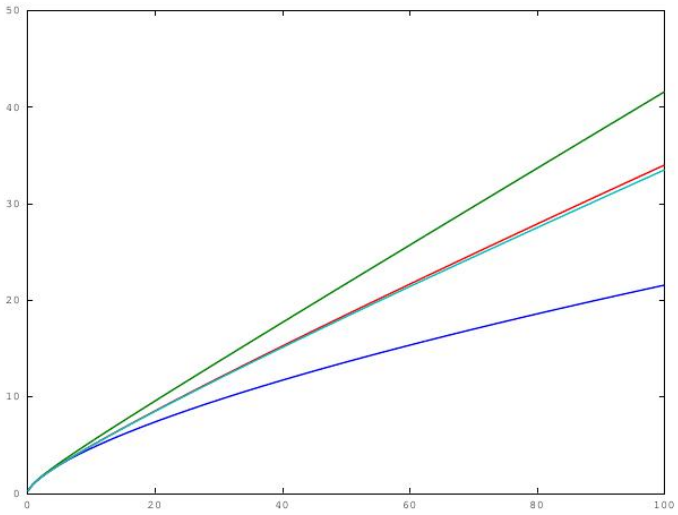

Figure 3.4. The diagram of $a_{\mathcal{D}}$ plotted over t for the case of $\lambda = 0$ and zero curvature background. The blue line corresponds to an Einstein-de Sitter (EdS) Universe. The green line corresponds to a scenario where the inhomogeneities have been taken into account, in the case of zero shear and ignoring the traceless part of the Ricci tensor. The red line corresponds to an inhomogeneous scenario where the inhomogeneous part of the rescaled Ricci tensor, $\bar{r}$ is modelled as constant. The line close to the previous one colored in cyan, indicates again an inhomogeneous scenario, however with considering the evolution of the non-constant $\bar{r}$. Figure credit: Skarke, [61].

3.7. Zalaletdinov's macroscopic gravity

In this section, we explain the concept of the covariant averaging of tensors and discuss what has been achieved in the work by Zalaletdinov.

As we saw earlier in this chapter, since Buchert has introduced his averaging approach in 2000, it has been used by many authors to explore the effects of backreaction, including the perturbative contexts mentioned in subsection 3.5.5, and has also been compared with observations [62]. The reason for the amount of attention it has since received, perhaps is its simplicity of application. In contrast, Zalaletdinov's averaging approach, which was developed even earlier than Buchert's work, is a technically rather challenging approach to handle. Its strength against Buchert's approach however lies on the fact of a fully covariant prescription which yields a tensorial object to remain to be a tensor after the process of taking averages. One important example is introducing a so called *averaged metric* on an *averaged manifold*. This eventually allows one to make physically exact statements about averaging in general relativity.

3.7.1. Introduction

There are a number of averaging procedures that have been introduced to resolve the averaging problem. An exact, non-perturbative and covariant approach that allows tensor quantities to be averaged, as well as scalars, was provided by Zalaletdinov [77] [78] and is called macroscopic gravity. The name comes from the analogy to Maxwell's electrodynamics (i.e. the Lorentz theory of electrons and Maxwell's electrodynamics are the microscopic and macroscopic theories respectively). Analogously, the goal of the macroscopic gravity formalism is to provide a link between the microscopic geometry of space-time, and the macroscopic averages that are used in cosmology. In this section, we will briefly summarize the macroscopic gravity formalism. In a better construction, the microscopic description is based on a discrete matter model, while the macroscopic description is based on a smooth continuous matter distribution [133].

This approach involves averaging the geometrical objects that exist on the space-time manifold, and constructing field equations for these averaged quantities based on averaging Cartan equations of the pseudo-Riemannian geometry of microscopic space-time.

In the real *lumpy* Universe with a discrete matter distribution on each physically distinct scale (of galaxies, clusters of galaxies, etc.), the stress-energy tensor $T_{\mu\nu} = T^{(discrete)}_{\mu\nu}$ can be adequately approximated by a smoothed one as

$$T_{\mu\nu} = \langle T^{(discrete)}_{\mu\nu} \rangle, \tag{3.57}$$

usually taken to be in the form of a perfect fluid.

As $T^{(discrete)}_{\mu\nu} \to \langle T^{(discrete)}_{\mu\nu} \rangle$ on the right-hand side of Einstein equations, the structure of the field operator in the left-hand side is kept unchanged under such a change and therefore the field equations hold:

$$R_{\mu\nu} - \frac{1}{2} g_{\mu\nu} R = 8\pi G \langle T^{(discrete)}_{\mu\nu} \rangle, \tag{3.58}$$

where $g_{\mu\nu}$, $R_{\mu\nu}$ and R are the metric, Ricci tensor and scalar curvature of a pseudo-Riemannian space-time geometry describing now the corresponding geometry created by the smoothed energy momentum tensor $\langle T^{(discrete)}_{\mu\nu} \rangle$.

However, for an exact proceeding, the Einstein equations themselves must have been consequently averaged out:

$$\langle R_{\mu\nu} \rangle - \frac{1}{2} \langle g_{\mu\nu} \rangle \langle g^{\alpha\beta} \rangle \langle R_{\alpha\beta} \rangle + \langle C_{\mu\nu} \rangle = 8\pi G \langle T^{(discrete)}_{\mu\nu} \rangle, \tag{3.59}$$

where the new variable $C_{\mu\nu}$ is a connection correlation function [134].

Let us call the averaged metric tensor $\langle g_{\mu\nu} \rangle$ the macroscopic metric tensor $\bar{g}_{\mu\nu}$. The macroscopic Einstein equations of macroscopic gravity become the Einstein equations of general relativity, for the macroscopic metric tensor $\langle g_{\mu\nu} \rangle$

$$M_{\mu\nu} - \frac{1}{2} \langle g_{\mu\nu} \rangle \langle g^{\alpha\beta} \rangle M_{\alpha\beta} = 8\pi G \langle T^{(discrete)}_{\mu\nu} \rangle, \tag{3.60}$$

where $M_{\mu\nu}$ is the macroscopic Riemannian curvature tensor.

3.7.2. The averaging operator

The starting point is "how can one average tensors while retaining their transformation properties under coordinate changes?" If the averaging operation is to involve an integral over a space-time region, then clearly only scalar objects can be averaged, since they change in a trivial way under coordinate transformation. However, averaging involves the integration of tensors over a (space-time or spatial or null) volume V, and is not easily well defined, because the result can change by changing the coordinates and is typically not unique. For treating this problem in a covariant way one needs to introduce some additional structure in the formalism (for a detailed review see [135] and [131]). This is achieved by using bilocal averaging operators over compact regions of space-time, Σ, that contain the supporting point x.

Our intent is to introduce a rigorously defined geometric averaging procedure that captures the intuition of averaging as integrating a quantity over Σ, and dividing by volume V_Σ. When we average a tensorial object P, in order for the averaged object $\langle P\rangle$ to transform tensorially, P could be parallel transported from each point x' within Σ to a common reference point x. However, no specific unique path has been identified here, such that the parallel transformation can be referred to.

For a vector field $v(x)$, this takes the form

$$\tilde{v}^a(x',x) = \mathcal{A}^a_{a'}(x,x')v^{a'}(x'). \tag{3.61}$$

The object $\mathcal{A}^a_{a'}(x,x')$ is an operator that maps a vector at point x' into the transported vector at reference point x.

One possibility is to define the operator as the product of a basis of vector fields (the tetrad fields) at two different points x and x' in Σ:

$$\mathcal{A}^a_{a'}(x,x') = e^a_I(x)e^I_{a'}(x'), \tag{3.62}$$

where the index I labels the basis vectors.

In particular, for this choice it can be noted that $\mathcal{A}^a_{a'}(x,x')$ depends only on the initial and final point and not on the choice of curve connecting the two points. We can follow this procedure for tensorial objects. The bilocal operator is then used to define the "bilocal extension" of an object. So the extension of P^a_b is

$$\tilde{P}^a_b(x',x) = \mathcal{A}^a_{c'}(x',x)P^{c'}_{d'}(x')\mathcal{A}^{d'}_b(x',x). \tag{3.63}$$

For higher rank tensors the bilocal extension works on each space-time index and the average is defined analogously

$$\tilde{T}^{a_1\ldots a_n}_{b_1\ldots b_m} = \mathcal{A}^{a'}_{a'_1}\ldots\mathcal{A}^{a_n}_{a'_n}\mathcal{A}^{b'_1}_{b_1}\ldots\mathcal{A}^{b'_n}_{b_n}T^{a'_1\ldots a'_n}_{b'_1\ldots b'_m}. \tag{3.64}$$

To begin with, we require that this bilocal operator be idempotent (i.e. square to itself)

$$\mathcal{A}^a_{b''}(x,x'')\mathcal{A}^{b''}_{a'}(x'',x') = \mathcal{A}^a_{a'}(x,x'), \tag{3.65}$$

and have coincidence limit

$$\lim_{x\to x'} \mathcal{A}^a_{a'}(x,x') = \delta^a_{a'}. \tag{3.66}$$

This ensures that $\mathcal{A}^a_{a'}(x,x')$ has the inverse operator $\mathcal{A}^{a'}_a(x',x)$.

We now define the average of a tensor field $P^a_b(x)$ as

$$\langle P^a_b(x)\rangle = \frac{1}{V_\Sigma}\int d^4x'\sqrt{-g'}\tilde{P}^a_b(x',x), \tag{3.67}$$

and in general

$$\langle T^{a_1\dots a_n}_{b_1\dots b_m}(x)\rangle = \frac{1}{V_\Sigma}\int d^4x\sqrt{-g'}\tilde{T}^{a_1\dots a_n}_{b_1\dots b_m}, \tag{3.68}$$

where V_Σ is the volume of the region Σ,

$$V_\Sigma = \int_\Sigma d^4x'\sqrt{-g'}. \tag{3.69}$$

With this definition we can now consider the average of various geometrical objects. Especially this allows us to define the bilocal extension of the metric tensor and the definition of an averaged metric.

3.7.3. The averaged manifold

With the averaging operation in place, we can turn to the description of an averaged geometry.

First we define a line element for the macroscopic space-time

$$ds^2 = \langle g_{\mu\nu}\rangle dx^\mu dx^\nu, \tag{3.70}$$

where the macroscopic metric tensor is used to calculate the macroscopic Christoffel symbols, denoted by $\langle\Gamma^\mu_{\nu\alpha}\rangle$. The so defined macroscopic Christoffel symbols guarantee that the macroscopic space-time is a Riemannian manifold itself [136]. Thus the averaged metric tensor $\langle g_{\mu\nu}\rangle$ and the averaged inverse metric tensor $\langle g^{\mu\nu}\rangle$ can be identified as metric tensors (we shall use this property, later in section 4.4). As we will explain there, it is essential for our work that a covariant procedure to average a space-time metric exists. However, it is irrelevant for our purpose how this is defined in detail.

If we assume that our microscopic space-time is a manifold $\mathcal{M}$ with metric $g_{\mu\nu}$, a Levi-Civita connection $\Gamma^\mu_{\nu\alpha}$, and Riemann curvature tensor $R^\mu_{\nu\alpha\beta} = 2\Gamma^\mu_{\nu[\beta,\alpha]} + 2\Gamma^\mu_{\epsilon[\alpha}\Gamma^\epsilon_{\nu\beta]}$, macroscopic gravity is based on the idea that the average of the Levi-Civita connection on $\mathcal{M}$ yields a Levi-Civita connection for the averaged or smoothes manifold $\bar{\mathcal{M}}$. Given $\langle\Gamma^\mu_{\nu\alpha}\rangle$, one can locally determine a metric $\langle g_{\mu\nu}\rangle$ for $\bar{\mathcal{M}}$ compatible with $\langle\Gamma^\mu_{\nu\alpha}\rangle$.

To proceed with the averaging, a correlation 2-form is defined as

$$Z^{\alpha\ \ \mu}_{\beta[\gamma\ \ \underline{\nu\sigma}]} = \langle\Gamma^\alpha_{\beta[\gamma}\Gamma^\mu_{\underline{\nu\sigma}]}\rangle - \langle\Gamma^\alpha_{\beta[\gamma}\rangle\langle\Gamma^\mu_{\underline{\nu\sigma}]}\rangle, \tag{3.71}$$

where underlined indices are not included in anti-symmetrization, and $Z^{\alpha}_{\mu\nu\beta} \equiv 2Z^{\alpha}_{\mu[\epsilon}{}^{\epsilon}{}_{\underline{\nu}\beta]}$.

This definition for connection correlation satisfies the algebraic conditions below [136][8]:

- The antisymmetry in the third and sixth indices,

$$Z^{\alpha}_{\beta\gamma}{}^{\mu}{}_{\nu\sigma} = -Z^{\alpha}_{\beta\sigma}{}^{\mu}{}_{\nu\gamma}. \tag{3.72}$$

- The antisymmetry in inter-change of the index pairs,

$$Z^{\alpha}_{\beta\gamma}{}^{\mu}{}_{\nu\sigma} = -Z^{\mu}_{\nu\gamma}{}^{\alpha}{}_{\beta\sigma}. \tag{3.73}$$

- The algebraic cycle identities

$$Z^{\alpha}_{\beta[\gamma}{}^{\mu}{}_{\nu\sigma]} = 0. \tag{3.74}$$

- The equi-affinity property,

$$Z^{\epsilon}_{\epsilon\gamma}{}^{\mu}{}_{\nu\sigma} = 0. \tag{3.75}$$

- And the algebraic symmetry of inter-change of the index triples from (3.72) to (3.73),

$$Z^{\alpha}_{\beta\gamma}{}^{\mu}{}_{\nu\sigma} = Z^{\mu}_{\nu\sigma}{}^{\alpha}{}_{\beta\gamma}. \tag{3.76}$$

Solving the differential equations for the connection correlation tensor $Z^{\alpha}_{\beta\gamma}{}^{\mu}{}_{\nu\sigma}$

$$Z^{\alpha}_{\beta[\gamma}{}^{\mu}{}_{\underline{\nu}\sigma||\lambda]} = 0, \tag{3.77}$$

where $||$ is the covariant derivative with respect to $\langle\Gamma^{\alpha}_{\beta\gamma}\rangle$, we find a set of connection correlation functions.

We have chosen $\bar{g}_{\mu\nu} = \langle g_{\mu\nu}\rangle$ as the averaged metric on the averaged manifold $\bar{\mathcal{M}}$. In general however, we have $\bar{g}_{\mu\nu} \neq \langle g_{\mu\nu}\rangle$, and can define the tensor $U^{\mu\nu} = \bar{g}^{\mu\nu} - \langle g^{\mu\nu}\rangle$ to keep track of this differences. However, we can say that when the averaged manifold is highly symmetric, as in the case of a manifold with homogeneous and isotropic spatial sections, which we will consider, one finds that $U^{\mu\nu} = 0$.

The average of the curvature 2-form $R^{\mu}_{\nu\alpha\beta}$ is denoted $\langle R^{\mu}_{\nu\alpha\beta}\rangle$ and the Ricci curvature 2-form on the averaged manifold $\bar{\mathcal{M}}$ is denoted $M^{\mu}_{\nu\alpha\beta}$,

$$M^{\mu}_{\nu\alpha\beta} = \partial_{\alpha}\langle\Gamma^{\mu}_{\nu\beta}\rangle - \partial_{\beta}\langle\Gamma^{\mu}_{\nu\alpha}\rangle + \langle\Gamma^{\mu}_{\sigma\alpha}\rangle\langle\Gamma^{\sigma}_{\nu\beta}\rangle - \langle\Gamma^{\mu}_{\sigma\beta}\rangle\langle\Gamma^{\sigma}_{\nu\alpha}\rangle, \tag{3.78}$$

where $M^{\mu}_{\nu\alpha\beta} \neq \langle R^{\mu}_{\nu\alpha\beta}\rangle$, in general. Likewise, it is assumed that there exists a non-metric (i.e. $\nabla_{\mu}\bar{g}_{\nu\rho} \neq 0$) and symmetric connection, $\Pi^{\mu}_{\nu\rho}$, such that

$$\langle R^{\mu}_{\nu\alpha\beta}\rangle = \partial_{\alpha}\Pi^{\mu}_{\nu\beta} - \partial_{\beta}\Pi^{\mu}_{\nu\alpha} + \Pi^{\mu}_{\sigma\alpha}\Pi^{\sigma}_{\nu\beta} - \Pi^{\mu}_{\sigma\beta}\Pi^{\sigma}_{\nu\alpha}, \tag{3.79}$$

where $\Pi^{\mu}_{\nu\alpha} \neq \langle\Gamma^{\mu}_{\nu\alpha}\rangle$, in general.

[8] These properties are directly mentioned from Zalaletdinov's paper [136].

Macroscopic parameter	Definition
$\mathcal{A}^{a}_{a'}$	Bilocal transformation operator
$\langle g_{\mu\nu}\rangle$	Averaged metric tensor
$\langle \Gamma^{\mu}_{\nu\rho}\rangle$	Averaged Levi-Civita connection
$\Pi^{\mu}_{\nu\rho}$	Non-metric connection
$Z^{\alpha\ \ \mu}_{\ \beta\gamma\ \ \nu\sigma}$	Connection correlation tensor
$M^{\mu}_{\nu\alpha\beta}$	Riemannian curvature tensor
$\langle R^{\mu}_{\ \nu\alpha\beta}\rangle$	Non-Riemannian curvature tensor
$Q^{\mu}_{\ \nu\alpha\beta}$	Polarization tensor
$A^{\mu}_{\nu\alpha\beta}$	Affine deformation tensor
$\langle T^{\mu}_{\nu}\rangle$	Averaged energy momentum tensor

Table 3.1. List of quantities and their definitions, used in Zalaletdinov's averaging approach on macroscopic gravity.

The difference between the macroscopic Riemannian curvature tensors $M^{\mu}_{\nu\alpha\beta}$ and the average of the non-Riemannian tensor $\langle R^{\mu}_{\ \nu\alpha\beta}\rangle$ is expressed as a polarization tensor $Q^{\mu}_{\ \nu\alpha\beta}$, so that

$$Q^{\mu}_{\ \nu\alpha\beta} = \langle R^{\mu}_{\ \nu\alpha\beta}\rangle - M^{\mu}_{\nu\alpha\beta} = 2\langle \Gamma^{\mu}_{\epsilon[\alpha}\Gamma^{\epsilon}_{\underline{\nu\beta}]}\rangle - 2\langle \Gamma^{\mu}_{\epsilon[\alpha}\rangle\langle \Gamma^{\epsilon}_{\underline{\nu\beta}]}\rangle. \tag{3.80}$$

Equation (3.80) shows that $Q^{\mu}_{\ \nu\alpha\beta}$ is a connection correction tensor,

$$Q^{\mu}_{\ \nu\alpha\beta} = -2Z^{\epsilon\ \ \mu}_{\ \nu\alpha\ \ \epsilon\beta}. \tag{3.81}$$

From the relation $Z^{\epsilon}_{\mu\nu\gamma} = 2Z^{\epsilon\ \ \ \sigma}_{\ \mu[\sigma\ \ \underline{\nu\gamma}]}$, one can obtain

$$Q_{\mu\nu} = Q^{\sigma}_{\mu\nu\sigma}. \tag{3.82}$$

The difference between the averaged connection and the connection of the averaged Riemann tensor yields an "affine deformation tensor"

$$A^{\mu}_{\nu\alpha} = \langle \Gamma^{\mu}_{\nu\alpha}\rangle - \Pi^{\mu}_{\nu\alpha}. \tag{3.83}$$

Solving the field equations for the non-Riemannian curvature tensor, $R^{\mu}_{\ \nu[\alpha\beta||\lambda]} = 0$, holds

$$A^{\epsilon}_{\ \nu[\alpha}R^{\mu}_{\ \underline{\epsilon\beta\lambda}]} - A^{\mu}_{\ \epsilon[\alpha}R^{\epsilon}_{\ \underline{\nu\beta\lambda}]} = 0, \tag{3.84}$$

and gives us a set of affine deformation functions.

3.7.4. The averaged Einstein equations

Under the assumption that the connection $\langle\Gamma^{\mu}_{\nu\alpha}\rangle$ is symmetric and compatible with the metric $\langle g_{\mu\nu}\rangle$, and that we assume the following splitting rules for products of connection and metric, $\langle\Gamma^{\mu}_{\nu\alpha}g^{\sigma}_{\tau}\rangle = \langle\Gamma^{\mu}_{\nu\alpha}\rangle\langle g^{\sigma}_{\tau}\rangle$ and $\langle\Gamma^{\alpha}_{\beta[\gamma}\Gamma^{\mu}_{\underline{\nu\rho]}}g^{\sigma}_{\tau}\rangle = \langle\Gamma^{\alpha}_{\beta[\gamma}\Gamma^{\mu}_{\underline{\nu\rho]}}\rangle\langle g^{\sigma}_{\tau}\rangle$, one can construct the field equations of macroscopic gravity.

The system of field equations of macroscopic gravity includes the macroscopic (averaged) Einstein equations. There is a system of equations for the macroscopic gravitational metric and connection correlation tensors.

$$\langle g^{\beta\epsilon}\rangle M_{\gamma\beta} - \frac{1}{2}\delta^{\epsilon}_{\gamma}\langle g^{\mu\nu}\rangle M_{\mu\nu} = 8\pi G\langle T^{\epsilon}_{\gamma}\rangle - (Z^{\epsilon}_{\mu\nu\gamma} - \frac{1}{2}\delta^{\epsilon}_{\gamma}Q_{\mu\nu})\langle g^{\mu\nu}\rangle, \tag{3.85}$$

where $\langle T^{\epsilon}_{\gamma}\rangle$ is the averaged energy-momentum tensor. We assume that it can be written as

$$\langle T^{\mu}_{\nu}\rangle = (\rho + p)u^{\mu}u_{\nu} + p\langle g^{\mu}_{\nu}\rangle + \Sigma^{\mu}_{\nu}, \tag{3.86}$$

where ρ, p and Σ^{μ}_{ν} are the energy density, isotropic pressure and anisotropic stress of the fluid, respectively. The 4-vector u^{μ} exists in the manifold with averaged geometry $\langle g_{\mu\nu}\rangle$, and is the velocity 4-vector of the fluid.

The averaged Einstein equations of macroscopic gravity agrees with the Einstein equations of general relativity for the macroscopic metric tensor $\langle g^{\mu}_{\nu}\rangle$ with a smoothed energy-momentum tensor only if all macroscopic gravitational metric and connection correlations vanish [134].

3.7.5. Macroscopic FL solutions

The solutions to the modified Einstein equations (3.85) have been studied by Coley, Pelavas and Zalaletdinov [137] and in a fully detailed discussion by Van den Hoogen [138], (see also [139] for the solutions at the perturbative level).

The macroscopic line element is assumed to be

$$d\bar{s}^2 = \langle g_{\mu\nu}\rangle dx^{\mu}dx^{\nu} = -dt^2 + a^2(t)[dx^2 + dy^2 + dz^2]. \tag{3.87}$$

They further assumed isotropy and homogeneity for the structure of the connection correlation tensor $Z^{\alpha\ \ \mu}_{\beta\gamma\ \ \nu\sigma}$.

The macroscopic field equations (3.85) thus give

$$\frac{\dot{a}^2}{a^2} = \frac{8\pi G}{3}\rho - \frac{\mathcal{K}^2}{a^2}, \tag{3.88}$$

$$\frac{\ddot{a}}{a} = -\frac{4\pi G}{3}(\rho + 3p), \tag{3.89}$$

where overdots denote differentiation with respect to t, and ρ is the macroscopic energy density that obeys

$$\dot{\rho} + 3\frac{\dot{a}}{a}(\rho + p) = 0, \tag{3.90}$$

and $\mathcal{K}$ comes from the correction part of the field equations and it is different from k in the standard model. The non-trivial components of the connection correlation and affine deformation tensors are

$$Z^{j\ k}_{jj\ jk} = Z^{j\ k}_{kj\ kk} = Z^{j\ j}_{jj\ kk} = Z^{k\ k}_{jj\ kk} = -\frac{2}{10}\mathcal{K}^2, \tag{3.91}$$

$$Z^{i\ k}_{jj\ ik} = Z^{j\ i}_{ij\ kk} = Z^{i\ i}_{jj\ kk} = Z^{j\ k}_{ij\ ik} = -\frac{1}{10}\mathcal{K}^2, \tag{3.92}$$

where $[ijk]$ can be ordered in of the triples of $[1,2,3],[2,3,1],[3,1,2]$ and

$$A^0_{ii} = \mathcal{K}a(t); \quad A^i_{i0} = A^0_{00} = \frac{\mathcal{K}}{a(t)}, \tag{3.93}$$

where i takes 1,2,3 values [139].

The macroscopic geometry therefore evolves like the FL solution of Einstein equation with an extra spatial curvature term in the macroscopic equivalent of the Friedmann equation, even though the macroscopic geometry is spatially flat.

Thus, the averaged Einstein field equations for a spatially flat, homogeneous, and isotropic macroscopic space-time geometry take the form of the Friedmann equations of general relativity for a non-flat FL geometry.

In any case, Zalaletdinov's approach leads to a complex set of equations that despite some valiant attempts have not been productive in terms of the cosmological backreaction problem yet.

3.7.6. Observational constraints

The observational consequences of the solution, explained above, have been recently investigated by Clarkson et al [140]. The spatial curvature of the macroscopic space-time is decoupled from the spatial curvature that appears in the macroscopic Friedmann equations. This is an important difference from the standard approach to cosmology, where it is assumed that Einstein field equations hold whatever the smoothing scale is, and that the spatial curvature in the Friedmann equation is therefore identical to the spatial curvature of the macroscopic space-time.

Writing the line element of the macroscopic geometry as

$$ds^2 = \langle g_{\mu\nu}\rangle dx^\mu dx^\nu = -dt^2 + a^2(t)[\frac{dr^2}{1-k_g r^2} + r^2 d\Omega], \tag{3.94}$$

where the geometrical curvature, k_g, is in general, a function of the scale of Σ. The scale factor $a(t)$ is that of the macroscopic space-time. On scales larger than Σ the macroscopic field equations then become

$$H^2 = \frac{\dot{a}^2}{a^2} = \frac{8\pi G}{3}\rho - \frac{k_d}{a^2} + \frac{\Lambda}{3}, \tag{3.95}$$

where the dynamical curvature, k_d is again a function of scale, and includes both spatial curvature in the metric, k_g, and the correlation tensor, $Z^{\alpha\ \mu}_{\beta[\gamma\ \nu\sigma]}$. We recover the case of usual result $k_g = k_d$, if and only if the contribution from $Z^{\alpha\ \mu}_{\beta[\gamma\ \nu\sigma]}$ vanishes.

More generally, in a space-time that is inhomogeneous on small scales, we do not expect these two spatial curvature terms to be equal. Defining $\Omega_{k_g} = -\frac{k_g}{a_0^2 H_0^2}$ and $\Omega_{k_d} = -\frac{k_d}{a_0^2 H_0^2}$, the macroscopic Friedmann equation becomes $\Omega_m + \Omega_{k_d} + \Omega_\Lambda = 1$ where Ω_m and Ω_Λ are the usual expressions for the fraction of the energy content of the Universe in matter and the cosmological constant, respectively.

Using the solutions to the macroscopic Friedmann equation (3.95) together with integrating a null trajectory in (3.94), one can derive the luminosity distance distance-redshift relation in the macroscopic geometry

$$d_L(z) = \frac{(1+z)}{H_0\sqrt{|\Omega_{k_g}|}} f_{k_g}\Big(\int_{\frac{1}{1+z}}^{1} \frac{\sqrt{|\Omega_{k_g}|}da}{\sqrt{\Omega_{k_d}a^2 + \Omega_\Lambda a^4 + \Omega_m a}} \Big), \tag{3.96}$$

where $f_{k_g}(x) = \sinh(x), x$ or $\sin(x)$ for the case of $k_g > 0$, $k_g = 0$ and $k_g < 0$, respectively.

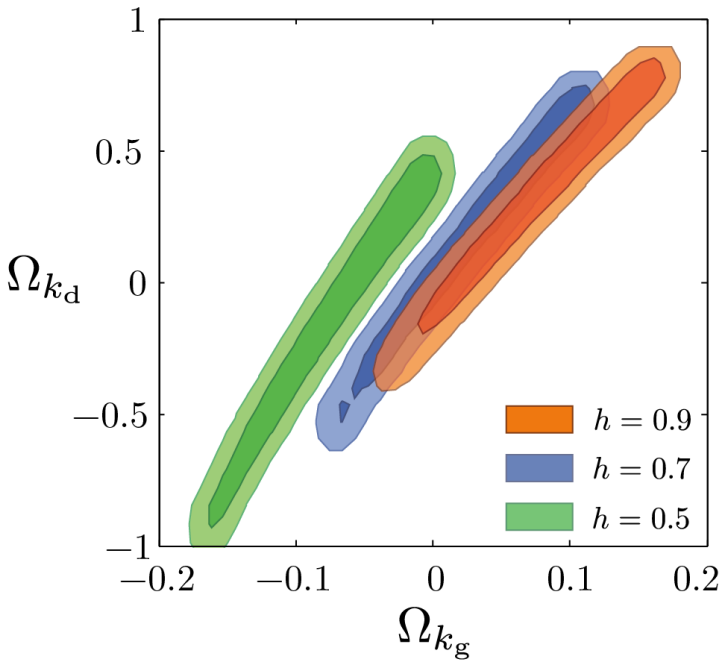

Figure 3.5. Constraints on the two curvature parameters, Ω_{k_g} and Ω_{k_d} from CMB+H_0 for $h = 0.9, 0.7$ and 0.5 at 68% and 95% confidence level for the shaded areas. The constraints are weakened compared to the case of the standard model where Ω_{k_d} and Ω_{k_d} are considered to be identical. Figure credit: Clarkson et al. [140].

Allowing the effects of Ω_{k_g} and Ω_{k_d} to be independent has considerable consequences for the measurement of cosmological parameters. As we see in Fig. 3.5, if we consider

CMB+H_0 constraints on spatial curvature in the standard model, we find that due to a degeneracy between the effects of Ω_{k_g} and Ω_{k_d} in equation (3.96) the significant constraints on spatial curvature that are obtained in the standard model, are gone. The combined constraints on Ω_{k_g} and Ω_{k_d} using data from the HST [141], the WMAP 7 year data of the temperature-temperature correlations in the CMB [1], the Union 2 [142] and SDSS SNIa data sets [143], and the constraints on the 'volume distance' from the BAOs [144] are shown in Fig. 3.6.

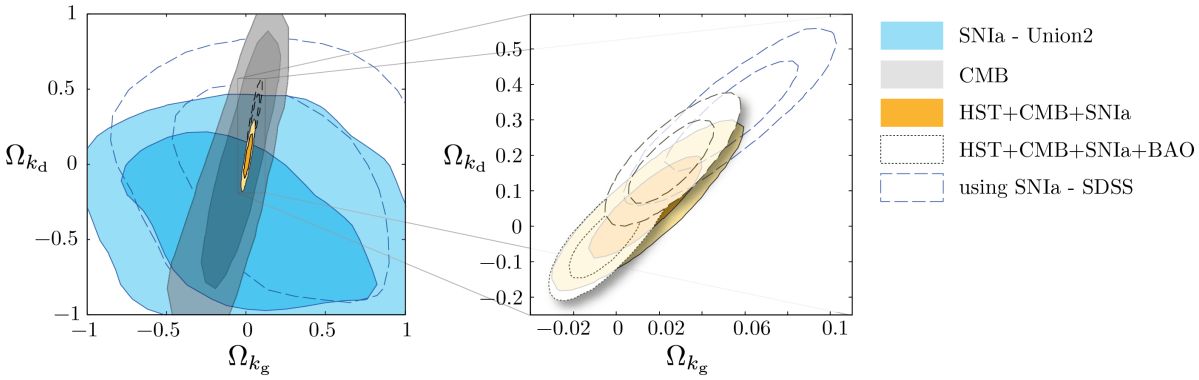

Figure 3.6. The left-hand plot shows the constraints on Ω_{k_g} and Ω_{k_d} from the CMB (gray), SNIa-Union2 (blue), and SNIa-SDSS (hollow and dashed), as well as the combined constraints including HST (orange). The one on the right-hand shows the combined constraints from these different data set including the BAO. The geometrical curvature is noticeably constrained rather than the dynamical one. The constraints from the CMB and SNIa individually are weak, but get more tight when combined with HST data. Figure credit: Clarkson et al. [140].

4. Effects of Inhomogeneity on the Propagation of Light

The aim of this chapter is to investigate the effects of averaging on light propagation in the Universe, or how to derive the equation of motion of light in an averaged description of the Universe from the null geodesic equation in the inhomogeneous Universe. Therefore we ask if some effects can be seen in observations in the lumpy Universe. For example how do averaged inhomogeneities affect the redshift of photons.

In the standard cosmology the background geometry is used for observing the large scale of Universe. Speaking of *background* means the homogeneous isotropic flat FL Universe with neglecting the details of small scales and local inhomogeneities.

Observational cosmology is based on light trajectories and the paths of light are on null geodesics. Inhomogeneity affects the light trajectories. Therefore we should see these effects on observations in the lumpy Universe.

Some aspects of this are very well understood and studied in great depth, e.g. CMB photons are related to density fluctuations by the Sachs-Wolfe effect. The integrated Sachs-Wolfe effect [26] is caused by gravitational redshift. The gravitational lensing [39] plays an important role in interpreting the effects of light propagation.

The motion of photons in an averaged geometry has already been studied in [145] and in a more precise way in [103, 146]. Yet in a different approach using a gauge-invariant formalism, the averaged geometry on the past null cone has been introduced [92, 147]. This allows to average the luminosity-redshift relation [149, 151, 152]. The study of light propagation in inhomogeneous Swiss-Cheese models by simulating Hubble diagrams has been probed recently in [153, 154, 155].

In this chapter, we shortly introduce the three works mentioned above, respectively in sections 4.1, 4.2 and 4.3.

In later sections, we follow a new approach and present our own work, which is the most general approach to trace the trajectories of light in the averaged Universe and includes some of the results of the mentioned works above.

In section 4.4 we outline the topic of the geodesic equation of motion in the averaged Universe and its differences to the background case. We do not limit the calculations to the spatial averaging model. In fact, it is essential for our work that a covariant procedure to average a space-time metric exists and thus the obtained results can be used for a general averaged model of the Universe. We make the plausible assumption that an averaging procedure that respects the causal structure of space-time exists. Though we are not able to explicitly construct it, it is obvious that the FL model is a good

description of the observed Universe at large scales. If this is the result of an average process, causality seems to be respected. Based on this and a second (more technical) assumption specified in that section, we derive an effective equation for light propagation in an averaged Universe.

We continue in section 4.5 to evaluate that equation for a Universe that can be described by a flat FL model after averaging. Finally, the last two sections 4.6 and 4.7 contain an estimation for the obtained effective Hubble expansion rate and a comparison to previous works.

4.1. Light propagation in an irrotational dust Universe

In studies of backreaction, the average expansion rate and other spatial averages have often been considered without relating them to observable quantities such as redshift and distance. Quantitative studies of light propagation were consistent with the idea that in statistically homogeneous and isotropic models, in which the average expansion rate is close to the FL case, deviations in the redshift and distance are negligible and results for light propagation are close to the FL case.

In contrast to these studies, Räsänen has assumed that the average expansion rate is not the same as in the exactly homogeneous and isotropic FL model of the Universe [103].

Here we explain the achievements of his work, where light propagates in an irrotational dust Universe, which is statistically homogeneous and isotropic (see [146] for the full discussion). We will see that redshift and distance are determined by an averaged expansion rate and the null geodesic shear.

4.1.1. The redshift

Let us consider the tangent vector u^μ for the general space-time geometry, determined by the Einstein equations. The light propagation in such a space-time traced by photon null geodesics with tangent vector k^μ. On the other hand, the redshift z of a source is defined by (1.20). The wavelength is proportional to the inverse of the frequency ω, so that

$$1 + z = \frac{\omega_s}{\omega_o}, \tag{4.1}$$

where ω_s and ω_o denote the frequency of the source and the observer, respectively.

The energy is related to the observer's velocity and can be defined as $\omega = -u_\mu k^\mu$. We can further decompose the tangent vector k^μ into its amplitude and the direction e^μ which is a unit vector, i.e. $e_\mu e^\mu = 1$ and it is orthogonal to the tangent vector u^μ such that $u_\mu e^\mu = 0$, thus

$$k^\mu = \omega(u^\mu + e^\mu). \tag{4.2}$$

The vector e^μ is spatial, i.e. $h^\mu_\nu e^\nu = e^\mu$.

Note that $h_{\mu\nu} \equiv g_{\mu\nu} + u_\mu u_\nu$ and thus $h_{\mu\nu}u^\nu = 0$. The covariant derivative of u^μ in an dust Universe can be written as [156, 87]

$$\nabla_\nu u_\mu = \theta_{\mu\nu} + w_{\mu\nu} = \frac{1}{3}h_{\mu\nu}\theta + \sigma_{\mu\nu} + w_{\mu\nu}, \tag{4.3}$$

where $\theta_{\mu\nu}$ is the symmetric part of the expansion tensor and $w_{\mu\nu}$ is the vorticity tensor. Note that $w_{\mu\nu} = 0$ for irrotational dust.

Now by means of equations (4.2) and (4.3) and taking into account $k^\mu \nabla_\mu k^\nu = 0$, we can take the derivative of ω with respect to an affine parameter λ, to see how it evolves along the null geodesic

$$\begin{aligned} \partial_\lambda \omega \equiv k^\mu \nabla_\mu \omega &= -k^\mu k^\nu \nabla_\mu u_\nu \\ &= -k^\mu k^\nu \theta_{\nu\mu} \\ &= -\omega^2 e^\mu e^\nu \theta_{\mu\nu} \\ &= -\omega^2 \Big(\frac{1}{3}\theta + \sigma_{\mu\nu} e^\mu e^\nu\Big). \end{aligned} \tag{4.4}$$

Integrating the above equation gives us $\omega \propto \exp\Big(\int d\lambda\, \omega\, \theta_{\mu\nu} e^\mu e^\nu\Big)$. We then get the following expression for the redshift, by using equation (4.1)

$$1 + z = \exp\Big(\int_{\lambda_s}^{\lambda_o} d\lambda\, \omega[\frac{1}{3}\theta + \sigma_{\mu\nu} e^\mu e^\nu]\Big), \tag{4.5}$$

where the integral is from the source to the observer along the geodesic. Since in the FL model, the result does not depend on the direction of the null geodesic, the shear also vanishes there, and the only remaining contribution must come from the expansion rate of the first term in the right hand side of equation (4.5).

If we assume statistically homogeneous and isotropic Universe, and split the expansion rate $\theta(t, x)$ into the average value on the hypersurface of constant time at each point along the geodesic, so that $\theta(t, x) \equiv \Delta\theta + \langle\theta\rangle(t)$. The redshift expression thus can be written as

$$1 + z \approx \exp\Big(\int_{t,\lambda}^{t_0} dt[\frac{1}{3}\langle\theta\rangle(t) + \frac{1}{3}\Delta\theta(t, x)]\Big). \tag{4.6}$$

Equation (4.6) corresponds to the first and higher orders of approximations for $1/a(t)$.

However, in the FL case, the contribution $\Delta\theta$ has been neglected, since we do not relate the redshift to any specific geodesic in homogeneous and isotropic model of the Universe. Thus the redshift to first approximation there, is given by

$$1 + z \approx 1 + \langle z\rangle \approx \frac{1}{a(t)}. \tag{4.7}$$

4.1.2. The angular diameter distance

Generally, the redshift should be related to other observable quantities such as luminosity distance, angular diameter distance, or the age of the Universe. Here we discuss the change in angular diameter distance. Following the same construction as (4.3), we can decompose the covariant derivative of k^μ as

$$\nabla_\nu k_\mu = \tilde{\theta}_{\mu\nu} = \frac{1}{2}\tilde{h}_{\mu\nu}\tilde{\theta} + \tilde{\sigma}_{\mu\nu}, \tag{4.8}$$

where $\tilde{\theta} = \nabla_\mu k^\mu = \tilde{h}^\mu_{\ \nu}\nabla_\mu k^\nu$ is the expansion rate and $\tilde{\sigma}_{\mu\nu} = \tilde{h}_\mu^{\ \gamma}\tilde{h}_\nu^{\ \delta}\nabla_\gamma k_\delta - \frac{1}{2}\tilde{h}_{\mu\nu}\tilde{\theta}$ is the shear. The vorticity of a light bundle vanishes, because unlike u^μ, k^μ is a gradient of a scalar.

By use of equation (4.8), the Einstein equation $R_{\mu\nu} - \frac{1}{2}g_{\mu\nu}R = 8\pi G T_{\mu\nu} = 8\pi G\rho u_\mu u_\nu$ and the null condition $k^\mu\nabla_\mu k^\nu$, we take the derivative of $\tilde{\theta}$ with respect to λ

$$\begin{aligned}
\partial_\lambda\tilde{\theta} \equiv k^\mu\nabla_\mu\nabla_\nu k^\nu &= k^\mu R_{\mu\ \nu}^{\ \nu\ \gamma} k_\gamma + k^\mu\nabla_\nu\nabla_\mu k^\nu \\
&= -R_{\mu\nu}k^\mu k^\nu - \nabla_\nu k^\mu\nabla_\mu k^\nu \\
&= -8\pi G\rho\omega^2 - 2\tilde{\sigma}^2 - \frac{1}{2}\tilde{\theta}^2 \\
&= -2\mu^2 - \frac{1}{2}\tilde{\theta}^2,
\end{aligned} \tag{4.9}$$

where $\tilde{\sigma}^2 = \frac{1}{2}\tilde{\sigma}_{\mu\nu}\tilde{\sigma}^{\mu\nu}$ and $\mu^2 = 4\pi G\rho\omega^2 + \tilde{\sigma}^2$. This will be used later on to determine the evolution of the angular diameter distance along the null geodesic.

On the other hand, according to [157] the angular diameter distance is proportional to the linear size of the null geodesics, $D_A \propto s$, and the expansion rate is expressed as $\tilde{\theta} = 2\partial_\lambda s/s$. Thus

$$D_A \propto \exp\left(\frac{1}{2}\int d\lambda\tilde{\theta}\right). \tag{4.10}$$

Using equation (4.9) together with (4.10), we obtain the relation below for the angular diameter distance

$$\partial_\lambda^2 D_A = -(4\pi G\rho\omega^2 + \tilde{\sigma}^2)D_A = -\mu^2 D_A. \tag{4.11}$$

Due to the assumption of spatial symmetry, the distance does not depend on the spatial position, so that $\partial_\lambda D_A = \omega\partial_t D_A = -\omega(1+z)H(z)\partial_z D_A$, where $H(z)$ is the Hubble expansion rate.

Considering $\omega \propto 1+z$ and $\rho \propto a^{-3} \propto (1+z)^3$, equation (4.10) can be written as

$$H\partial_z\Big[(1+z)^2 H\partial_z D_A\Big] = -4\pi G\rho D_A = -4\pi G\rho_0(1+z)^3 D_A, \tag{4.12}$$

where energy density ρ should be replaced by $\langle\rho\rangle$ in the averaged case.

As a result of equation (4.12), we see that the distance is determined by the Hubble expansion rate $H(z)$. Therefore the equation for the average angular diameter distance

in terms of $H(z)$ in a statistically homogeneous and isotropic dust Universe is the same as in the FL model, only if we did not have any changes in the average Hubble expansion rate (and also in the average energy density). However, backreaction is not expected to produce an expansion rate identical to the FL model.

In Räsänen's work, both equations (4.6) and (4.12) rely on Buchert's scalar averaging, and cannot be generalized to the real Universe with tensorial geometries. We will derive a more general result for propagation of light in an averaged Universe in section 4.4.

4.2. The light cone averaging procedure

A covariant prescription for scalar averaging on null hypersurfaces has been proposed by Veneziano and collaborations [92, 147, 149]. This can be applied to the past light cone of an observer in the context of an inhomogeneous metric. In order to do so, a *geodesic light cone frame* has been introduced, where the averaging prescription can be simplified.

This prescription has been called as "the light cone averaging procedure". Two possible applications to this procedure are the averaging of the redshift parameter and the luminosity-redshift relation. Here we briefly review this procedure (see [151, 152] for further discussions).

Let us consider a four dimensional integral of a scalar, $F(x)$, as

$$I(F,\Omega)=\int_{\Omega}d^4x\sqrt{-g(x)}F(x)\equiv\int_{\mathcal{M}_4}d^4x\sqrt{-g(x)}F(x)\mathrm{W}_{\Omega}(x), \tag{4.13}$$

where the integration region Ω, is defined in terms of a suitable scalar window function, W_{Ω}.

Now let us recall the three-dimensional spacelike hypersurface $\Sigma(A)$ and assume the hypersurface is defined via a scalar field, $A(x)$, with timelike gradient, $\partial_\mu A(x)$. The window function, W, selects a region with temporal boundaries determined by the hypersurfaces $\Sigma(A)$. Also, the spatial boundary determined by the coordinate condition $B<r_0$, where B is a scalar function of the coordinates with spacelike gradient $\partial_\mu B$, satisfying $\partial_\mu B\partial^\mu B=0$, and r_0 is a positive constant. Thus the window function can be written as [150]

$$\mathrm{W}_{\Omega}(x)=n^\mu\nabla_\mu\Theta(A(x)-A_0)\Theta(r_0-B(x)), \tag{4.14}$$

where Θ is the Heaviside step function, and the unit normal n_μ is

$$n_\mu=-\frac{\partial_\mu A}{\sqrt{-\partial_\nu A\partial^\nu A}};\quad n_\mu n^\mu=-1. \tag{4.15}$$

Using the window function in equation (4.14), the gauge-invariant definition of the integral of a scalar function $F(x)$ in (4.13) becomes

$$I(F;A_0)=\int d^4x\sqrt{-g(x)}\delta(A(x)-A_0)\sqrt{-\partial_\mu A\partial^\mu A}\;\Theta(r_0-B(x))\;F(x). \tag{4.16}$$

Another hypersurface integral, which indicates the volume integral is

$$I(1;A_0)=\int d^4\sqrt{-g}\Theta(r_0-B)\delta(A-A_0)\sqrt{-\partial_\mu A\partial^\mu A}, \tag{4.17}$$

where the integration region describes the causally connected section of Σ by varying the light cone hypersurface.

Therefore, the averaging prescription for a scalar $F(x)$ on the hypersurfaces of constant A, following [147], is defined as

$$\langle F\rangle_{A_0}=\frac{I(F;A_0)}{I(1;A_0)}. \tag{4.18}$$

4.2.1. Geodesic light cone coordinate

The integral equations and their averages can take a simpler form in a so-called *geodesic light cone (GLC) coordinates*, where the averaging prescription greatly simplifies, while keeping all the required degrees of freedom. This is in analogy with choosing the synchronous gauge coordinates for spatial averaging, such that the timelike coordinate of the GLC gauge can be identified with the cosmic time t of the synchronous gauge. The coordinates, $x^\mu=(\tau,w,\theta^\alpha)$, specifies the metric of GLC coordinates as

$$ds^2=\Upsilon^2dw^2-2\Upsilon dwd\tau+\gamma_{\alpha\beta}(d\theta^\alpha-U^\alpha dw)(d\theta^\beta-U^\beta dw), \tag{4.19}$$

where Υ is an arbitrary function, U^α is a two dimensional vector and $\gamma_{\alpha\beta}$ is a symmetric tensor of which $\alpha,\beta=1,2$. One can choose w as a null coordinate, i.e. $\partial_\mu w\partial^\mu w=0$, and $\partial_\mu\tau$ as a geodesic flow, so that $(\partial^\nu\tau)\nabla_\nu(\partial_\mu\tau)\equiv 0$.

In a more familiar way, these parameters can be easily written in a limiting case of the spatially flat Robertson-Walker metric be setting

$$\begin{aligned} w\equiv r+\eta;\quad \tau\equiv t;\\ \Upsilon\equiv a(t);\quad U^\alpha\equiv 0;\\ \gamma_{\alpha\beta}d\theta^\alpha d\theta^\beta\equiv a^2(t)r^2(d\theta^2+\sin^2\theta d\phi^2),\end{aligned} \tag{4.20}$$

where η is the conformal time of the homogeneous metric ($d\eta=dt/a(t)$).

Finally, from equation (4.18), the average of a scalar quantity $F(\tau,w,\theta^\alpha)$ over the compact surface Σ, defined by the intersection of our past light-cone $w=w_0$ with the spacelike hypersurface $\tau=\tau_s$ is given by [147, 148]

$$\begin{aligned}\langle F\rangle_{w_0,\tau_s}&=\frac{\int_\Sigma d^4x\sqrt{-g}\delta(w-w_0)\delta(\tau-\tau_s)F(\tau,w,\theta^\alpha)|\partial_\mu\tau\partial^\mu w|}{\int_\Sigma d^4x\sqrt{-g}\delta(w-w_0)\delta(\tau-\tau_s)|\partial_\mu\tau\partial^\mu w|}\\ &=\frac{\int d^2\theta\sqrt{\gamma(w_0,\tau_s,\theta^\alpha)}F(w_0,\tau_s,\theta^\alpha)}{\int d^2\theta\sqrt{\gamma(w_0,\tau_s,\theta^\alpha)}},\end{aligned} \tag{4.21}$$

where $\gamma=\det\gamma_{\alpha\beta}$.

4.2.2. Luminosity-redshift relation

The next step is to apply the light cone averaging formalism to some physical applications such as the luminosity-distance relation.

In GLC, the null geodesics connecting sources and observer are characterized by the tangent vector, $k^\mu = g^{\mu\nu}\partial_\nu w = -\delta^\mu_\tau \Upsilon^{-1}$, where the photons reach the observer travelling at constant w and θ^α. Consider a light ray emitted at the intersection between the past light-cone of the observer, $w = w_0$ and the spatial hypersurface $\tau = \tau_s$, and received to the observer at $\tau = \tau_0 > \tau_s$. The redshift parameter z_s in GLC coordinates becomes

$$1 + z_s = \frac{(k^\mu u_\mu)_s}{(k^\mu u_\mu)_o} = \frac{\Upsilon_0}{\Upsilon_s}, \tag{4.22}$$

where $\Upsilon_0 = \Upsilon(w_0, \tau_0, \theta^\alpha)$ and $\Upsilon_s = \Upsilon(\omega_0, \tau_s, \theta^\alpha)$.

For light-cone averages on surfaces of redshift $z = z_s$, equation (4.21) becomes

$$\langle F \rangle_{w_0, z_s} = \frac{\int d^2\theta \sqrt{\gamma(w_0, \tau(z_s, w_0, \theta^\alpha), \theta^\beta)} F(w_0, \tau(z_s, w_0, \theta^\alpha), \theta^\beta)}{d^2\theta \sqrt{\gamma(w_0, \tau(z_s, w_0, \theta^\alpha), \theta^\beta)}}. \tag{4.23}$$

The luminosity-redshift relation has been studied within a gauge-invariant approach for linearly perturbed FL model of the Universe in [158].

The luminosity distance d_L of a source at redshift z is related to the angular distance d_A of the source, as $d_L = (1+z)^2 d_A$.

One can obtain the average value of the luminosity distance, d_L, on the two-sphere embedded in the light cone, by inserting this result into equation (4.23) (see [147, 148] for the full discussion). The expression for $\langle d_L \rangle$ as a function of z_s, in the GLC gauge is

$$\langle d_L \rangle_{w_0, z} = (1 + z_s)^2 \frac{\int d^2\theta \sqrt{|\gamma(w_0, \tau(z_s, w_0, \theta^\alpha), \theta^\beta)|}\, d_A(w_0, \tau(z_s, w_0, \theta^\alpha), \theta^\beta)}{\int d^2\theta \sqrt{|\gamma(w_0, \tau(z_s, w_0, \theta^\alpha), \theta^\beta)|}}. \tag{4.24}$$

The latter equation shows the effects of inhomogeneities on observables related to light cones, with the use of light like hypersurfaces and two-surfaces embedded on a past light cone.

The second order expression for $\langle d_L \rangle$ has been studied in [152].

4.3. Propagation of light in Swiss-Cheese models

One of the relativistic toy models for the inhomogeneous Universe is known as *Swiss-Cheese* model [96, 97, 98]. This scenario is constructed by removing spherical regions from a homogeneous FL background (the *cheese*) and replacing them with inhomogeneous density distributions with the same gravitating mass (mass-compensated *voids*).

One of the solution in Swiss-Cheese models for the Einstein equations is the Szekeres model [159, 160]. Results of the impact of inhomogeneities on the expansion rate (which is a good description of light propagation) for the exact dust solutions in the Szekeres model can be found in [161] where the authors claim the results remain close to the background case.

Another solution in the context of Swiss-Cheese models is the Lemaitre-Tolmann-Bondi (LTB) solution, which is a general spherically symmetric solution to Einstein equations for dust. The later model is a useful toy for studying backreaction effects, because the symmetry allows quantitative studies without the use of approximations. Moreover, it is a suitable choice to model the observed voids in the Universe. Therefore, it is perhaps the most studied model in this context. In the earliest work [162] the author used the LTB model to obtain a reasonable fit to supernovae luminosity densities and showed that the acceleration implied by the supernovae data can be explained by a large scale inhomogeneity without the need for a cosmological constant. A later study [163] showed that backreaction slows down the expansion if measured in terms of the proper time, but speeds it up if measured in terms of the energy density or the scale factor. However, although there are many other studies about the averaged luminosity and angular diameter distances (see for example [164, 165, 166, 167]) in this model, it remains a toy model which is not suitable to describe the real Universe.

The propagation of light in a Swiss-Cheese model was first studied by Kontowski [168] and in a wider investigation by Dyer and Roeder [169]. It was shown in both works that in a clumpy Universe, a lower deceleration parameter appears on the Hubble diagram, and the luminosity-redshift relation will be different with respect to the one from the purely homogeneous Universe[1].

Moreover, the inhomogeneities in Swiss-Cheese models are used to address to the so-called *Ricci-Weyl focussing problem*. The FL model of the Universe contains a non-zero Ricci tensor, but a vanishing Weyl tensor, while the real Universe must contain a non-vanishing Weyl tensor as well. Since the Ricci tensor vanishes inside the holes, we consider the Swiss-Cheese models with zero Ricci tensor and non-zero Weyl tensor.

The approach presented by Fleury and his collaborators [153, 154] is justified for this class of Swiss-Cheese models (i.e. it is in the line with [168] and [169]), yet keeps a well-defined FL averaged behavior, so that one starts from a spatially homogeneous and isotropic FL geometry, then considers individual masses embedded in a spatially homogeneous fluid. Each of these masses are lying at the center of a spherical voids where a light beam can travel through them (see Fig. 4.1). This keeps the same dynamics and average properties for the model as the FL model. However, conversely to the FL model where a beam of light experiences the Riemannian curvature via contribution from the Ricci tensor, here the Weyl tensor dominates.

[1] This differs from the case for the sub-model of Swiss-Cheese with LTB solution inside the holes where the luminosity-redshift relation remains unchanged with respect to the homogeneous Universe [170, 171].

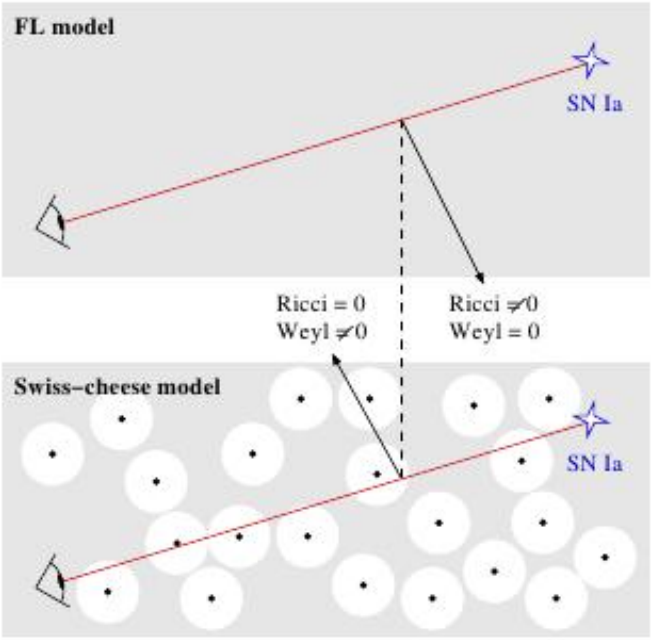

Figure 4.1. A light beam travels through a Swiss-Cheese Universe from a source to an observer. The dynamics of the model is identical to the FL model, yet with a zero Ricci tensor and non-vanishing Weyl tensor converse to the FL case. Figure credit: Fleury et al. [153].

The geometry outside the holes is described by the standard FL geometry and RW metric. Inside the holes however, the geometry is described by an extension of Schwarzschild metric with a cosmological constant, known as the Kottler solution [172] (see also [173] for a review).

Indeed, a light beam is described by a bundle of null geodesics encoded in a 2×2 matrix $\mathcal{D}^A_B$ called the Jacobi map [153]. Thus the angular and luminosity distances read

$$D_A = \sqrt{|det\mathcal{D}^A_B|}; \qquad D_L = (1+z)^2 D_A. \tag{4.25}$$

The evolution of the Jacobi map with light propagation is governed by the Sachs equation [174], where an observer with four velocity u^μ has been considered and the wave vector k^μ satisfies the geodesic equation. The Sachs basis $(s^\mu_A)_{A=1,2}$ has been then introduced as an orthogonal basis of a plane orthogonal to u^μ and k^μ,

$$s^\mu_A u_\mu = s^\mu_A k_\mu = 0, \tag{4.26}$$

such that it spans a screen on which the observer projects the beam of light. The Sachs equation thus read

$$\frac{d^2}{dv^2}\mathcal{D}^A_B = \mathcal{R}^A_C \mathcal{D}^C_B, \tag{4.27}$$

where v denotes an affine parameter along the geodesics, and $\mathcal{R}_{AB} = R_{\mu\nu\alpha\beta}k^\nu k^\alpha s^\mu_A s^\beta_B$ is the projection of the Riemann tensor. As the same way that the Riemann tensor can be decomposed into a Ricci part $R_{\mu\nu}$ and a Weyl part $C_{\mu\nu\alpha\beta}$, we can also split $\mathcal{R}_{AB}$ into Ricci and Weyl focussing parts as

$$(\mathcal{R}_{AB}) = \begin{pmatrix} \Phi_{00} & 0 \\ 0 & \Phi_{00} \end{pmatrix} + \begin{pmatrix} -\mathrm{Re}\Psi_0 & \mathrm{Im}\Psi_0 \\ \mathrm{Im}\psi_0 & \mathrm{Re}\Psi_0 \end{pmatrix}, \tag{4.28}$$

with

$$\Phi_{00} \equiv -\frac{1}{2}R_{\mu\nu}k^\mu k^\nu; \qquad \Psi_0 \equiv -\frac{1}{2}C_{\mu\nu\alpha\beta}(s^\mu_1 - is^\mu_2)k^\nu k^\alpha(s^\beta_1 - is^\beta_2). \tag{4.29}$$

From equations (4.27) and (4.28) one can claim that the Ricci term tends to isotropically focus the light beam, while the Weyl term tends to shear and/or rotate the beam[2].

Compared to the FL model, propagation of light through such a Swiss-Cheese model goes along with a reduced Ricci focussing and thus an increased luminosity distance for high redshifts (see equations (4.25-4.28)). These changes due to the inhomogeneities will affect the Hubble diagram in a way that the determination of cosmological parameters is biased. Consider the given Swiss-Cheese Universe where its FL regions are characterized by the background cosmological parameters $(\Omega_m, \Omega_k, \Omega_\Lambda)$. If an observer sits in the homogeneous part and observes a supernovae in this inhomogeneous Universe and fits the FL luminosity-redshift relation, he will obtain a set of apparent cosmological parameters $(\bar{\Omega}_m, \bar{\Omega}_k, \bar{\Omega}_\Lambda)$, which differ from the background values. An example of a mock Hubble diagram corresponding to the given Swiss-Cheese model with $(\Omega_m, \Omega_k, \Omega_\Lambda) = (1, 0, 0)$ is plotted in Fig. 4.2, where it has been compared to a homogeneous universe with the same parameters and with $(\Omega_m, \Omega_k, \Omega_\Lambda) = (0.3, 0, 0.7)$.

The results of the current model has been furthermore compared to the Dyer-Roeder approximation in [155], which shows both procedures are in a good agreement for predicting the distance-redshift relation.

[2]The problem of how Weyl focussing associated with point-like matter sources is converted into Ricci focussing of smooth matter sources, has been discussed in a great detail in [175].

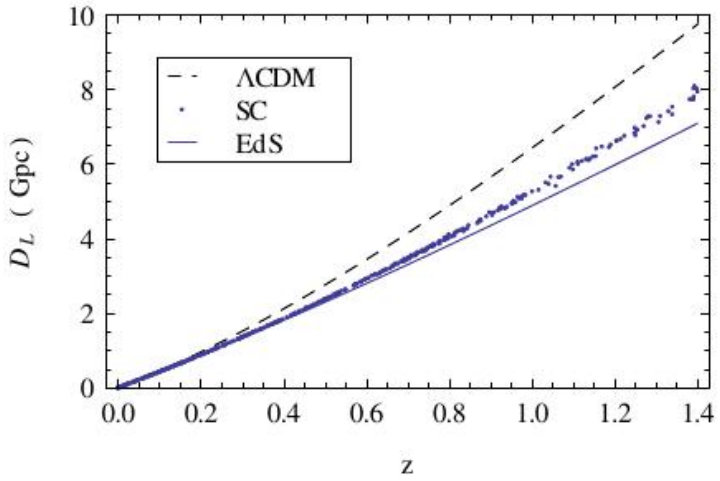

Figure 4.2. Hubble diagram of a Swiss-Cheese Universe (plotted with dots), in comparison with the displayed $D_L(z)$ for homogeneous Universes of EdS and ΛCDM background. The EdS case with parameters $(1, 0, 0)$ is plotted as a blue solid line and the ΛCDM model with $(0.3, 0, 0.7)$ is the black dashed line. Figure credit: Fleury et al. [153].

4.4. Propagation of light in an averaged space-time

The work presented below contains the main result of my thesis. The essence of it has been published in [8].

The crucial issue is how we justify the smaller scales to the background geometry and transform from a lumpy Universe to the smoothed one.

A problematic aspect of spatial averaging is that we do not observe spatial volumes, but rather null volumes and that Buchert's, Skarke's and Zalaletdinov's approaches neglect possible effects on the propagation of photons. Also, the work of Räsänen and Veneziano is restricted to the perturbation level and the work of Fleury is based on a toy model.

The key point here will be to use an averaged metric that describes the smoothed manifold. This allows us to consider the paths of light propagation in the averaged space-time. But the metric tensor cannot be averaged easily, and many current approaches of averaging cannot be used to construct such an averaged metric [8]. The exception is the averaging procedure defined by Zalaletdinov and we view it as a proof of existence of such an average. Thus we are going to assume that the average of a metric is a metric. Zalaletdinov showed that an average procedure with that property exists, but it is not unique.

According to Zalaletdinov, a line element for the macroscopic space-time is defined as

$$ds^2 = \bar{g}_{\mu\nu} dx^\mu dx^\nu, \tag{4.30}$$

where $\bar{g}_{\mu\nu}$ is the macroscopic metric tensor, which is used to calculate the macroscopic Christoffel symbols. The so defined macroscopic Christoffel symbols guarantee that the macroscopic space-time is a Riemannian manifold itself and that there are no metric correlations [136]. Thus the averaged metric tensor $\langle g_{\mu\nu}\rangle$ and the averaged inverse metric tensor $\langle g^{\mu\nu}\rangle$ can be identified as

$$\langle g_{\mu\nu}\rangle = \bar{g}_{\mu\nu}, \quad \langle g^{\mu\nu}\rangle = \bar{g}^{\mu\nu}. \tag{4.31}$$

As a second critical assumption, we are proposing that the averaged space-time agrees perfectly with the causal structure of the microscopic space-time. We think that this is a plausible assumption. At least this assumption is implicitly made in modern cosmology when it is assumed that the light-rays in the Universe that is assumed to be isotropic and homogeneous on large scales are null in a FL model. The example of the bilocal extension, based on the tetrad fields (3.62) has this property. Unfortunately, it is not useful for our purpose as it gives $\langle g_{\mu\nu}\rangle = g_{\mu\nu}$. Nevertheless, this proves that at least one bilocal extension that satisfies both required properties exists.

Let k^μ denote a null vector field. Its geodesic equation reads

$$k^\mu_{;\nu} k^\nu = 0, \tag{4.32}$$

whereby the covariant derivative can be split into the normal derivative and the Christoffel symbols $\Gamma^\mu_{\nu\rho}$ as

$$k^\mu_{,\nu} k^\nu + \Gamma^\mu_{\nu\rho} k^\nu k^\rho = 0. \tag{4.33}$$

The Christoffel symbol can be calculated from the metric,

$$\Gamma^\mu_{\nu\rho} = \frac{1}{2} g^{\mu\sigma}(g_{\sigma\rho,\nu} + g_{\sigma\nu,\rho} - g_{\nu\rho,\sigma}). \tag{4.34}$$

We cancel out the inverse metric in (4.33) by a multiplication with $g_{\lambda\mu}$, to avoid non-linearities in the metric,

$$g_{\lambda\mu}\left(k^\mu_{,\nu} k^\nu + \frac{1}{2} g^{\mu\sigma} g_{\sigma\rho,\nu} k^\nu k^\rho + \frac{1}{2} g^{\mu\sigma} g_{\sigma\nu,\rho} k^\nu k^\rho - \frac{1}{2} g^{\mu\sigma} g_{\nu\rho,\sigma} k^\nu k^\rho\right) = 0. \tag{4.35}$$

Simplifying the latter equation we get

$$g_{\mu\lambda} k^\mu_{,\nu} k^\nu + \left(g_{\nu\lambda,\mu} - \frac{1}{2} g_{\nu\mu,\lambda}\right) k^\mu k^\nu = 0. \tag{4.36}$$

Now we use the null condition $g_{\mu\nu} k^\mu k^\nu = 0$. Its derivative is also equal to zero. This can be expressed as

$$\left(k^\mu g_{\mu\nu} k^\nu\right)_{,\lambda} = k^\mu_{,\lambda} g_{\mu\nu} k^\nu + k^\mu g_{\mu\nu,\lambda} k^\nu + k^\mu g_{\mu\nu} k^\nu_{,\lambda} = 0. \tag{4.37}$$

Using this expression in the last term of equation (4.36) gives us

$$g_{\mu\lambda} k^\mu_{,\nu} k^\nu + g_{\nu\lambda,\mu} k^\mu k^\nu - \frac{1}{2}\Big[\underbrace{\left(k^\mu g_{\mu\nu} k^\nu\right)_{,\lambda}}_{=0} - g_{\mu\nu} k^\mu_{,\lambda} k^\nu - g_{\mu\nu} k^\mu k^\nu_{,\lambda}\Big] = 0. \tag{4.38}$$

From equation (4.38), we thus arrive at a more convenient form of the geodesic equation for null vector fields as

$$(k^{\mu}_{,\nu} g_{\mu\lambda} + k^{\mu}_{,\lambda} g_{\mu\nu} + k^{\mu} g_{\mu\lambda,\nu}) k^{\nu} = 0. \tag{4.39}$$

The big advantage for our purpose is that this form is linear in the metric.

As a next step, we average this equation in the following sense: We consider a particular light-ray, so k^{μ} is not subject to the averaging, but the metric and its derivative are.

In contrast to other approaches, this is not necessarily an average over a space-time region, it could also be an average over many realizations of space-times between a source and an observer, i.e. the bilocal extension operator could be viewed as connecting a given space-time to all its possible deformations and in this sense we can arrive at an average metric.

Thus we assume that averaging and contractions with k^{μ} commute. This assumption might not hold for all possible averaging schemes, but we think that this is a sensible assumption to make. Finally, we also assume that derivatives of the wave vector are not subject to averages. The reason is again that we take the point of view that we only average over the metric of space-time, but consider the same light-ray in the averaged and microscopic space-time. Thus the coordinate derivatives of the wave vector should not be affected by this averaging procedure. In other words, the same coordinate values correspond to the same physical event in the averaged and microscopic space-times. Distances, angles and time intervals between physical events are different however.

A consequence of the two assumptions mentioned above is that we preserve the null condition,

$$\langle k^{\mu} g_{\mu\nu} k^{\nu} \rangle = k^{\mu} \langle g_{\mu\nu} \rangle k^{\nu} = 0. \tag{4.40}$$

Note that in general the derivative of an averaged metric is different from the average of the derivative of the metric, i.e. $\langle g_{\mu\lambda,\nu} \rangle \neq \langle g_{\mu\lambda} \rangle_{,\nu}$. As this should be the leading correction, affecting the geodesic equation, we write

$$k^{\mu}_{,\nu} \langle g_{\mu\lambda} \rangle k^{\nu} + k^{\mu}_{,\lambda} \langle g_{\mu\nu} \rangle k^{\nu} + k^{\mu} \langle g_{\mu\lambda} \rangle_{,\nu} k^{\nu} + k^{\mu} \langle g_{\mu\lambda,\nu} \rangle k^{\nu} - k^{\mu} \langle g_{\mu\lambda} \rangle_{,\nu} k^{\nu} = 0. \tag{4.41}$$

Therefore we arrive at an averaged version of equation (4.39),

$$\left(k^{\mu}_{,\nu} \langle g_{\mu\lambda} \rangle + k^{\mu}_{,\lambda} \langle g_{\mu\nu} \rangle + k^{\mu} \langle g_{\mu\lambda} \rangle_{,\nu} \right) k^{\nu} = k^{\mu} T_{\mu\lambda\nu} k^{\nu} \equiv I_{\lambda}, \tag{4.42}$$

where $T_{\mu\lambda\nu}$ is equal to

$$T_{\mu\lambda\nu} = \langle g_{\mu\lambda} \rangle_{,\nu} - \langle g_{\mu\lambda,\nu} \rangle, \tag{4.43}$$

and we have called the whole expression $k^{\mu} T_{\mu\lambda\nu} k^{\nu}$ as a new variable, I_{λ}. The left hand side of (4.42) represents the equation of a null geodesic of an averaged metric and the right hand side represents the modification due to averaging. From the right side however, we face two important properties for $T_{\mu\lambda\nu}$ and I_{λ}, which we shall explain and prove in the following:

(I) Firstly, it turns out that the object $T^{\mathrm{sym}}_{\mu\lambda\nu} = (T_{\mu\lambda\nu} + T_{\nu\lambda\mu})/2$ is a tensor. This is a non-trivial and non-obvious statement.

Proof of the tensor property follows from a brute force argument, based on the well know transformation properties of vectors and tensors (the averaged metric has been assumed to be a tensor itself),

$$k'^{\mu}(x') = \frac{\partial x'^{\mu}}{\partial x^{\alpha}} k^{\alpha}(x), \tag{4.44}$$

and

$$\langle g'_{\mu\nu}\rangle(x') = \frac{\partial x^{\alpha}}{\partial x'^{\mu}} \frac{\partial x^{\beta}}{\partial x'^{\nu}} \langle g_{\alpha\beta}\rangle(x), \tag{4.45}$$

and transformation properties of their derivatives

$$\frac{\partial k'^{\mu}}{\partial x'^{\nu}} = \frac{\partial x^{\beta}}{\partial x'^{\nu}} \frac{\partial x'^{\mu}}{\partial x^{\alpha}} \frac{\partial k^{\alpha}}{\partial x^{\beta}} + \frac{\partial x^{\beta}}{\partial x'^{\nu}} \frac{\partial^2 x'^{\mu}}{\partial x^{\alpha} \partial x^{\beta}} k^{\alpha}, \tag{4.46}$$

and

$$\begin{aligned} \frac{\partial \langle g'_{\mu\nu}\rangle}{\partial x'^{\lambda}} = {} & \frac{\partial x^{\sigma}}{\partial x'^{\lambda}} \frac{\partial^2 x^{\alpha}}{\partial x^{\sigma} \partial x'^{\mu}} \frac{\partial x^{\beta}}{\partial x'^{\nu}} \langle g_{\alpha\beta}\rangle \\ & + \frac{\partial x^{\sigma}}{\partial x'^{\lambda}} \frac{\partial x^{\alpha}}{\partial x'^{\mu}} \frac{\partial^2 x^{\beta}}{\partial x^{\sigma} \partial x'^{\nu}} \langle g_{\alpha\beta}\rangle \\ & + \frac{\partial x^{\sigma}}{\partial x'^{\lambda}} \frac{\partial x^{\alpha}}{\partial x'^{\mu}} \frac{\partial x^{\beta}}{\partial x'^{\nu}} \frac{\partial \langle g_{\alpha\beta}\rangle}{\partial x^{\sigma}}. \end{aligned} \tag{4.47}$$

We then check explicitly that the left hand side of (4.42) is a vector. We start from

$$\begin{aligned} \left(\frac{\partial k'^{\mu}}{\partial x'^{\nu}} \langle g'_{\mu\lambda}\rangle + \frac{\partial k'^{\mu}}{\partial x'^{\lambda}} \langle g'_{\mu\nu}\rangle + k'^{\mu} \frac{\partial \langle g'_{\mu\lambda}\rangle}{\partial x'^{\nu}} \right) = {} & \\ & \frac{\partial x^{\beta}}{\partial x'^{\nu}} \frac{\partial x'^{\mu}}{\partial x^{\alpha}} \frac{\partial k^{\alpha}}{\partial x^{\beta}} \frac{\partial x^{\epsilon}}{\partial x'^{\mu}} \frac{\partial x^{\eta}}{\partial x'^{\lambda}} \langle g_{\epsilon\eta}\rangle \\ & + \frac{\partial x^{\beta}}{\partial x'^{\nu}} \frac{\partial^2 x'^{\mu}}{\partial x^{\alpha} \partial x^{\beta}} k^{\alpha} \frac{\partial x^{\epsilon}}{\partial x'^{\mu}} \frac{\partial x^{\eta}}{\partial x'^{\lambda}} \langle g_{\epsilon\eta}\rangle \\ & + \frac{\partial x^{\beta}}{\partial x'^{\lambda}} \frac{\partial x'^{\mu}}{\partial x^{\alpha}} \frac{\partial k^{\alpha}}{\partial x^{\beta}} \frac{\partial x^{\varepsilon}}{\partial x'^{\mu}} \frac{\partial x^{\xi}}{\partial x'^{\nu}} \langle g_{\varepsilon\xi}\rangle \\ & + \frac{\partial x^{\beta}}{\partial x'^{\lambda}} \frac{\partial^2 x'^{\mu}}{\partial x^{\alpha} \partial x^{\beta}} k^{\alpha} \frac{\partial x^{\varepsilon}}{\partial x'^{\mu}} \frac{\partial x^{\xi}}{\partial x'^{\nu}} \langle g_{\varepsilon\xi}\rangle \\ & + \frac{\partial x'^{\mu}}{\partial x^{\alpha}} k^{\alpha} \frac{\partial x^{\sigma}}{\partial x'^{\nu}} \frac{\partial^2 x^{\kappa}}{\partial x^{\sigma} \partial x'^{\mu}} \frac{\partial x^{\varrho}}{\partial x'^{\lambda}} \langle g_{\kappa\varrho}\rangle \\ & + \frac{\partial x'^{\mu}}{\partial x^{\alpha}} k^{\alpha} \frac{\partial x^{\sigma}}{\partial x'^{\nu}} \frac{\partial x^{\kappa}}{\partial x'^{\mu}} \frac{\partial^2 x^{\varrho}}{\partial x^{\sigma} \partial x'^{\lambda}} \langle g_{\kappa\varrho}\rangle \\ & + \frac{\partial x'^{\mu}}{\partial x^{\alpha}} k^{\alpha} \frac{\partial x^{\sigma}}{\partial x'^{\nu}} \frac{\partial x^{\kappa}}{\partial x'^{\mu}} \frac{\partial x^{\varrho}}{\partial x'^{\lambda}} \frac{\partial \langle g_{\kappa\varrho}\rangle}{\partial x^{\sigma}}. \end{aligned} \tag{4.48}$$

In the following, besides the null condition, one has to use the relation

$$\frac{\partial^2 x'^{\mu}}{\partial x^{\gamma}\partial x^{\alpha}}\frac{\partial x^{\beta}}{\partial x'^{\mu}} = -\frac{\partial x'^{\mu}}{\partial x^{\alpha}}\frac{\partial^2 x^{\beta}}{\partial x^{\gamma}\partial x'^{\mu}}, \tag{4.49}$$

obtained from $\partial\delta^{\mu}_{\nu}/\partial x^{\gamma} = 0$.

Thus the second and fourth terms cancel out the fifth and sixth terms in the right hand side of equation (4.48), and the remaining terms are

$$\begin{aligned} &\frac{\partial k^{\alpha}}{\partial x'^{\nu}}\frac{\partial x'^{\mu}}{\partial x^{\alpha}}\frac{\partial x^{\epsilon}}{\partial x'^{\mu}}\frac{\partial x^{\eta}}{\partial x'^{\lambda}}\langle g_{\epsilon\eta}\rangle \\ &+\frac{\partial k^{\alpha}}{\partial x'^{\lambda}}\frac{\partial x'^{\mu}}{\partial x^{\alpha}}\frac{\partial x^{\varepsilon}}{\partial x'^{\mu}}\frac{\partial x^{\xi}}{\partial x'^{\nu}}\langle g_{\varepsilon\xi}\rangle \\ &+\frac{\partial x'^{\mu}}{\partial x^{\alpha}}k^{\alpha}\frac{\partial x^{\epsilon}}{\partial x'^{\mu}}\frac{\partial x^{\eta}}{\partial x'^{\lambda}}\frac{\langle g_{\epsilon\eta}\rangle}{\partial x^{\sigma}}\frac{\partial x^{\sigma}}{\partial x'^{\nu}}, \end{aligned} \tag{4.50}$$

which shows that it preserves the tensor property of $\left(k^{\mu}_{,\nu}\langle g_{\mu\lambda}\rangle + k^{\mu}_{,\lambda}\langle g_{\mu\nu}\rangle + k^{\mu}\langle g_{\mu\lambda}\rangle_{,\nu}\right)k^{\nu}$. Finally we can argue that as $I_{\lambda} = k^{\mu}T_{\mu\lambda\nu}k^{\nu}$ is a vector, the symmetric part, $T^{\rm sym}_{\mu\lambda\nu} = (T_{\mu\lambda\nu} + T_{\nu\lambda\mu})/2$, must also be a tensor, since k^{ν} itself is a vector.

Notice that by construction $T_{\mu\lambda\nu}$ is a symmetric object under the exchange of μ and λ, $T_{\mu\lambda\nu} = T_{\lambda\mu\nu}$, but not necessarily a tensor. Also note that $T^{\rm sym}_{\mu\lambda\nu} \neq T^{\rm sym}_{\lambda\mu\nu}$. In fact only $T^{\rm sym}_{\mu\lambda\nu}$ is of relevance to the averaged null geodesic equation.

(II) Secondly, multiplying the term I_{λ} with k^{λ} would give us $I_{\lambda}k^{\lambda} = 0$.

The second property, $I_{\lambda}k^{\lambda} = 0$, follows from contracting the left hand side of equation (4.42) with k^{λ}

$$k^{\mu}T_{\mu\lambda\nu}k^{\nu}k^{\lambda} = k^{\mu}_{,\nu}\langle g_{\mu\lambda}\rangle k^{\nu}k^{\lambda} + k^{\mu}_{,\lambda}\langle g_{\mu\nu}\rangle k^{\nu}k^{\lambda} + k^{\mu}\langle g_{\mu\lambda}\rangle_{,\nu}k^{\nu}k^{\lambda}. \tag{4.51}$$

We then use the fact that the null property of the wave vector is preserved,

$$\left(k^{\mu}\langle g_{\mu\lambda}\rangle k^{\lambda}\right)_{,\nu} = 0. \tag{4.52}$$

Multiplying the latter equation by k^{ν} gives us

$$\left(k^{\mu}_{\nu}\langle g_{\mu\lambda}\rangle k^{\lambda} + k^{\mu}\langle g_{\mu\lambda,\nu}\rangle k^{\lambda} + k^{\mu}\langle g_{\mu\lambda}\rangle k^{\lambda}_{,\nu}\right)k^{\nu} = 0. \tag{4.53}$$

By comparing equation (4.51) with (4.53), it is straightforward that the right hand side of (4.51) vanishes identically and thus the second statement holds.

4.5. Propagation of light through an averaged Universe

Let us denote the metric of a FL model by $\bar{g}_{\mu\nu}$ and the four-velocity of a comoving observer (the one that sees the light-ray under consideration) by $\bar{u}^\mu$. The observed photon frequency is then given by

$$\omega \equiv -\bar{u}_\mu k^\mu. \tag{4.54}$$

We assume that $\langle g_{\mu\nu} \rangle = \bar{g}_{\mu\nu}$, as the cosmological principle tells us that we should be able to describe the averaged Universe by an isotropic and homogeneous model. We still do not define how this average works in detail, but we assume that it exists and argue that observations confirm that such an approach must be possible.

Applying the cosmological principle to the tensor $T^{\text{sym}}_{\mu\lambda\nu}$, we can write down the most general algebraic structure compatible with isotropy and homogeneity. It is

$$T^{\text{sym}}_{\mu\lambda\nu} = \frac{f_1}{2}(\bar{g}_{\mu\lambda}\bar{u}_\nu + \bar{g}_{\nu\lambda}\bar{u}_\mu) + f_2\bar{u}_\mu\bar{u}_\lambda\bar{u}_\nu + f_3\bar{g}_{\mu\nu}\bar{u}_\lambda, \tag{4.55}$$

as $\bar{u}^\mu$ and $\bar{g}_{\mu\nu}$ are the only non-trivial tensors of first and second rank that can be used to construct a third rank tensor that is symmetric in two of its indices. f_1, f_2 and f_3 are three functions of cosmic time t only, which cannot be fixed by pure symmetry considerations. However, only the combination

$$I_\lambda = k^\mu T^{\text{sym}}_{\mu\lambda\nu} k^\nu = f_1(-\omega)\bar{g}_{\mu\lambda}k^\mu + f_2\omega^2\bar{u}_\lambda, \tag{4.56}$$

enters the averaged light geodesic equation. We further consider the contraction

$$I_\lambda k^\lambda = -f_2\omega^3, \tag{4.57}$$

which must vanish as shown in the previous section and thus $f_2 \equiv 0$.

Thus the inhomogeneity of the light propagation equation is given by

$$I_\lambda = -f_1\omega\bar{g}_{\mu\lambda}k^\mu, \tag{4.58}$$

and all effects of averaging on the light propagation must be encoded in a single function $f_1(t)$. Without any further knowledge, this generic structure of the inhomogeneity of the null geodesic equation allows us to make some non-trivial and generic statements about light propagation in an averaged Universe.

The Hubble rate $H = \dot{a}/a$, where $a(t)$ denotes the scale factor of the averaged FL metric and the dot denotes a derivative with respect to cosmic time. For a comoving observer with $\bar{u}_\mu = (-1, 0)$ we find

$$k^0 = \omega; \quad k^i = \omega e^i/a, \tag{4.59}$$

where e^i is a spatial unit vector, indicating the spatial direction the light-ray is pointing at. So that,

$$e^\mu \equiv (0, \frac{1}{a}e^i), \quad e_\mu \equiv (0, ae_i). \tag{4.60}$$

Keeping this information, we can write the derivatives of the time component and spatial components of the vector field k as,

$$k^0_{,0} = \dot{\omega}, \quad k^0_{,i} = \omega_{,i}, \quad k^i_{,0} = \frac{1}{a}(\dot{\omega}e^i + \dot{e}^i\omega - H\omega e^i), \quad k^i_{,j} = \omega_{,j}\frac{e^i}{a} + \frac{\omega}{a}e^i_{,j}. \tag{4.61}$$

Let us first look at the time component of the averaged null geodesic equation. The left hand side is well known from the equation of null geodesic motion in the FL model,

$$(-\omega)(\dot{\omega} + \frac{e^i}{a}\omega_{,i} + H\omega) = I_0 = f_1\omega^2. \tag{4.62}$$

In order to obtain equation (4.62), we have considered all possible terms with $\lambda = 0$,

$$2k^0_{,0}k^0\bar{g}_{00} + k^0\bar{g}_{00,0}k^0 + k^0_{,i}\bar{g}_{00}k^i + k^i_{,0}\bar{g}_{ij}k^j = I_0, \tag{4.63}$$

where $\bar{g}_{ij} = a^2\gamma_{ij}$. Trivially the terms containing $\bar{g}_{i0}$, $\bar{g}_{i0,j}$ and $\bar{g}_{00,i}$ vanish.

Moreover, we have considered the conditions

$$\gamma_{ij}e^ie^j = a^2, \quad \gamma_{ij}\dot{e}^ie^j = Ha^2, \tag{4.64}$$

obtained from the null geodesic equation $\bar{g}_{\mu\nu}k^\mu k^\nu = 0$ in the FL model.

Equation (4.62) might be more familiar in terms of the affine parameter

$$\frac{\mathrm{D}\,\omega}{\mathrm{d}\lambda} = \frac{\mathrm{d}\,\omega}{\mathrm{d}\lambda} = k^\mu\frac{\partial\,\omega}{\partial x^\mu} = \omega(\dot{\omega} + \frac{e^i}{a}\omega_{,i}), \tag{4.65}$$

and thus

$$\frac{\mathrm{d}\,\omega}{\mathrm{d}\lambda} + H_{\mathrm{eff}}\,\omega^2 = 0, \quad H_{\mathrm{eff}} \equiv H + f_1. \tag{4.66}$$

For $f_1 = 0$, this reduces to the famous result $\omega \propto 1/a$, the redshift of photons (note that $\mathrm{d}t = \omega\mathrm{d}\lambda$). Thus we conclude that any $f_1 \neq 0$ leads to a modification of the redshift of photons, so we would expect that the actual redshift of a photon in an averaged description of an inhomogeneous Universe must differ from the redshift that the same photon would have in the corresponding homogeneous and isotropic Universe.

Similar to equation (4.63), we derive the non-zero spatial components of (4.42), i.e. for $\lambda \neq 0$,

$$k^j_{,0}k^0\bar{g}_{ij} + k^j_{,k}k^k\bar{g}_{ij} + k^0_{,i}k^0\bar{g}_{00} + k^j_{,i}k^k\bar{g}_{jk} + k^jk^0\bar{g}_{ij,0} + k^jk^k\bar{g}_{ij,k} = I_{,i}, \tag{4.67}$$

since we consider only the flat FL case, the last term of the equation above vanishes. The spatial components of the modified light propagation equation becomes

$$a\gamma_{ij}e^j\omega\left(\dot{\omega} + \frac{e^k}{a}\omega_{,k} + H\omega\right) + a\omega^2\gamma_{ij}\left(\dot{e}^j + e^j_{|k}e^k\right) = I_{,i} = -\omega^2 a\gamma_{ij}e^j f_1, \tag{4.68}$$

where | denotes a covariant derivative with respect to the 3-metric γ_{ij}. By means of (4.62), equation (4.68) can be further simplified to yield

$$\dot{e}^j + e^j_{|k} e^k = 0, \tag{4.69}$$

or in terms of the affine parameter

$$\frac{\mathrm{D}e^i}{\mathrm{d}\lambda} = 0, \tag{4.70}$$

i.e. light-rays propagate along straight lines. This result holds for exact FL models and for light in the averaged Universe.

To sum up, based on the principles of statistical isotropy and homogeneity, there is one global effect on the propagation of light, which is a modification of the redshift of a photon, which can be described by an effective Hubble expansion rate.

4.6. Estimation for the effective Hubble rate

In order to estimate the function $f_1(t)$ we consider an irrotational model without gravitational waves. Then an ansatz for the metric that allows for density perturbations and can easily be compared with the zero shear gauge (or longitudinal Newtonian gauge) of linear perturbation theory is

$$ds^2 = -e^{2\phi}\mathrm{d}t^2 + a^2(t)e^{-2\psi}\gamma_{ij}\mathrm{d}x^i\mathrm{d}x^j. \tag{4.71}$$

We split the exact metric $g_{\mu\nu} = \bar{g}_{\mu\nu} + \delta g_{\mu\nu}$, where we do not make the assumption that $\delta g_{\mu\nu}$ is small. By construction $\langle \delta g_{\mu\nu} \rangle = 0$.

As it was mentioned earlier, the only non-zero components of the symmetric tensor $T^{\mathrm{sym}}_{\mu\lambda\nu}$ are T^{sym}_{000} and T^{sym}_{ij0}. We now evaluate

$$T^{\mathrm{sym}}_{000} = -\langle \delta g_{00,0} \rangle = 2\langle e^{2\phi}\dot{\phi} \rangle. \tag{4.72}$$

Note that $\bar{g}_{00} = -1$ and thus its derivative vanishes before and after averaging. By comparing this result with our ansatz for $T^{\mathrm{sym}}_{000} = f_1$ we have

$$f_1 = 2\langle e^{2\phi}\dot{\phi} \rangle. \tag{4.73}$$

Alternatively $\delta g_{ij} = a^2(e^{-2\psi} - 1)\gamma_{ij}\psi$ allows us to estimate f_1 from T^{sym}_{ij0},

$$T^{\mathrm{sym}}_{ij0} = \frac{1}{2}(T^{\mathrm{sym}}_{ij0} + T^{\mathrm{sym}}_{0ij}) = -\frac{1}{2}(\langle \delta g_{ij,0} \rangle), \tag{4.74}$$

where we compare to our ansatz for $T^{\mathrm{sym}}_{ij0} = -\frac{1}{2}f_1 a^2 \gamma_{ij}$. This gives us $f_1 = 2\langle e^{2\psi}\dot{\psi} \rangle$. Without anisotropic pressure, the off-diagonal components of the Einstein tensor must vanish, which implies $\phi = \psi$ and thus both estimates are consistent with each other.

Proof of $\phi = \psi$ in the absence of the anisotropic pressure, follows from writing the Ricci tensor (1.23) for the metric (4.71)

$$\begin{aligned} R_{ij} &= \partial_i\partial_j\phi - 3\partial_i\partial_j\psi + \partial_i\phi\,\partial_j\phi \\ &\quad - \partial_k(-\partial_i\psi\delta^k_j - \partial_j\psi\delta^k_i + \partial_m\psi\delta^{km}\delta_{ij}) \\ &\quad - \partial_n\phi(-\partial_i\psi\delta^n_j - \partial_j\psi\delta^n_i + \partial_l\psi\delta^{nl}\delta_{ij}) \\ &\quad + 3\partial_n\psi(-\partial_j\psi\delta^n_i - \partial_i\psi\delta^n_j + \partial_l\psi\delta^{nl}\delta_{ij}) \\ &\quad + (-\partial_k\psi\delta^n_i - \partial_i\psi\delta^n_k + \partial_s\psi\delta^{ns}\delta_{ik})(-\partial_n\psi\delta^k_j - \partial_j\psi\delta^k_n + \partial_r\psi\delta^{kr}\delta_{jn}), \end{aligned} \tag{4.75}$$

thus

$$\begin{aligned} R_{ij} &= \partial_i\partial_j\phi - 3\partial_i\partial_j\psi + \partial_i\phi\,\partial_j\phi + 2\partial_i\partial_j\psi - \partial_m\partial_k\psi\delta^{mk}\delta_{ij} \\ &\quad + \partial_i\phi\,\partial_j\psi - \partial_j\phi\,\partial_i\psi - \partial_n\phi\,\partial_l\psi\delta^{nl}\delta_{ij} \\ &\quad - 3\partial_i\psi\,\partial_j\psi - 3\partial_i\psi\,\partial_j\psi + 3\partial_n\psi\,\partial_l\psi\delta^{nl}\delta_{ij} \\ &\quad + 5\partial_i\psi\,\partial_j\psi - \partial_k\psi\,\partial_r\psi\delta^{kr}\delta_{ij} - \partial_s\psi\,\partial_n\psi\delta^{ns}\delta_{ij}, \end{aligned} \tag{4.76}$$

which at the end gives us

$$R_{ij} = \partial_i\partial_j\phi - \partial_i\partial_j\psi + \partial_i\phi\,\partial_j\phi - \partial_i\psi\,\partial_j\psi + \partial_i\phi\,\partial_j\psi - \partial_j\phi\,\partial_i\psi. \tag{4.77}$$

The case of $\phi = \psi$, satisfies the condition $G_{ij} = 0$ in the Einstein equation.

As already stated above, $\langle e^{2\phi}\rangle \equiv 1$ (by construction). However, since averaging and time derivative do not commute in general, f_1 is in general non-zero. In linear perturbation theory, $\dot\phi = 0$ in the Einstein-de Sitter model (EdS), but this is not the case for the ΛCDM model. For higher orders in perturbation, both the EdS and the ΛCDM model have $\dot\phi \neq 0$ (these are the integrated Sachs-Wolfe effect [26] and the Rees-Sciama effect [176]). Consequently, this implies that for the fully non-linear theory we have $\langle e^{2\phi}\dot\phi\rangle \neq 0$ in general.

Let us now estimate qualitatively what are the effects of the effective Hubble expansion rate H_{eff}. By means of (4.66), we get

$$H_{\text{eff}} = H + 2\langle e^{2\phi}\dot\phi\rangle. \tag{4.78}$$

In the following, we define the density contrast w.r.t. the averaged matter density $\bar\rho(t)$, i.e.

$$\delta(\mathbf{r}, t) \equiv \frac{\rho(\mathbf{r}, t) - \bar\rho(t)}{\bar\rho(t)}. \tag{4.79}$$

$\rho \geq 0$ implies $\delta \geq -1$. For an over-dense, collapsing region ($\delta > 0$), we expect from Newtonian reasoning that $\dot\phi < 0$. Similarly, for an underdense, expanding region ($\delta < 0$), $\dot\phi > 0$. However, if the over-dense region is virialized, its gravitational potential does not change any more and we expect no effect. Thus it is impossible to predict the sign of f_1 without a detailed investigation. Another important aspect is that most of the

volume of the Universe is under-dense. An arbitrary light-ray will typically pass through a dominantly under-dense universe, and thus we expect that $H_{\text{eff}} > H$ at times long after the formation of cosmic structure started. On the other hand, observed light is typically emitted in an over-dense and observed in an over-dense region. Thus for objects at not too far distances we expect that over-densities dominate the trajectory of the light-ray. For a quantitative discussion, which is beyond the scope of this work, some numerical simulations are necessary.

We can nevertheless conclude that the one-to-one association of redshift with the scale factor and thus with cosmic time that we know from the standard model of cosmology is not possible if the effect from the averaged description is taken into account.

4.7. Comparison to other results

Let us finally put our work in the context of the previous results. In the work of Räsänen [146, 88] (see also section 4.1) the propagation of a bundle of light has been studied. The redshift $z \equiv (\omega_{\text{s}} - \omega_{\text{o}})/\omega_{\text{o}}$ is found to be

$$1 + z = \exp\Big(\int_{\lambda_{\text{s}}}^{\lambda_{\text{o}}} \mathrm{d}\lambda\omega\big[\frac{1}{3}\theta + \sigma_{\mu\nu}e^{\mu}e^{\nu}\big]\Big), \tag{4.80}$$

where $\sigma_{\mu\nu}$ denotes the shear and θ the expansion rate and e^{μ} denotes as above the spatial direction of light propagation. This result agrees very well with our result in equation (4.66), which after integration can be written as (using $\mathrm{d}t = \omega\mathrm{d}\lambda$)

$$1 + z = \exp\Big[\int_{t_{\text{s}}}^{t_{\text{o}}} H_{\text{eff}}\,\mathrm{d}t\Big]. \tag{4.81}$$

Räsänen argued that the shear is negligible for the averaged geometry, and that the only important contribution would come from the averaged expansion rate. Therefore the distance redshift relation is in terms of the averaged expansion rate. In [177] it has been discussed that if the metric remains close to a FL model, the change in redshift with respect to its background value is small.

In addition to the agreement with these non-perturbative investigations, we are also able to compare our result to perturbative studies of Veneziano and his collaborations. So that our equation (4.81) is in agreement with equation (4.24) where the use of past null cones have been considered.

Furthermore, studies of Fleury and co-workers on the effects on the Hubble diagram in Swiss-Cheese toy models [153] are also in line with the above results.

5. Conclusion and Outlook

In this work, we have considered the propagation of light-rays in an averaged space-time. Our central result is a modification of the equation of null geodesic motion, see (4.42). This new equation of motion is a fully covariant vector equation for the wave-vector k^μ. Rays describing the propagation of light in an averaged space-time are generated by this wave vector, which is null w.r.t. the averaged space-time. In order to prove those points we assume that the averaged space-time (pseudo-)metric is a tensor and that it respects the causal structure of the microscopic space-time. That such averaging procedures exist has been shown by Zalaletdinov [136]. However, the particular averaging proposed by Zalaletdinov does not result in an isotropic and homogeneous metric. As we consider a fixed light-ray (source and observer are fixed events on the manifold), we think that it is justified not to average the wave vector and its derivative, but to just average the metric and its derivatives.

We then apply this light propagation equation (recall, it is not the geodesic equation of the averaged space-time) to a cosmological model. We assume that the averaged metric is a flat, spatially isotropic and homogeneous (as suggested by the success of the standard model of cosmology). We have shown that the relation between photon frequency and affine parameter is modified. This modification can be expressed as an effective Hubble rate, as shown in (4.66).

Thus the central finding of our work is that photons in an averaged Universe follow a FL geodesic equation of motion, but with the Hubble rate replaced by an effective Hubble rate that does not coincide with the Hubble rate that one would infer from the averaging of the space-time itself. In contrast to many previous studies, this result is not based on a perturbative approach and does not make use of a toy model. Moreover, our result is in perfect agreement with previous non-perturbative investigations [177] and with the results of the study of toy models, like the Swiss-Cheese model [155]. Also perturbative studies are in line with our findings [152].

We thus have shown that the Hubble rate associated with the averaged space-time metric does not necessarily coincide with the effective Hubble rate that should be considered for photon propagation. A quantitative study of the order of magnitude of the effect seems to require detailed numerical simulation, and is thus beyond the scope of this work. The most important result of this work is that the averaging effects on light propagation can be absorbed into an effective Hubble rate. This might be one of the more fundamental reasons for the great success of the Friedmann-Lemaître models.

Some interesting lines of research opened up by this work are the following:

So far we restricted our attention to the study of a single light-ray. The next logical step is to study the equation of geodesic deviation in order to ask if an analogous modification occurs, which would allow us to find a modification to the luminosity and angular diameter distances.

Furthermore, we notice that Buchert's formalism has been considered in FL space-time where the Weyl tensor vanishes and thus bundles of light-rays are subject to Ricci focussing (i.e. associated with a smooth distribution of matter). However, in a clumpy Universe, light-rays propagate in underdense regions and are sensitive to Weyl focussing (i.e. induced by the gradient of the gravitational potential). The issue of relating Weyl focussing of point like sources to Ricci focussing of smooth matter sources has been considered recently in [175]. In this context it will be interesting in our work to ask if it is true that a microscopic Weyl focussing leads to an effective Ricci focusing after averaging.

Another interesting aspect is that we can treat the distribution of inhomogeneities as stochastic random fields. The spatial distribution of inhomogeneities remains Gaussian. An important property of Gaussian random processes is that the spatial averages taken over a large volume in our Universe will be equal to expectations taken over an ensemble of regions of the Universe, as of course we are unable to measure quantities over an ensemble of Universes. Keeping this in mind, in our work, we can take the average over the statistical ensembles and calculate the redshift, and check whether it is equal to the case when we first determine the redshift for each individual distribution and then average over all redshifts. The possible differences in the redshift will lead us to interpret the effects of averaging on the observational data.

Difference between the observed redshift defined by spectral lines, and the model redshift from the theory may create tension between different estimates of parameters like H_0 [178]. We showed in our work that the average over inhomogeneous distributions affects the Hubble expansion rate. This might explain the tension between Hubble rates from cosmological probes like WMAP and Planck and other probes like SN Ia. Consequently, we expect that the effects could be related to explain dark energy. However, the evidence should be probed in the cosmological experimental surveys, such as SN Ia observations and galaxy redshift surveys. Thus an important next step is to find experimental evidence in favour or against the existence of two different Hubble parameters.

Bibliography

[1] E. Komatsu, et al., *Seven-year Wilkinson Microwave Anisotropy Probe (WMAP) Observations: Cosmological Interpretation.* Astrophys. J. Suppl. **192** (2011) 18 [arXiv:1001.4538].

[2] Planck Collaboration I, *Planck 2013 results: Overview of products and scientific results.* (2013) [arXiv:1303.5062].

[3] A. G. Riess, et al., *Observational Evidence from Supernovae for an Accelerating Universe and a Cosmological Constant.* Astron. J. **116** (1998) 1009 [arXiv:astro-ph/9805201].

[4] S. Perlmutter, et al., *Measurements of Omega and Lambda from 42 High-Redshift Supernovae.* Astrophys. J. **517** (1999) 565 [arXiv:astro-ph/9812133].

[5] D. J. Eisenstein, et al., *Detection of the Baryon Acoustic Peak in the Large-Scale Correlation Function of SDSS Luminous Red Galaxies.* Astrophys. J. **633** (2005) 560 [arXiv:astro-ph/0501171].

[6] D. W. Hogg, et al., *Cosmic homogeneity demonstrated with luminous red galaxies.* Astrophys. J. **624** (2005) 54 [arXiv:astro-ph/0411197].

[7] M. Scrimgeour, et al., *The WiggleZ Dark Energy Survey: the transition to large-scale cosmic homogeneity.* Mon. Not. Roy. Astron. Soc. **425** (2012) 116 [arXiv:1205.6812].

[8] S. Bagheri and D. J. Schwarz, *Light propagation in the averaged universe.* J. Cosmol. Astropart. Phys. **10** (2014) 073 [arXiv:astro-ph/1404.2185].

[9] A. R. Liddle and D. H. Lyth, *Cosmological inflation and large scale structure.* Cambridge Univ. Press. Cambridge (2000).

[10] S. M. Carrol, *Lecture Notes on General Relativity.* NSF-ITP. Chicago (1997) 97 [arXiv:gr-qc/9712019].

[11] A. H. Guth, *Inflationary universe: A possible solution to the horizon and flatness problems.* Phys. Rev. **D 23** (1981) 347.

[12] E. W. Kolb and M. S. Turner, *The Early Universe.* Westview Press. (1990).

[13] A. Linde, *Particle Physics and Inflationary Cosmology.* CRC Press. (1990) [arXiv:hep-th/0503203].

[14] Planck Collaboration XVI, *Planck 2013 results: Cosmological parameters.* (2013) [arXiv:1303.5076].

[15] V. F. Mukhanov, *Physicsl fundations of cosmology.* Cambridge Univ. Press. Cambridge (2005).

[16] M. Colless, et al., *The 2dF Galaxy Redshift Survey: spectra and redshifts.* Mon. Not. Roy. Astron. Soc. **328** (2001) 1039 [arXiv:astro-ph/0106498].

[17] J. R. I. Gott, et al., *A Map of the Universe.* Astrophys. J. **624** (2005) 463 [arXiv:astro-ph/0310571].

[18] D. H. Lyth and A. R. Liddle, *The primordial density perturbation: Cosmology, inflation and the origin of structure.* Cambridge Univ. Press. Cambridge (2009).

[19] S. Weinberg, *Cosmology.* Oxford Univ. Press. (2008).

[20] S. Dodelson, *Modern Cosmology.* Academic Press. (2003).

[21] D. H. Lyth and E. D. Stewart, *Inflationary density perturbations with* omega < 1. Phy. Lett. **252** (1990) 336.

[22] J. M. Bardeen, *Gauge-invariant cosmological perturbations.* Phys. Rev. **D 22** (1980) 1882.

[23] E. R. Harrison, *Fluctuations at the Threshold of Classical Cosmology.* Phys. Rev. **D 1** (1970) 2726.

[24] R. A. Sunyaev, B. Zel'dovich *The spectrum of primordial radiation, its distortions and their significance.* Astrophys. and Spacephys. **2** (1970) 66.

[25] D. J. Fixsen, *The Temperature of the Cosmic Microwave Background.* Astrophys. J. **707** (2009) 916 [arXiv:0911.1955].

[26] R. K. Sachs and A. M. Wolfe, *Perturbations of a cosmological model and angular variations of the microwave background.* Astrophys. J. **147** (1967) 73.

[27] H. K. Suonio, *Lecture notes on cosmology, Chap.12: cosmic microwave background anisotropy.* (2006).

[28] G. F. Smoot, et al., (1992). *Structure in the COBE differential microwave radiometer first-year maps.* Aastrophys. J. **396** (1992) L1.

[29] E. L. Wright, et al., *Interpretation of the cosmic microwave background radiation anisotropy detected by the COBE Differential Microwave Radiometer.* Astrophys. J. **396** (1992) L13.

[30] C. L. Bennett, et al., *Nine-Year Wilkinson Microwave Anisotropy Probe (WMAP) Observations: Final Maps and Results.* Astrophy. J. **208** (2013) 20 [arXiv:1212.5225].

[31] G. Hinshaw, et al., *Nine-Year Wilkinson Microwave Anisotropy Probe (WMAP) Observations: Cosmological Parameter Results.* Astrophys. J. **208** (2013) 19 [arXiv:1212.5226].

[32] P. G. E. Peebles, et al., *Finding the Big Bang.* Princeton Univ. New Jersey (2009).

[33] M. J. Lamarre, et al., *Planck pre-launch status: The HFI instrument, from specification to actual performance.* Astron. Astrophys. **520** (2010) A9.

[34] Planck HFI Core Team, *Planck early results, IV. First assessment of the High Frequency Instrument in-flight performance.* Astron. Astrophys. **536** (2011) A4 [arXiv:1101.2039];

Planck HFI Core Team, *Planck early results, VI. The High Frequency Instrument data processing.* Astron. Astrophys. **536** (2011) A6 [arXiv:1101.2048].

[35] M. Bersanelli, et al., *Planck pre-launch status: Design and description of the Low Frequency Instrument.* Astron. Astrophys. **520** (2010) A4 [arXiv:1001.3321].

[36] A. Mennella, et al., *Planck early results.III. First assessment of the Low Frequency Instrument. flight performance.* Astron. Astrophys. **536** (2011) A3 [arXiv:1101.2038].

[37] E. Hivon, et al., *A fast method for statistical analysis of large and complex cosmic microwave background data sets.* Astrophys. J. **567** (2002) 2 [arXiv:astro-ph/0105302].

[38] F. R. Bouchet, *The Planck mission.* (2014) [arXiv:1405.0439].

[39] A. Blanchard and J. Schneider, *Gravitational lensing effect on the fluctuations of the cosmic background radiation.* Astron. Astrophys. **184** (1987) 1.

[40] U. Seljak, *Gravitational lensing effect on cosmic microwave background anisotropies: a power spectrum approach.* Astrophys. J. **463** (1996) 1 [arXiv:astro-ph/9505109].

[41] F. Bernardeau, *Weak lensing detection in CMB maps. Astron. Astrophys.* **324** (1997) 15 [arXiv:astro-ph/9611012].

[42] R. M. Zaldarriaga, et al., *Gravitational lensing effect on cosmic microwave background polarization.* Phys. Rev. **D 58** (1998) 023003 [arXiv:astro-ph/9803150].

[43] A. Challinor and A. Lewis. *Lensed CMB power spectra from all sky correlation function.* Phy. Rev. **D 71** (2005) 103010 [arXiv:astro-ph/0502425].

[44] W. Hu and T. Okamoto, *Mass reconstruction with CMB polarisation.* Astrophy. J. **574** (2002) 566 [arXiv:astro-ph/0111606];

T. Okamoto and W. Hu, *CMB lensing reconstruction on the full sky.* Phys. Rev. **D 67** (2003) 083002 [arXiv:astro-ph/0301031];

C. M. Hirata, et al., *Analyzed weak lensing of the cosmic microwave background using the likelihood function.* Phy. Rev. **D 67** (2003) 043001 [arXiv:astro-ph/0209489].

[45] S. Das, et al., *The Atacama cosmology Telescope: Temperature and Gravitational lensing power spectrum measurements from three seasons of data. J. Cosmol.* Astropart. Phys. **4** (2013) 014 [arXiv:1301.1037].

[46] A. V. Engelen, et al., *A measurement of gravitational lensing of the cosmic microwave background using south pole telescope data.* Astrophys. J. **756** (2012) 142 [arXiv:1202.0546].

[47] Planck Collaboration XVII, *Planck 2013 results: Gravitational lensing by large scale structure.* (2013) [arXiv:1303.5077].

[48] Planck Collaboration XXII, *Planck 2013 results: Constraints on inflation.* (2013) [arXiv:astro-ph 1303.5082].

[49] K. N. Abazajian, et al., *The Seventh Data Release of the Sloan Digital Sky Survey.* Astrophys. j. **182** (2009) 543 [arXiv:0812.0649].

[50] M. J. Drinkwater, et al., *The WiggleZ Dark Energy Survey: survey design and first data release.* Mon. Not. Roy. Astron. Soc. **401** (2010) 1429 [arXiv:0911.4246].

[51] K. S. Dawson, et al., *The Baryon Oscillation Spectroscopic Survey of SDSS-III.* Astrophys. J. **145** (2013) [arXiv:1208.0022];

L. Anderson, et al., *The clustering of galaxies in the SDSS-III Baryon Oscillation Spectroscopic Survey: Baryon Acoustic Oscillations in the Data Release 10 and 11 galaxy samples.* Mon. Not. Roy. Astron. Soc. **441** (2013) 24 [arXiv:1312.4877].

[52] F. S. Labini, et al., *Absence of anti-correlations and of baryon acoustic oscillations in the galaxy correlation function from the Sloan Digital Sky Survey data release 7.* Astron. Astrophys. **505** (2009) 981 [arXiv:0903.0950].

[53] W. J. Percival, et al., *The Shape of the Sloan Digital Sky Survey Data Release 5 Galaxy Power Spectrum.* Astrophys. J. **657** (2007) 645 [arXiv:astro-ph/0608636].

[54] C. Blake, et al., *The WiggleZ Dark Energy Survey: mapping the distance-redshift relation with baryon acoustic oscillations.* Mon. Not. Roy. Astron. Soc. **418** (2011) 1707 [arXiv:1108.2635].

[55] V. J. Martinez, *The large scale structure in the Universe: from power-laws to acoustic peaks.* In "Data Analysis in Cosmology", Lecture Notes in Physics, eds. V. J. Martinez, et al., Springer-Verlag. (2009) [arXiv:0804.1536].

[56] M. J. Geller and J. P. Huchra, *Mapping the Universe.* Science **246** (1989) 897.

[57] R. P. Kirshner, et al., *A million cubic megaparsec void in Bootes.* Astrophys. J. **248** (1981) 57.

[58] P. J. E. Peebles, *Principles of Physical Cosmology.* Princeton Univ. Press. New Jersey (1993).

[59] T. Buchert and S. Räsänen, *Backreaction in late time cosmology.* Ann. Rev. Nucl. Part. Science. **62** (2012) 57 [arXiv:1112.5335].

[60] H. Skarke, *Inhomogeneity implies Accelerated Expansion.* Phys. Rev. **D 89** (2014) 043506 [arXiv:1310.1028].

[61] H. Skarke, *The evolution of an inhomogeneous universe.* (2014) [arXiv:1407.6602v1].

[62] J. Larena, et al., *Testing backreaction effects with observations.* Phys. Rev. **D 79** (2009) 083011 [arXiv:0808.1161];

E. Rosenthal and E. E. Flanagan, *Cosmological backreaction and spatially averaged spatial curvature.* (2008) [arXiv:0809.2107];

K. Bolejko, et al., *Bayesian analysis of the backreaction models.* Phys. Rev. **D 81** (2010) 063515 [arXiv:0811.4487].

[63] J. Larena, *Averaged inhomogeneous cosmologies and accelerated expansion: the morphon field.* 2.Kosmologietag, Univ. Bielefeld (2007) [www.physik.uni-bielefeld.de/igs/schools/cosmology/2007/larena.pdf].

[64] M. F. Shirokov and I. Z. Fisher, *Isotropic space with discrete gravitational field sources. on the theory of non homogeneous isotropic universe.* Sov. Astron. J. **6**, 699 (1963), Reprinted in: *Gen. Rel. Grav.* **30** (1998) 1411.

[65] R. A. Isaacson, *Gravitational Radiation in the Limit of High Frequency. II. Nonlinear Terms and the Effective Stress Tensor.* Phys. Rev. **166** (1968) 1272.

[66] D. R. Brill and J. B. Hartle, *Method of the Self-Consistent Field in General Relativity and its Application to the Gravitational Geon.* Phys. Rev. **135** (1964) B271.

[67] T. W. Noonan, Gen. Rel. Grav. **16** (1984) 1103.

[68] G. F. R. Ellis, *Relativistic cosmology: its nature, aims and problems.* In: General Relativity and Gravitation, Eds. B. Bertotti et al., (Reidel, Dordrecht) (1984) 215.

[69] N. V. Zotov and W. R. Stoeger, *Averaging Einstein's equations.* Class. Quantum Grav. **9** (1992) 1023.

[70] T. Futamase, *Approximation scheme for constructing a clumpy universe in General Relativity.* Phys. Rev. Lett. **61** (1988) 2175.

[71] T. Futamase, *Averaging of a locally inhomogeneous realistic universe.* Phys. Rev. **D 53** (1996) 681.

[72] J. P. Boersma, *Averaging in cosmology.* Phys. Rev. **D 57** (1998) 798 [arXiv:gr-qc/9711057]

[73] W. R. Stoeger, et al., *The relationship between continuum homogeneity and statistical homogeneity in cosmology.* Mon. Not. Roy. Astron. Soc. **226** (1987) 373.

[74] M. Carfora and K. Piotrkowska, *A renormalization group approach to relativistic cosmology.* Phys. Rev. **D 52** (1995) 4393 [arXiv:gr-qc/9502021].

[75] N. Mustapha, et al., *The distortion of the area distance-redshift relation in inhomogeneous isotropic universes.* Class. Quant. Grav. **15** (1998) 2363 [arXiv:gr-qc/9708043].

[76] A. Krasinski, *Inhomogeneous Cosmological Models.* Cambridge Univ. Press. Cambridge (1997).

[77] R. M. Zalaletdinov, *Averaging out the Einstein equations.* Gen. Rel. Grav. **24** (1992) 1015.

[78] R. M. Zalaletdinov, *Toward a theory of macroscopic gravity.* Gen. Rel. Grav. **25** (1993) 673.

[79] T. Buchert, *On average properties of inhomogeneous fluids in general relativity I: dust cosmologies.* Gen. Rel. Grav. **32** (2000) 105 [arXiv:gr-qc/9906015].

[80] T. Buchert, *On average properties of inhomogeneous fluids in general relativity II: perfect fluid cosmologies.* Gen. Rel. Grav. **33** (2001) 1381 [arXiv:gr-qc/0102049].

[81] T. Buchert, *On average properties of inhomogeneous cosmologies.* In: General relativity and gravitation, proc. 9th JGRG meeting, ed. Y. Eriguchi. (2000) 306 [arXiv:gr-qc/0001056].

[82] C. Wetterich, *Can Structure Formation Influence the Cosmological Evoluti on?* Phys. Rev. **D 67** (2003) 043513 [arXiv:astro-ph/0111166].

[83] D. J. Schwarz, *Accelerated expansion without dark energy.* In: On the nature of dark energy, 18th IAP Astrophysics Colloquium, Eds. P. Brax eet al., (2002) pp. 331 [arXiv:astro-ph/0209584].

[84] S. Räsänen, *Backreaction of linear perturbations and dark energy.* (2004) [arXiv:astro-ph/0407317].

[85] S. Räsänen, *Dark energy from backreaction.* J. Cosmol. Astropart. Phys. **02** (2004) 003 [arXiv:astro-ph/0311257].

[86] T. Buchert and M. Carfora, *On the curvature of the present-day universe.* Class. Quant. Grav. **25** (2008) 195001 [arXiv:0803.1401].

[87] C. G. Tsagas, et al., *Relativistic cosmology and large-scale structure.* Phys. Rept. **465** (2008) 61 [arXiv:0705.4397].

[88] S. Räsänen, *Light propagation in statistically homogeneous and with general matter content.* J. Cosmol. Astropart. Phys. **1003** (2010) 018 [arXiv:0912.3370].

[89] E. Gourgoulhon, *3+1 formalism and bases of numerical relativity.* (2007) [arXiv:gr-qc/0703035].

[90] R. Arnowitt, et al., *The Dynamics of General Relativity.* Gen. Rel. Grav. **40** edited by L. Witten (1962) 1997 [arXiv:gr-qc/0405109].

[91] J. Larena, *Spatially averaged cosmology in an arbitrary coordinate system.* Phys. Rev. **D 79** (2009) 084006 [arXiv:0902.3159].

[92] M. Gasperini, et al., *Gauge invariant averages for the cosmological backreaction.* J. Cosmol. Astropart. Phys. **03** (2009) 011 [arXiv:0901.1303].

[93] M. Gasperini, et al., *A covariant and gauge invariant formulation of the cosmological backreaction.* J. Cosmol. Astropart. Phys. **02** (2010) 009 [arXiv:0912.3244].

[94] G. Marozzi, *The cosmological backreaction: gauge (in)dependence, observers and scalars.* J. Cosmol. Astropart. Phys. **01** (2011) 012 [arXiv:1011.4921].

[95] T. Buchert and M. Carfora, *Cosmological parameters are dressed.* Phys. Rev. Lett. **90** (2003) 031101 [arXiv:gr-qc/0210045].

[96] A. Lemaitre, *The expanding universe.* Class. and Quant. Grav. **29** (1997) 637.

[97] J. Plebanski and A. Krasinski, *An introduction to General Relativity and Cosmology.* Cambridge Univ. Press. Cambridge (2006).

[98] H. Bondi, *Spherically symmetrical models in general relativity.* Gen. Rel. Grav. **31** (1999) 1777.

[99] T. Buchert, *On globally static and stationary cosmologies with or without a cosmological constant and the dark energy problem.* Class. Quant. Grav. **23** (2006) 817 [arXiv:gr-qc/0509124].

[100] N. Li and D. J. Schwarz, *On the onset of cosmological backreaction.* Phys. Rev. **D 76** (2007) 083011 [arXiv:gr-qc/0702043].

[101] T. Buchert, et al., *Correspondence between kinematical backreaction and scalar field cosmologies, the morphon field.* Class. Quant. Grav. **23** (2006) 6379 [arXiv:gr-qc/0606020].

[102] D. L. Wiltshire. *Exact Solution to the Averaging Problem in Cosmology.* Phys. Rev. Lett. **99** (2007) 251101 [arXiv:0709.0732].

[103] S. Räsnen, *Evaluating backreaction with the peak model of structure formation.* J. Cosmol. Astropart. Phys. **04** (2008) 026 [arXiv:0801.2692].

[104] D. L. Wiltshire. *Average observational quantities in the timescape cosmology.* Phys. Rev. **D 80** (2009) 123512 [arXiv:0909.0749].

[105] X. Roy and T. Buchert. *Chaplygin gas and effective description of inhomogeneous universe models in general relativity.* Class. Quant. Grav. **27** (2010) 175013 [arXiv:0909.4155].

[106] A. Wiegand and T. Buchert. *Multiscale cosmology and structure emerging dark energy: A plausibility analysis.* Phys. Rev. **D 82** (2010) 023523 [arXiv:1002.3912].

[107] E. W. Kolb, et al., *On cosmic acceleration without dark energy.* New J. Phys. **8** (2006) 322 [arXiv:astro-ph/0506534].

[108] N. Li and D. J. Schwarz, *Scale dependence of cosmological backreaction.* Phys. Rev. **D 78** (2008) 083531 [arXiv:0710.5073].

[109] I. A. Brown, et al., *Averaging Robertson-Walker cosmologies.* J. Cosmol. Astropart. Phys. **4** (2009) 16 [arXiv:0811.4495].

[110] I. A. Brown, et al., *Gauges and cosmological backreaction.* J. Cosmol. Astropart. Phys. **11** (2009) 27 [arXiv:0903.3264].

[111] S. Räsänen, *Applicability of the linearly perturbed FLRW metric and Newtonian cosmology.* Phys. Rev. **D 81** (2010) 103512 [arXiv:1002.4779].

[112] A. Ishibashi and R. M. Wald, *Can the acceleration of our universe be explained by the effects of inhomogeneities?* Class. Quant. Grav. **23** (2006) 235 [arXiv:gr-qc/0509108].

[113] T. Buchert, et al., *Geometrical order of magnitude estimates for spatial curvature realistic models of the universe.* Gen. Rel. Grav. **41** (2009) 2017 [arXiv:0906.0134].

[114] N. Li and D. J. Schwarz, *Scale dependence of cosmological backreaction.* Phys. Rev. **D 78** (2008) 083531 [arXiv:0710.5073].

[115] N. Li, *Cosmological backreaction : from the local Hubble expansion rate to dark energy.* Dissertation, Univ. Bielefeld (2008). [http://bieson.ub. uni-bielefeld.de/volltexte/2008/1372].

[116] D. L. Wiltshire, *Viable inhomogeneous model universe without dark energy from primordial inflation.* (2005) [arXiv:gr-qc/0503099];

D. L. Wiltshire, *Dark energy without dark energy.* In: Dark Matter in Astroparticle and Particle Physics, Eds. H. V. Klapdor-Kleingrothaus and G. F. Lewis (2008) 565 [arXiv:0712.3984].

[117] E. W. Kolb, et al., *Primordial inflation explains why the universe is accelerating today.* (2005) [arXiv:hep-th/0503117].

[118] C. M. Hirata and U. Seljak, *Can superhorizon cosmological perturbations explain the acceleration of the universe?* Phys. Rev. **D 72** (2005) 083501 [arXiv:astro-ph/0503582].

[119] G. Geshnizjani, et al., *Do large-scale inhomogeneities explain away dark energy?* Phys. Rev. **D 72** (2005) 023517 [arXiv:astro-ph/0503553].

[120] E. E. Flanagan, *Can superhorizon perturbations drive the acceleration of the Universe?* Phys. Rev. **D 71** (2005) 103521 [arXiv:hep-th/0503202].

[121] S. Räsänen, *Constraints on backreaction in dust universes.* Class. Quant. Grav. **23** (2006) 1823 [arXiv:astro-ph/0504005].

[122] M. F. Parry, *A rule of thumb for cosmological backreaction.* J. Cosmol. Astropart. Phys. **0606** (2006) 016 [arXiv:astro-ph/0605159].

[123] N. Kumar and E. E. Flanagan, *Backreaction of superhorizon perturbations in scalar field cosmologies.* Phys. Rev. **D 78** (2008) 063537 [arXiv:0808.1043].

[124] S. R. Green and R. M. Wald, *A new framework for analysing the effects of small scale inhomogeneities in cosmology.* Phys. Rev. **D 83** (2011) 084020 [arXiv:1011.4920].

[125] A. A. Coley, *Averaging in cosmological models.* (2010) [arXiv:1001.0791].

[126] E. W. Kolb, et al., *Cosmological background solutions and cosmological backreactions.* Gen. Rel. Grav. **42** (2010) 1399 [arXiv:0901.4566].

[127] S. Räsänen, *Accelerated expansion from structure formation.* J. Cosmol. Astropart. Phys. **0611** (2006) 003 [arXiv:astro-ph/0607626].

[128] C. Clarkson et al., *Does the growth of structure affect our dynamical models of the universe? The averaging, backreaction and fitting problems in cosmology.* Rept. Prog. Phys. **74** (2011) 112901 [arXiv:1109.2314].

[129] D. L. Wiltshire, *Cosmic clocks, cosmic variance, cosmic averages.* New. J. Phys. **9** (2007) 377 [arXiv:gr-qc/0702082].

[130] A. Paranjape, *A covariant road to spatial averaging in cosmology: scalar corrections to the cosmological equations.* Int. J. Mod. Phys. **D 17** (2008) 597 [arxiv: 0705.2380].

[131] A. Paranjape, *The averaging problem in cosmology.* Dissertation (2009) [arXiv:0906.3165].

[132] T. Buchert, *Dark energy from structure.* Gen. Rel. Grav. **40** (2008) 467 [arXiv: 0707.2153].

[133] R. Tavakol and R. Zalaletdinov, *On the domain of applicability of general relativity.* Found. Phys. **28** (1998) 307 [arXiv:gr-qc/9703025].

[134] R. M. Zalaletdinov, *Averaging problem in cosmology and macroscopic gravity.* Online Proceedings of the Atlantic Regional Meeting on General Relativity and Gravitation, Univ. of New Brunswick. (2007) [arXiv:gr-qc/0701116].

[135] J. Brannlund, et al., *Averaging geometrical objects on a differentiable manifold.* Int. J. Mod. Phys. **D 19** (2010) 1915. [arxiv:1003.2014].

[136] R. M. Zalaletdinov, *The averaging problem in cosmology and macroscopic gravity.* Int. J. Mod. Phys. **A 23** (2008) 1173 [arXiv:0801.3256].

[137] A. A. Coley, et al., *Cosmological solutions in macroscopic gravity.* Phys. Rev. Lett. **95** (2005) 151102 [arXiv:gr-qc/0504115].

[138] R. J. van den Hoogen, *A complete cosmological solution to the averaged Einstein field equations as found in macroscopic gravity.* J. Math. Phys. **50** (2009) 082503 [arXiv:0909.0070].

[139] T. Clifton, et al., *Observational Cosmology in Macroscopic Gravity.* J. Cosmol. Astropart. Phys. **10** (2012) 044 [arXiv:1209.1085].

[140] C. Clarkson, et al., *Observational constraints on the averaged universe.* (2014) [arxiv:1111.2214].

[141] A. G. Riess, et al., *A redetermination of the Hubble constant with the Hubble space telescope from a differential distance ladder.* Astrophys. J. **699** (2009) 539 [arXiv:0905.0695].

[142] R. Amanullah, et al., *Spectra and light curves of six type Ia Supernovae at* $0.511 < z < 1.12$ *and the Union2 compilation.* Astrophys. J. **716** (2010) 712.

[143] R. Kessler, et al., *First-year Sloan Digital Sky Survey-II (SDSS-II) Supernova results: Hubble diagram and cosmological parameters.* Astrophys. J. Suppl. **185** (2009) 32 [arXiv:0908.4274].

[144] W. J. Percival, et al., *Baryon Acoustic Oscillations in the Sloan Digital Sky Survey data release 7 galaxy sample.* Mon. Not. Roy. Astron. Soc. **401** (2010) 2148 [arXiv:0907.1660].

[145] A. A. Coley, *Null geodesics and observational cosmology.* (2008) [arXiv:0812.4565].

[146] S. Räsänen, *Light propagation in statistically homogeneous and isotropic dust universes.* J. Cosmol. Astropart. Phys. **0902** (2009) 011 [arXiv:0812.2872].

[147] M. Gasperini, et al., *Light-cone averaging in cosmology: formalism and applications.* J. Cosmol. Astropart. Phys. **1107** (2011) 008 [arXiv:1104.1167].

[148] I. Ben-Dayan, et al., *Backreaction on the luminosity-redshift relation from gauge invariant light-cone averaging* J. Cosmol. Astropart. Phys. **04** (2012) 036 [arXiv:1202.1247].

[149] I. Ben-Dayan, et al., *Backreaction on the luminosity-redshift relation from gauge invariant light-cone averaging.* J. Cosmol. Astropart. Phys. **1204** (2012) 036 [arXiv:1202.1247].

[150] M. Gasperini, et al., *A covariant and gauge invariant formulation of the cosmological backreaction* J. Cosmol. Astropart. Phys. 1002 (2010) 009 [arXiv:0912.3244].

[151] I. Ben-Dayan, et al., *Do stochastic inhomogeneities affect dark-energy precision measurements?* Phys. Rev. Lett. **110** (2013) 021301 [arXiv:1207/1286].

[152] I. Ben-Dayan, et al., *Average and dispersion of the luminosity-redshift relation in the concordance model.* J. Cosmol. Astropart. Phys. **1306** (2013) 002 [arXiv:1302.0740].

[153] P. Fleury, et al., *Interpretation of the Hubble diagram in a nonhomogeneous universe.* Phys. Rev. **D 87** (2013) 123526 [arXiv:1302.5308].

[154] P. Fleury, et al., *Can all cosmological observations be accurately interpreted with a unique geometry?* Phys. Rev. Lett. **111** (2013) 091302 [arXiv:1304.7791].

[155] P. Fleury, *Swiss-cheese models and the Dyer-Roeder approximation.* J. Cosmol. Astropart. Phys. **06** (2014) 054 [arXiv:1402.3123].

[156] G. Ellis, *Relativistic Cosmology, General Relativity and Cosmology.* ed R. K. Sachs Academic Press Inc. London (1971) 104;

J. Wainwright and G. Ellis, *Dynamical Systems in Cosmology.* Cambridge Univ. Press. Cambridge (1997).

[157] M. Sasaki, *Cosmological Gravitational Lens Equation: Its Validity And Limitation.* Prog. Theor. Phys. **90** (1993) 753.

[158] M. Sasaki, *The Magnitude-Redshift relation in a perturbed Friedmann universe.* Mon. Not. Roy. Astron. Soc. **228** (1987) 653;

M. Kasai and M. Sasaki, *The Number Count Redshift Relation in a Perturbed Friedmann Universe.* Mod. Phys. Lett. **A2** (1987) 727.

[159] P. Szekeres, *A class of inhomogeneous cosmological models.* Commun. Math. Phys. **41** (1975) 55;

C. Hellaby and A. Krasinski, *You can't get through Szekeres wormholes: Or, regularity, topology and causality in quasispherical Szekeres models.* Phys. Rev. **D 66** (2002) 084011 [arXiv:0206052].

[160] C. Hellaby and A. Krasinski, *Physical and geometrical interpretation of the $\epsilon < 0$ Szekeres models.* Phys. Rev. **D 77** (2008) 023529 [arXiv:0710.2171];

A. Krasinski, *Geometry and topology of the quasi-plane Szekeres model.* Phys. Rev. **D 78** (2008) 064038. Erratum Phys. Rev. **D 85** (2012) 069903 [arXiv:0805.0529].

[161] M. Lavinto, et al., *Average expansion rate and light propagation in a cosmological Tardis space time.* J. Cosmol. Astropart. Phys. **12** (2013) 051 [arXiv:1308.6731].

[162] M. N. Celerier, *Do we really see a cosmological constant in the supernovae data?* Astron. Astrophys. **353** (2000) 63 [astro-ph/9907206].

[163] S. Räsänen, *Backreaction in the Lemaitre-Tolman-Bondi model.* J. Cosmol. Astropart. Phys. **0411** (2004) 010 [gr-qc/0408097].

[164] H. Alnes, et al., *An inhomogeneous alternative to dark energy?* Phys. Rev. **D 73** (2006) 083519 [astro-ph/0512006].

[165] K. Enqvist, *Lemaitre-Tolman-Bondi model and accelerating expansion.* Gen. Rel. Grav. **40** (2008) 451 [arXiv:0709.2044].

[166] T. Mattsson and M. Ronkainen, *Exploiting scale dependence in cosmological averaging.* J. Cosmol. Astropart. Phys. **0802** (2008) 004 [arXiv:0708.3673].

[167] R. A. Vanderveld, et al., *Mimicking Dark Energy with Lemaitre- Tolman-Bondi Models: Weak Central Singularities and Critical Points.* Phys. Rev. *D 74* (2006) 023506 [astro-ph/0602476].

[168] R. Kantowski, *Corrections in the Luminosity-Redshift Relations of the Homogeneous Friedmann Models.* Astrophys. J. **155** (1969) 89.

[169] C. C. Dyer and R. C. Roeder, Astrophys. J. **189** (1974) 167.

[170] N. Brouzakis, et al., *The effect of large scale inhomogeneities on the luminosity distance.* J. Cosmol. Astropart. Phys. **02** (2007) 013 [arXiv:astro-ph/0612179].

[171] V. Marra et al., *On cosmological observables in a swiss-cheese universe.* Phys. Rev. **D 76** (2007) 1230004 [arXiv:0708.3622].

[172] F. Kottler, *About the physical foundations of Einstein's theory,* (German version) Ann. Phys. **361** (1918) 401.

[173] V. Perlick, *Gravitational lensing from a space time perspective.* Rev. Relativity **7** (2004) 9 (section 5.2) [http://relativity.livingreviews.org/ Articles/lrr-2004-9/].

[174] R. Sachs, *Gravitational waves in general relativity. IV. The outgoing radiation condition.* Proc. R. Soc. London. **A 264** (1961) 309;

P. Schneider, et al., *Gravitational Lenses.* Springer, New York (1992).

[175] C. Clarkson, et al., *(Mis-)Interpreting supernovae observations in a lumpy universe.* Mon. Not. R. Astron. Soc. **426** (2012) 1121 [arXiv:1109.2484v3].

[176] M. J. Rees and D. W. Sciama, *Large-scale density inhomogeneities in the universe.* Nature. **217** (1968) 511.

[177] S. Räsänen, *Light propagation and the average expansion rate in near FRW universes.* Phys. Rev. **D 85** (2012) 083528 [arXiv:1107.1176].

[178] B. A. Bassett, et al., *A Tale of Two Redshifts.* (2013) [arXiv:1312.2593].

A. List of Abbreviations

Abbreviation	Use	Full name
ΛCDM	1	Lambda Cold Dark Matter model
ACBAR	2.5.1	Arcminute Cosmology Bolometer Array Receiver
ACT	2.5.5	Atacama Cosmology Telescope
ADM	3.4	Arnowitt-Deser-Misner
BAO	1	baryon acoustic oscillations
BBN	1.1	Big Bang Nucleosynthesis
BOSS	2.6	Baryonic Oscillation Spectroscopic Survey
CMB	1	cosmic microwave background
COBE	2.5.1	Cosmic Background Explorer
EdS	3.6.2	Einstein-de Sitter
ESA	2.5.2	European Space Agency
FL	1	Friedmann-Lemaître model of the Universe
GLC	4.2.1	Geodesic Light Cone Coordinates
GR	1.2	general relativity
HFI	2.5.2	High Frequency Instrument
ISW	2.4	Integrated Sachs Wolfe Effect
ΛCDM	1	Λ cold dark matter
LFI	2.5.2	Low Frequency Instrument
LTB	3.5.2	Lemaître-Tolman-Bondi
LSS	2.5.1	large scale structure
RW	1.4	Robertson Walker
SDSS	2.6	Sloan Digital Sky Survey
SPT	2.5.5	South Pole Telescope
WiggleZ	1	An Australian Galaxy survey
WMAP	1	Wilkinson Microwave Anisotropy Probe
WMAP7	2.5.1	WMAP 7-year data release

B. List of Figures and Tables

List of Figures

List of Tables

Acknowledgements

First of all, I want to thank my supervisor Prof. Dominik Schwarz for offering me an opportunity to pursue my study in his group, for his support and encouragement during my time as a Ph.D. student at Bielefeld University, and for the many opportunities to participate in fruitful conferences, workshops and schools. Without his help, this thesis would obviously not have been possible!

I am also grateful to my second supervisor, Prof. Domenico Giulini for valuable discussions and comments.

Many thanks go to my friends in the physics department: Ioan and Flo, for being wonderful office-mates, Isabel, for her kind and supportive friendship, and of course to Thomas, Daniel, Song, Alex and Benedict. Thank you all, for the friendships that made my Ph.D. life so enjoyable.

Thanks also go to my Iranian friends in Bielefeld, Masoumeh, Farideh, Mahshid and many others who were accompanying me through the challenges over the last few years.

Finally, I wish to express my deepest gratitude to my family.

My work was supported by Deutsche Forschungsgemeinschaft (DFG) within the International Research Training Group (IRTG 881) and the Research Training Group (RTG 1620) “Models of Gravity”.